Universität zu Lübeck
SS 2012

Interdisziplinäre Vorlesung zur Lasermedizin

Prof. Alfred Vogel

Laserdisruption: Plasma-mediated surgery

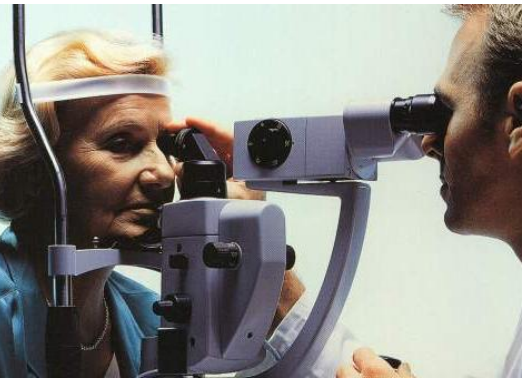

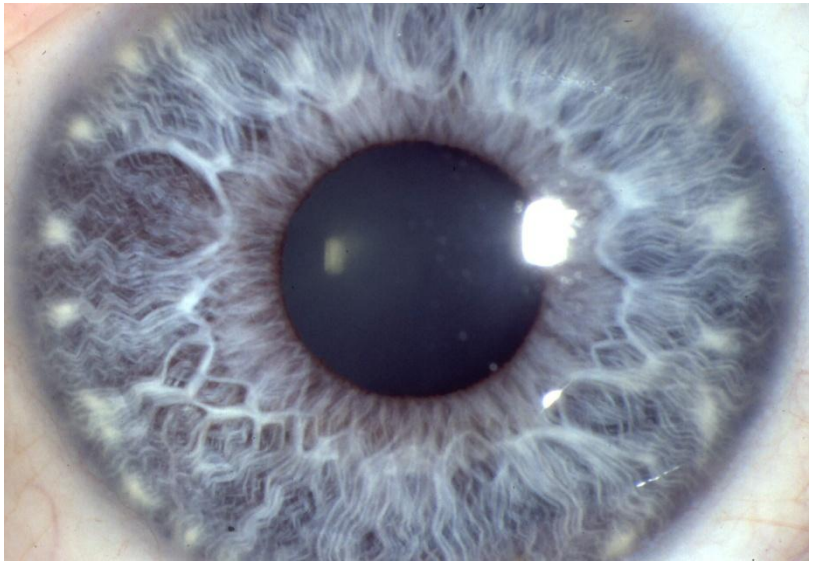

Outline:
Plasma-mediated surgery

1

- Principle and applications of intraocular surgery
- Plasma-mediated fragmentation: laser lithotripsy

2

- Femtosecond laser cell surgery
- Nanocavitation for cell transfection

3

- Plasma-mediated transport of biomaterials

Mechanical damage and bleeding from explosive vaporization induced by *linear* absorption at the RPE

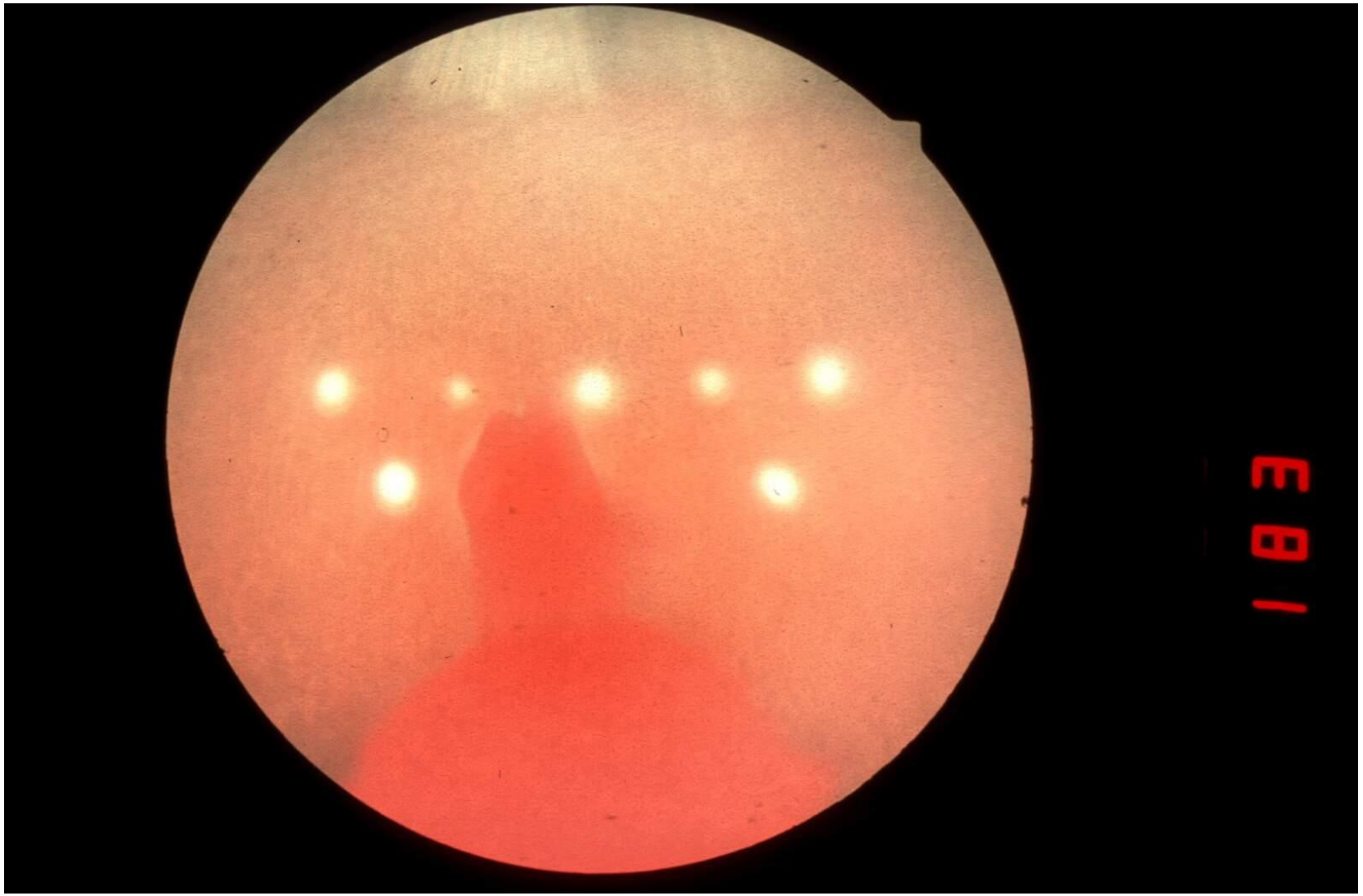

Light absorption of cells & tissues ⇔ Localized energy deposition

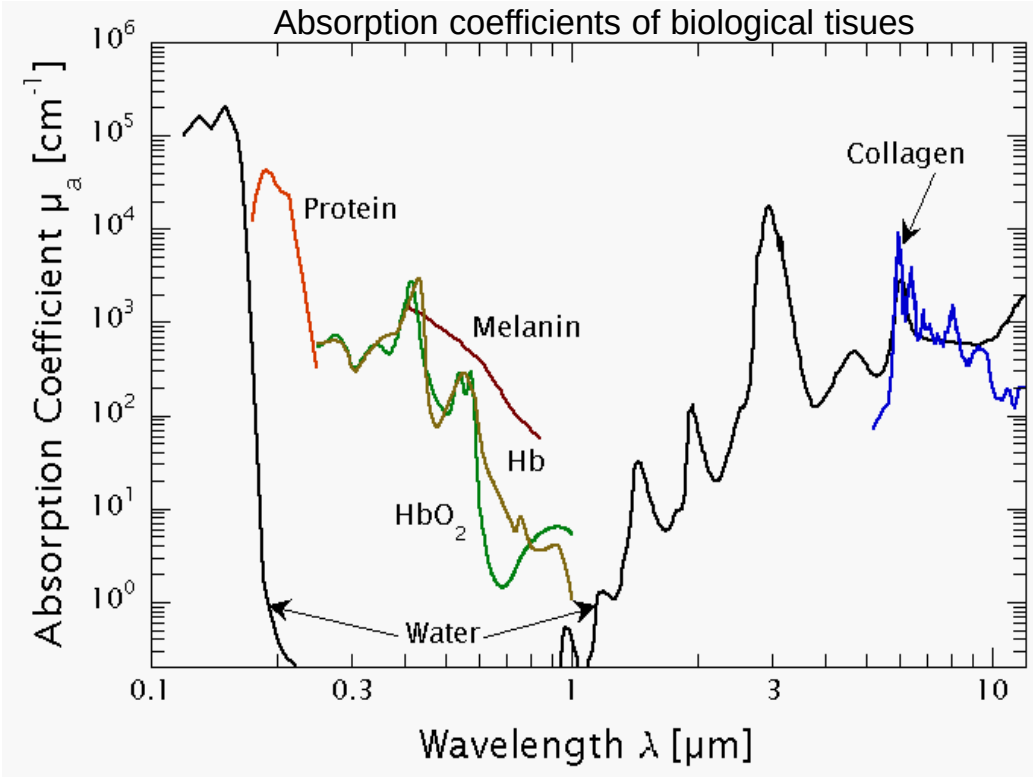

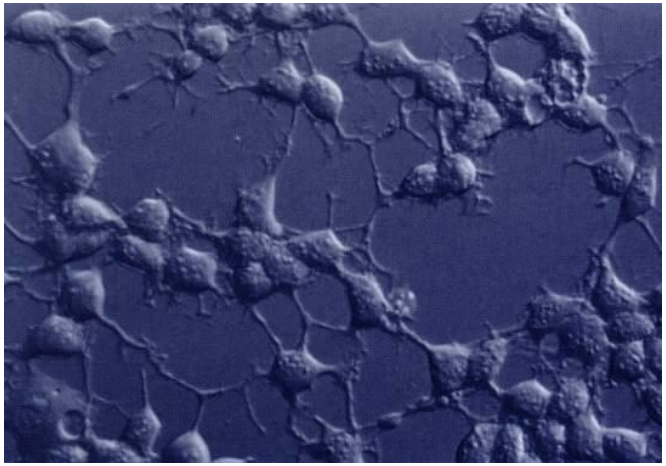

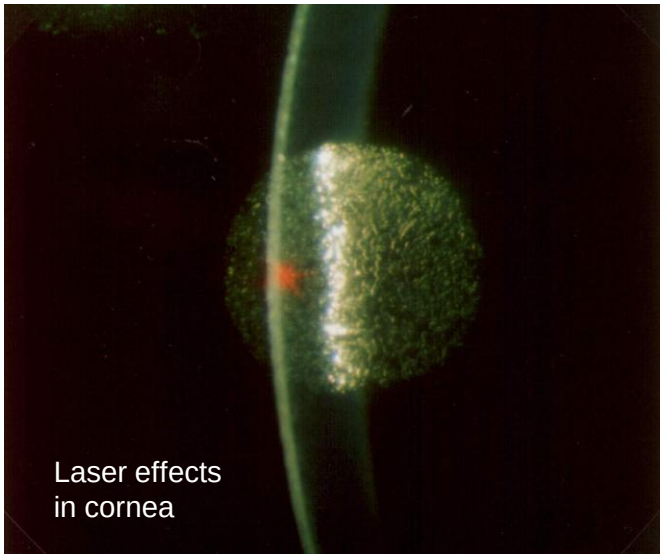

Localized energy deposition
within transparent tissues or cells requires:

- wavelengths that can penetrate,
- tight focusing, and
- *nonlinear absorption*

Example: Intraocular dissection and disruption

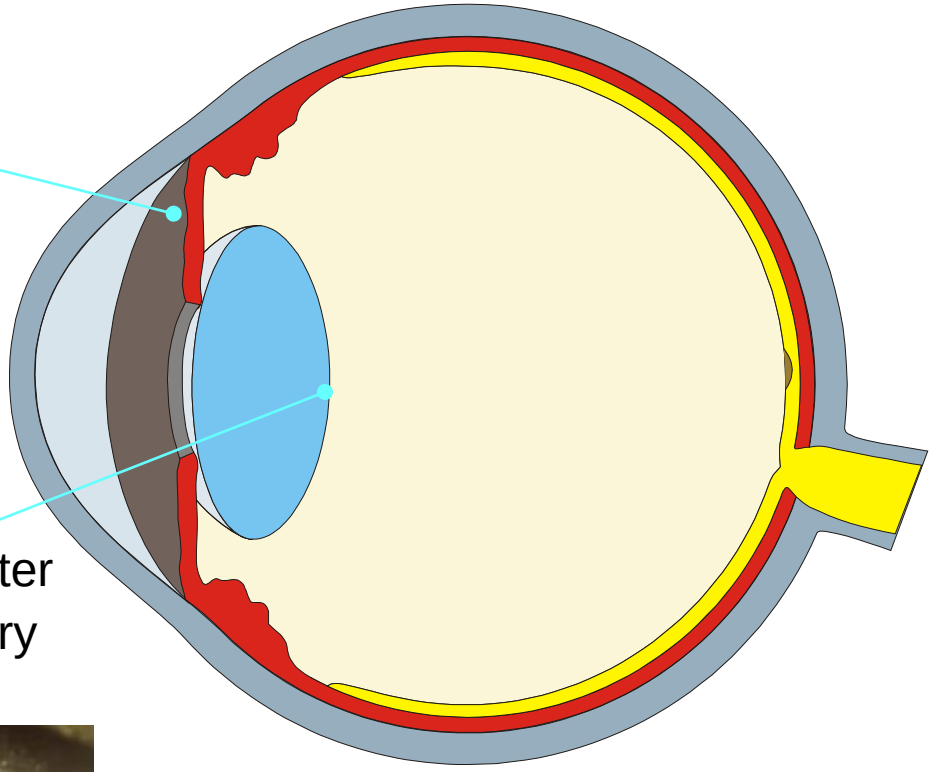

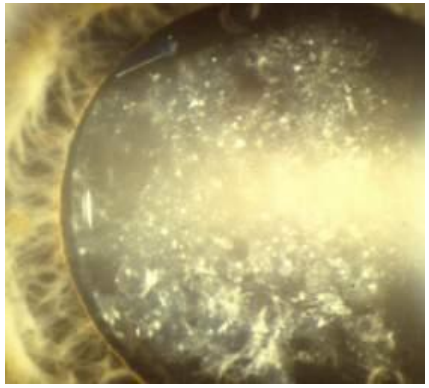

Conflicting tasks:

Light must penetrate into the eye

+

localized energy deposition

⇒ **nonlinear absorption required !**

Discovery of “laser lightning”

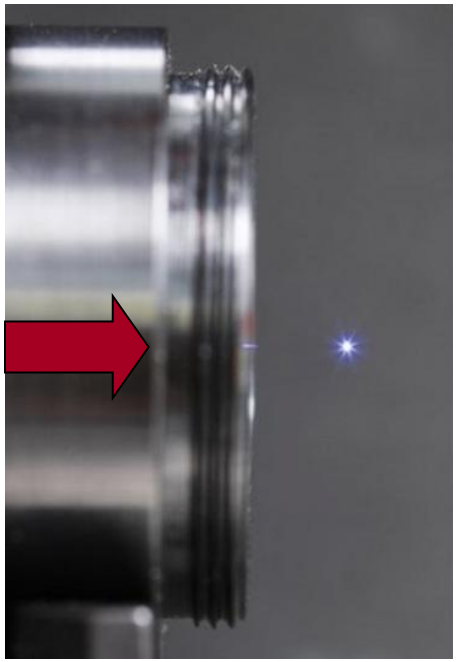

1963 Maker et al. observed plasma sparks when „giant“ ruby laser pulses were focused in air

Threshold 10^{12} W/cm^2

Name: „optical breakdown“

1964 Discovery of optical breakdown in liquids and solids

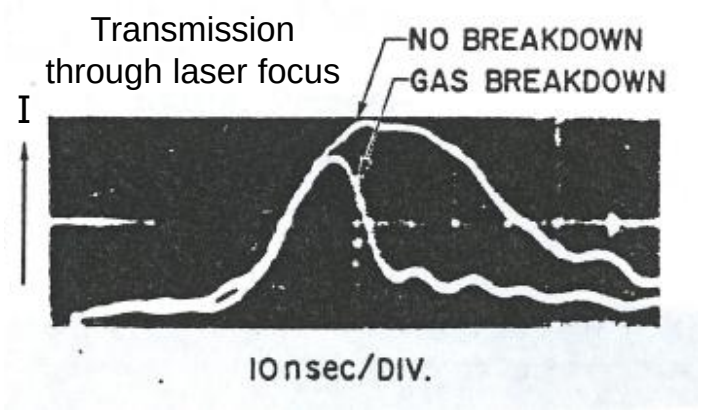

(Meyerand & Haught, Phys. Rev. Lett. 1964)

Optical breakdown = nonlinear absorption

Local energy deposition within transparent dielectrics becomes possible

Laser-lightning

Energy deposition by nonlinear absorption

($I \geq 10^{11}$ W/cm^2 $\Leftrightarrow$ coagulation: $\approx 10^3$ W/cm^2)

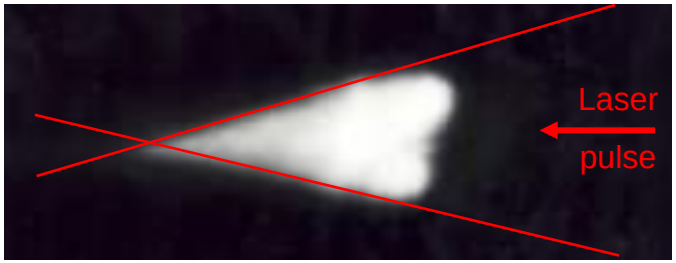

Large irradiance in laser focus leads to localized energy deposition via plasma formation („optical breakdown“)

$\Rightarrow$ The pulse duration must be short (≤ ns) to minimize the amount of deposited energy

Energy density in luminescent ns plasma:
$\approx$ 40 kJ/cm^3

Vaporization enthalpy of water: 2.6 kJ/cm^3
Energy density of TNT: $\approx$ 6.9 kJ/cm^3

DC breakdown

Devices and considerations for laser treatment

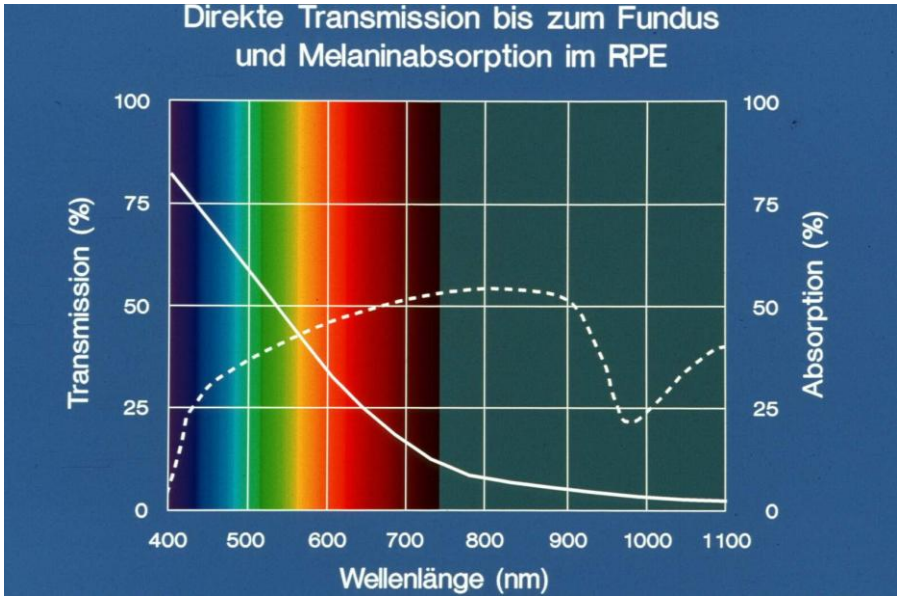

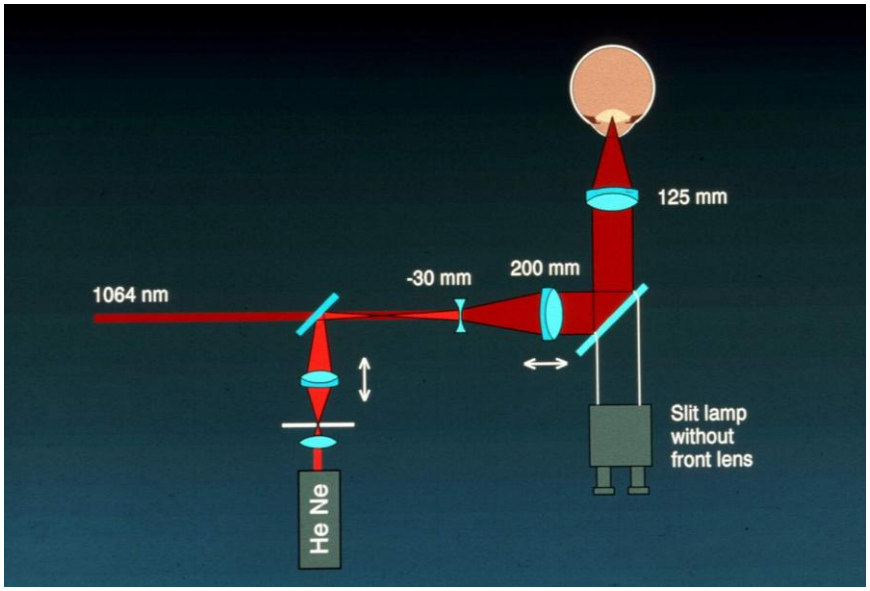

Plasma-mediated intraocular laser surgery

- ‘no hole’ surgery -

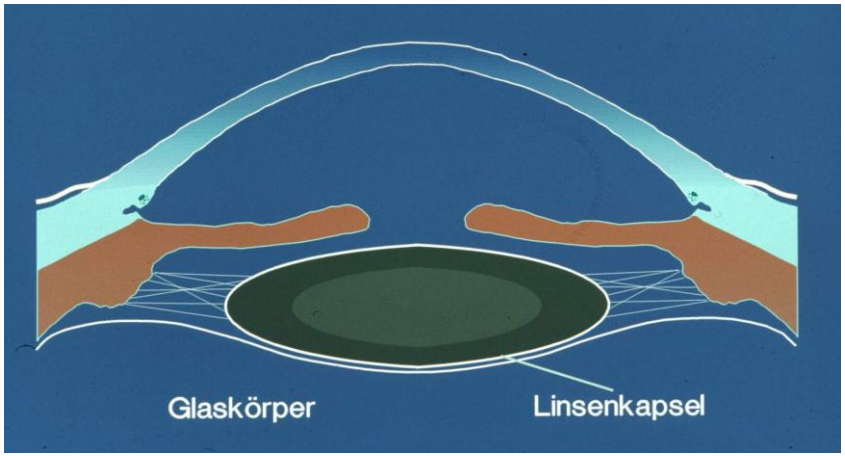

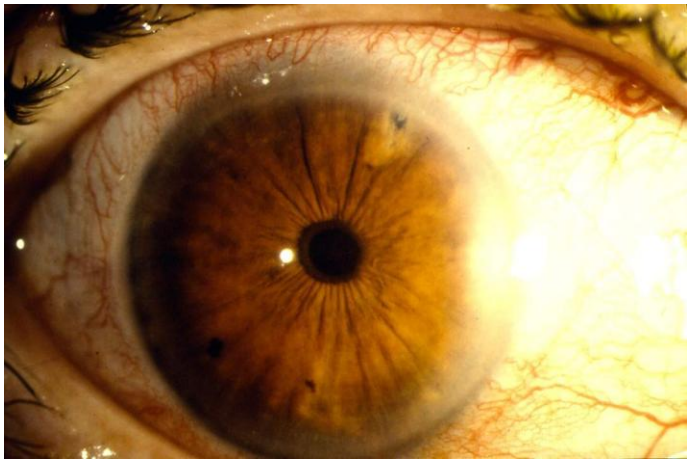

Iridotomy

Capsulotomy

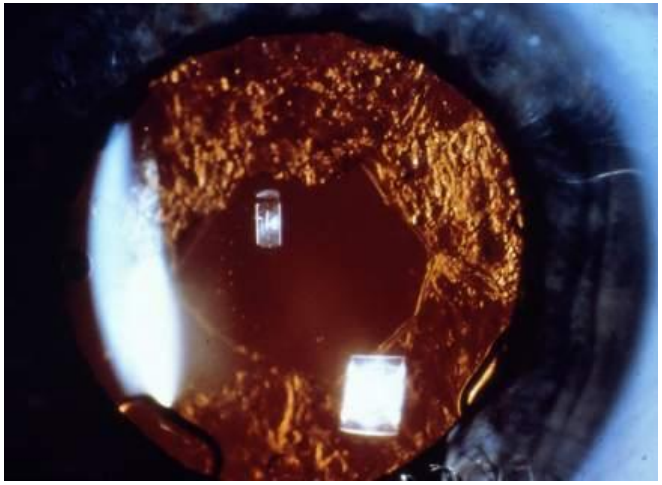

Dissection of a vitreal strand to stop retinal traction

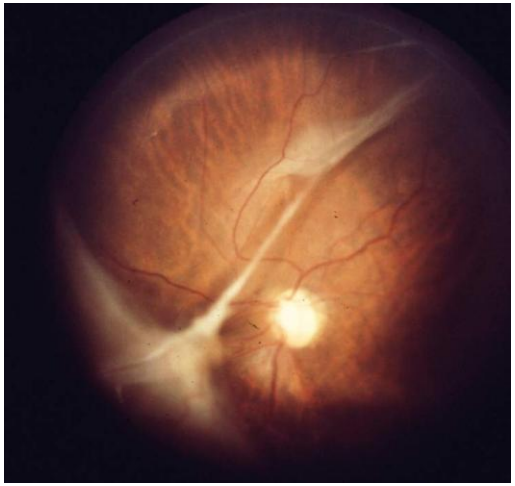

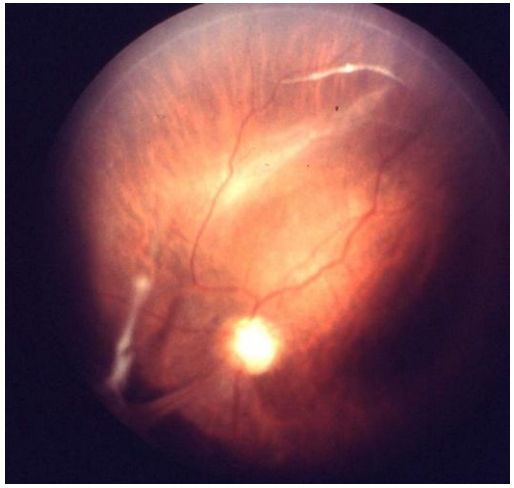

Dynamics of plasma formation (“Optical breakdown”)

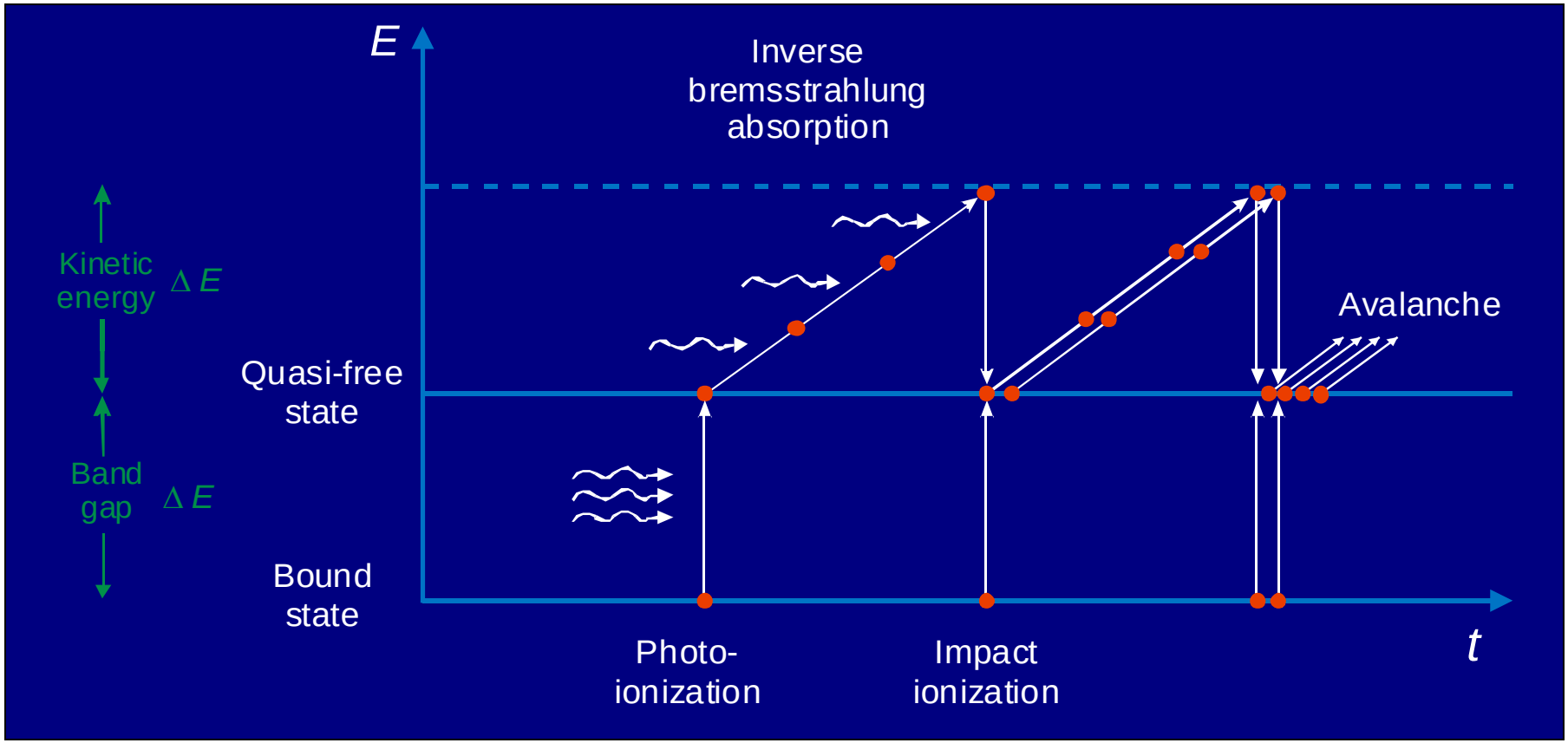

- Initial free electrons are generated by **photoionization** (multiphoton ionization or tunneling)
- Free electrons gain energy by „inverse bremsstrahlung absorption“ of photons
- When the free electrons have gained sufficient kinetic energy, they produce more free electrons by impact ionization $\Rightarrow$ **ionization avalanche**

Wavelength dependence of threshold portrays interplay of multiphoton and avalanche ionization

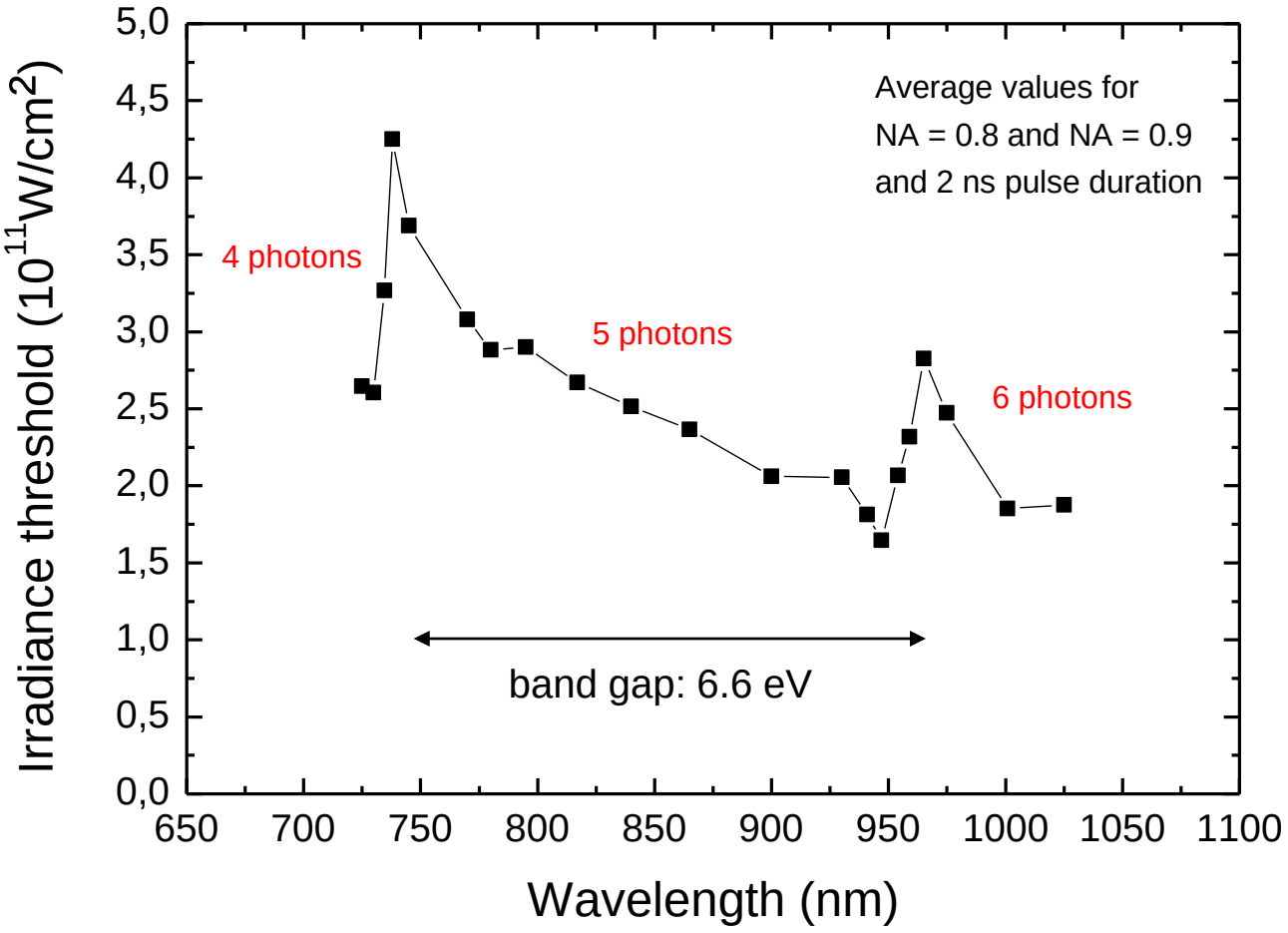

- Breakdown threshold increases with number of photons required for MPI
  - Rate of avalanche ionization increases with λ^2

Plasma grows above threshold by ‘breakdown wave’

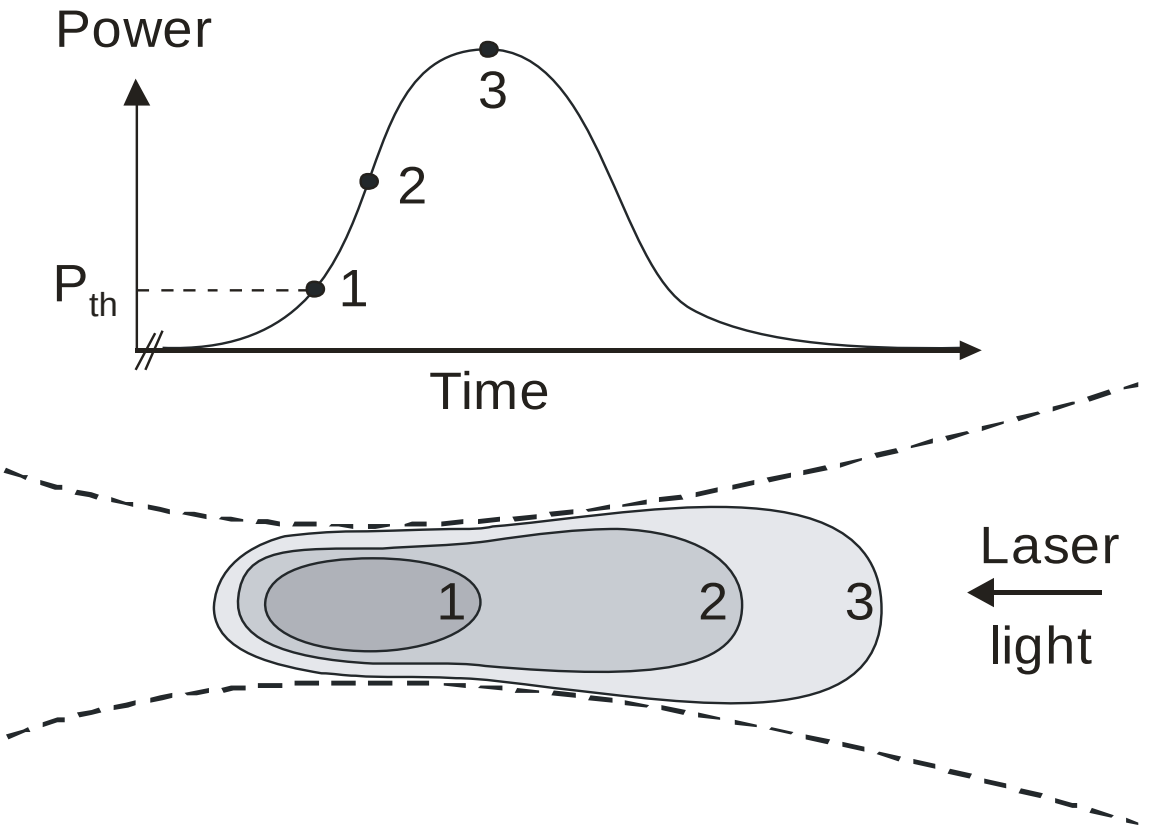

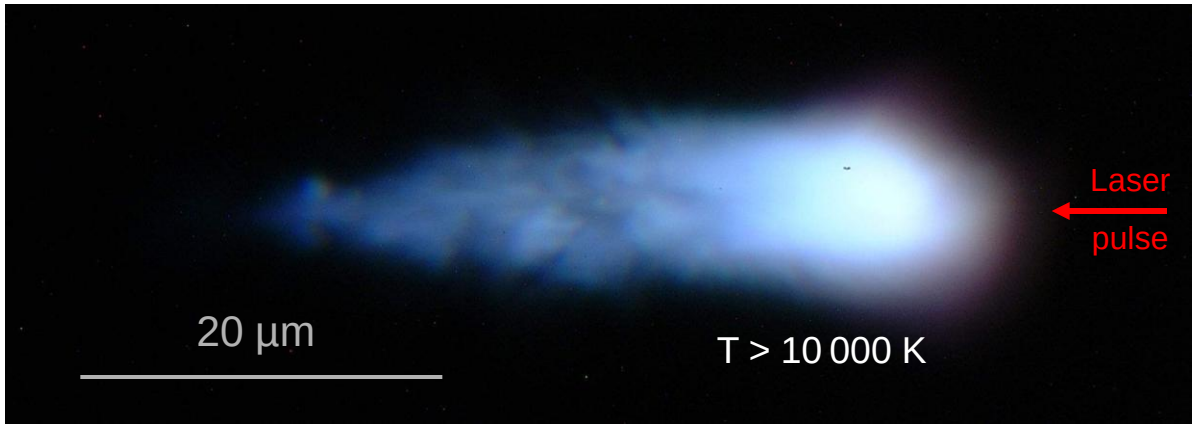

Shock wave emission

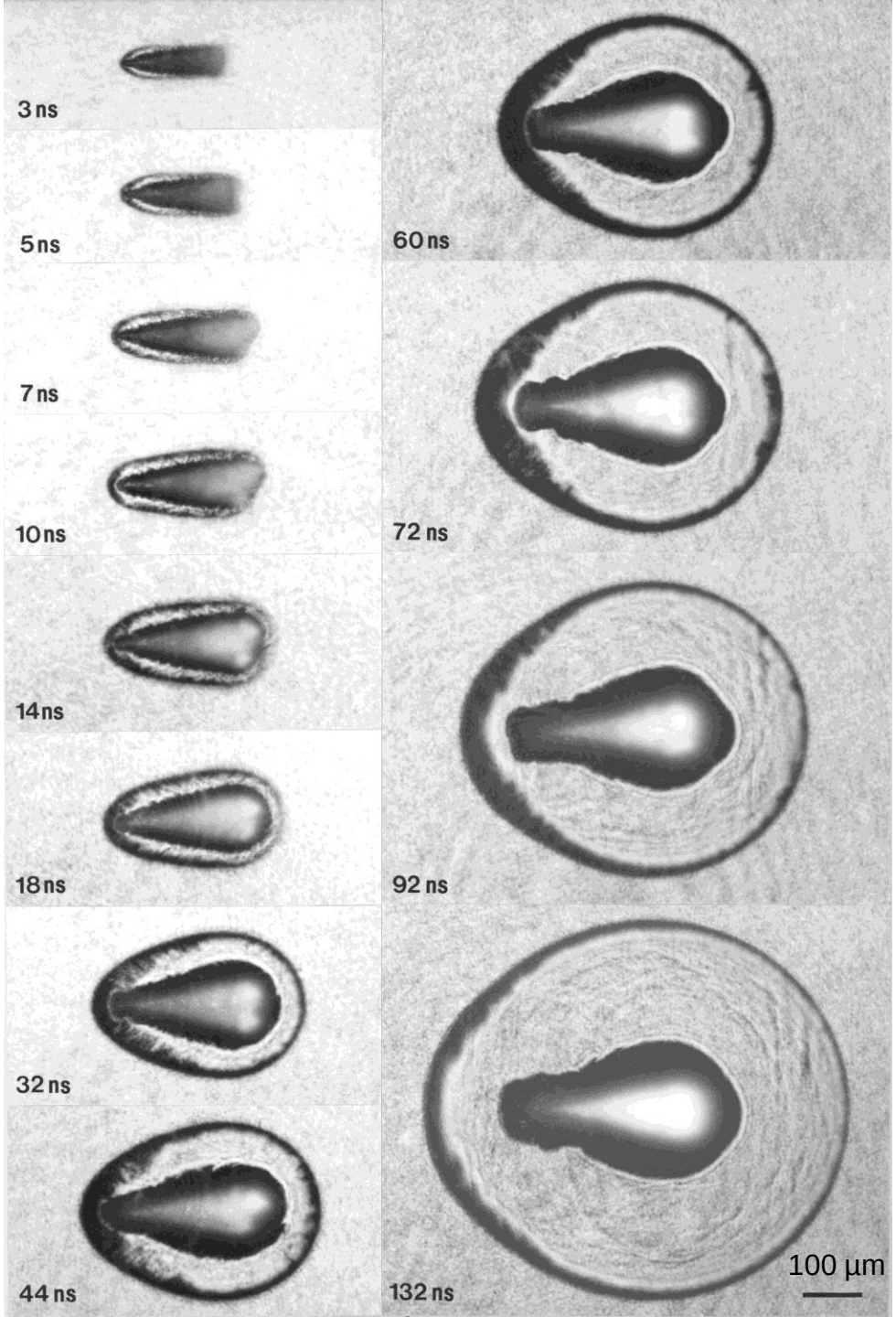

6 ns , 1064 nm, 10 mJ

Shock wave velocity and pressure

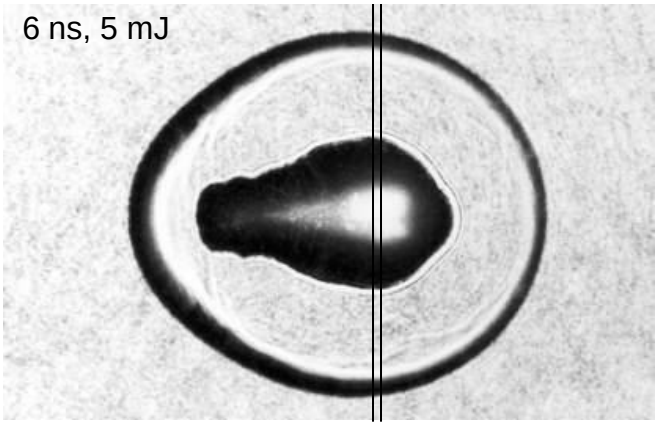

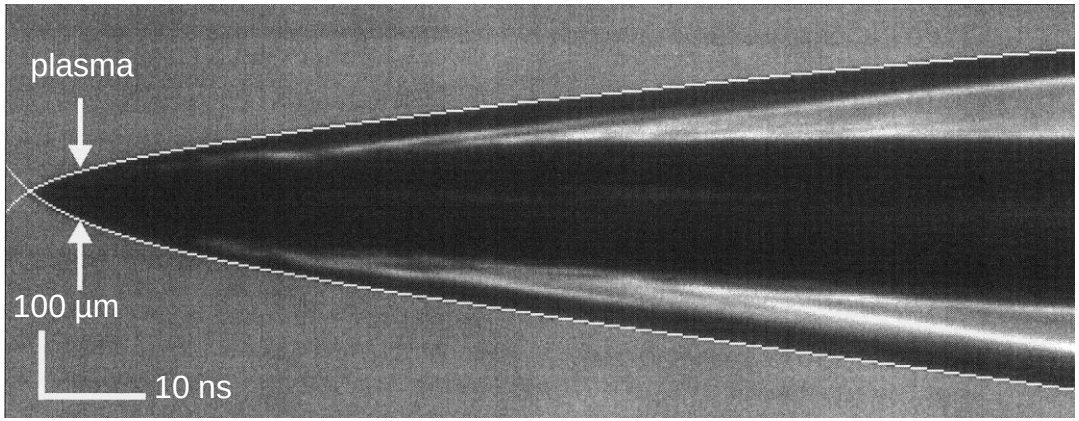

Shock wave velocity ⇒ shock wave pressure:

$$p_s = c_1 \rho_0 u_s \left(10^{(u_s - c_0)c_2} - 1\right) + p_\infty$$

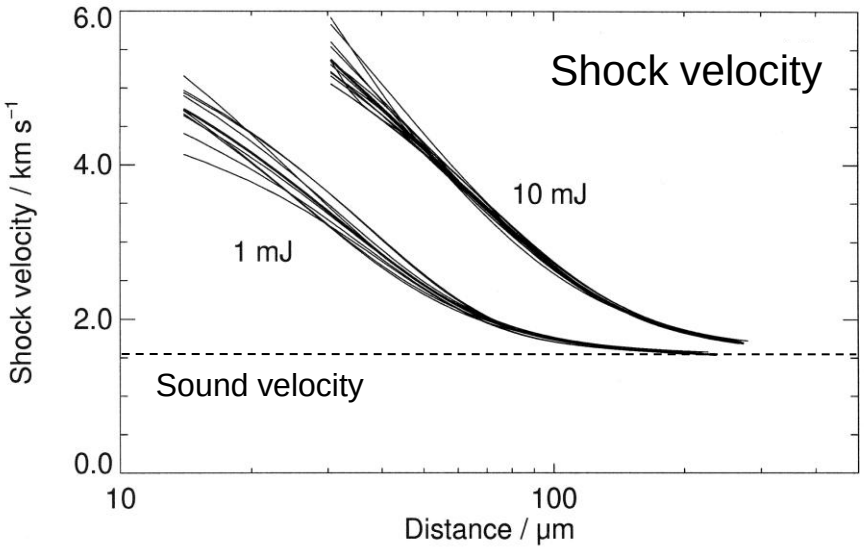

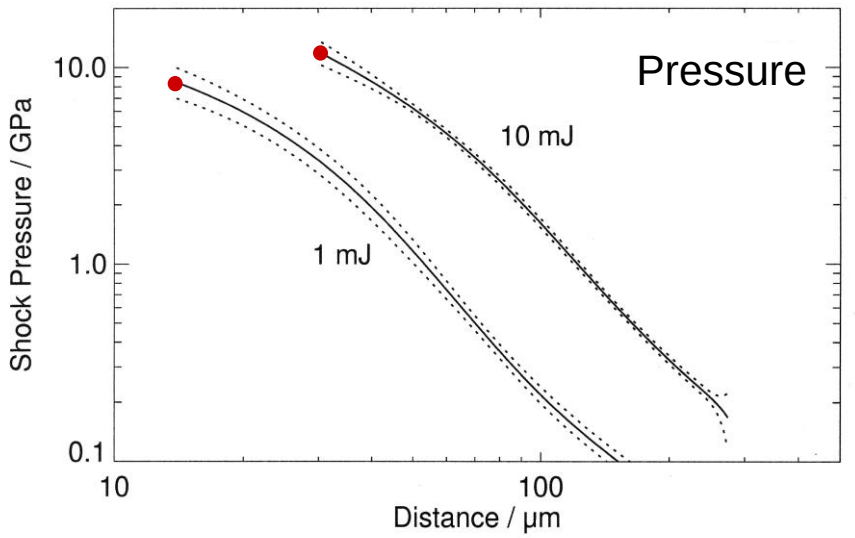

Initial pressure at plasma rim: ≈ 100 kbar

Cavitation bubble dynamics

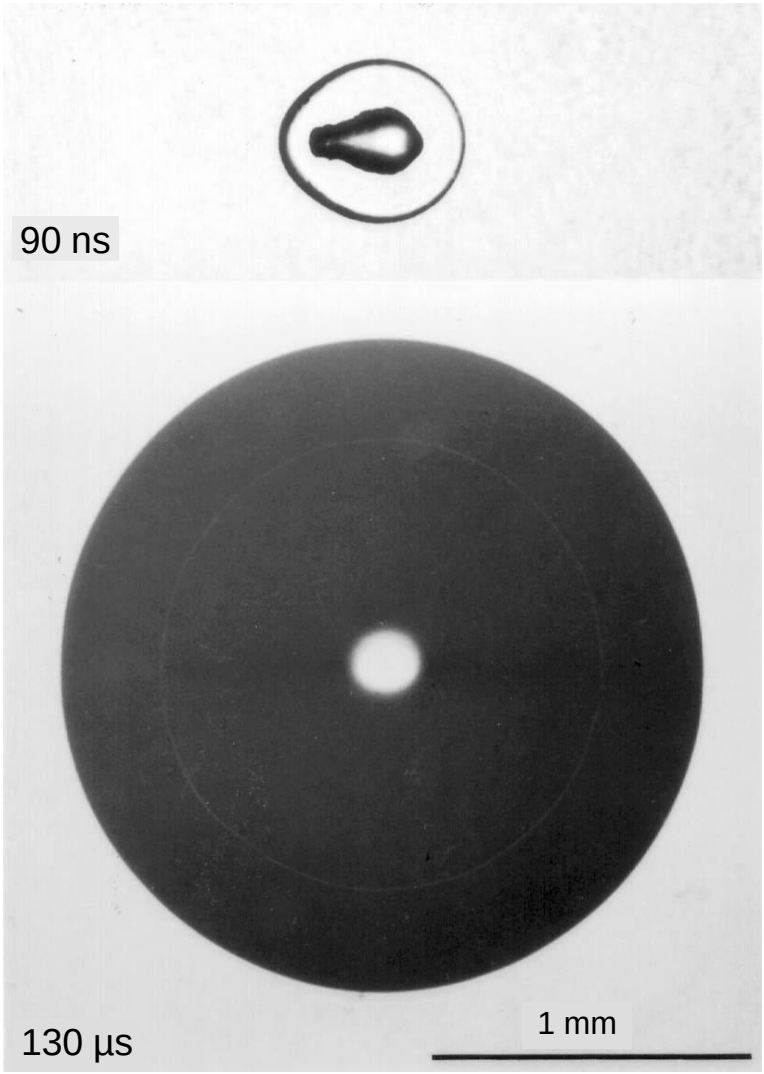

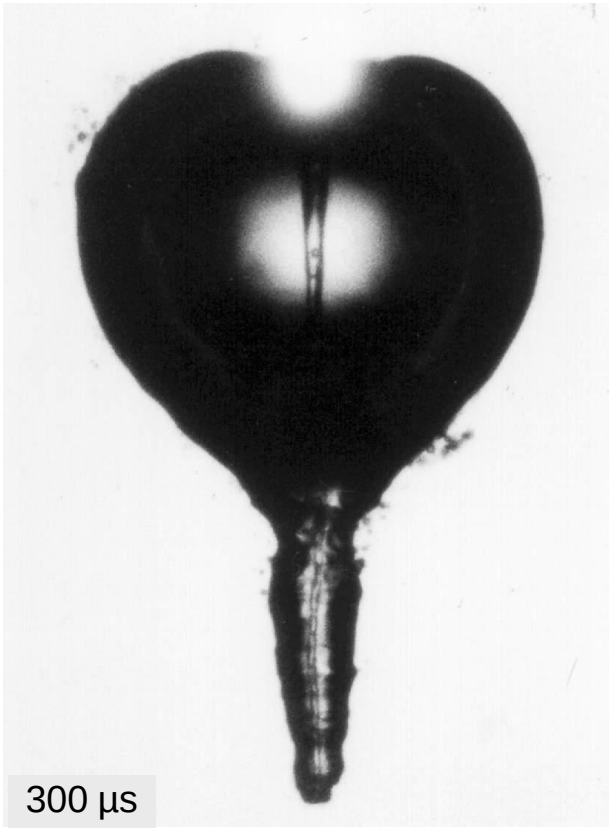

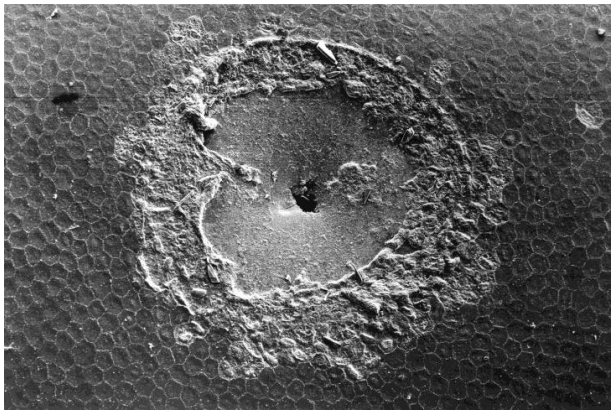

Expansion velocity > 500 m/s for 30-50 ns

Jet velocity: ≈ 100 m/s

IR ns breakdown is highly disruptive

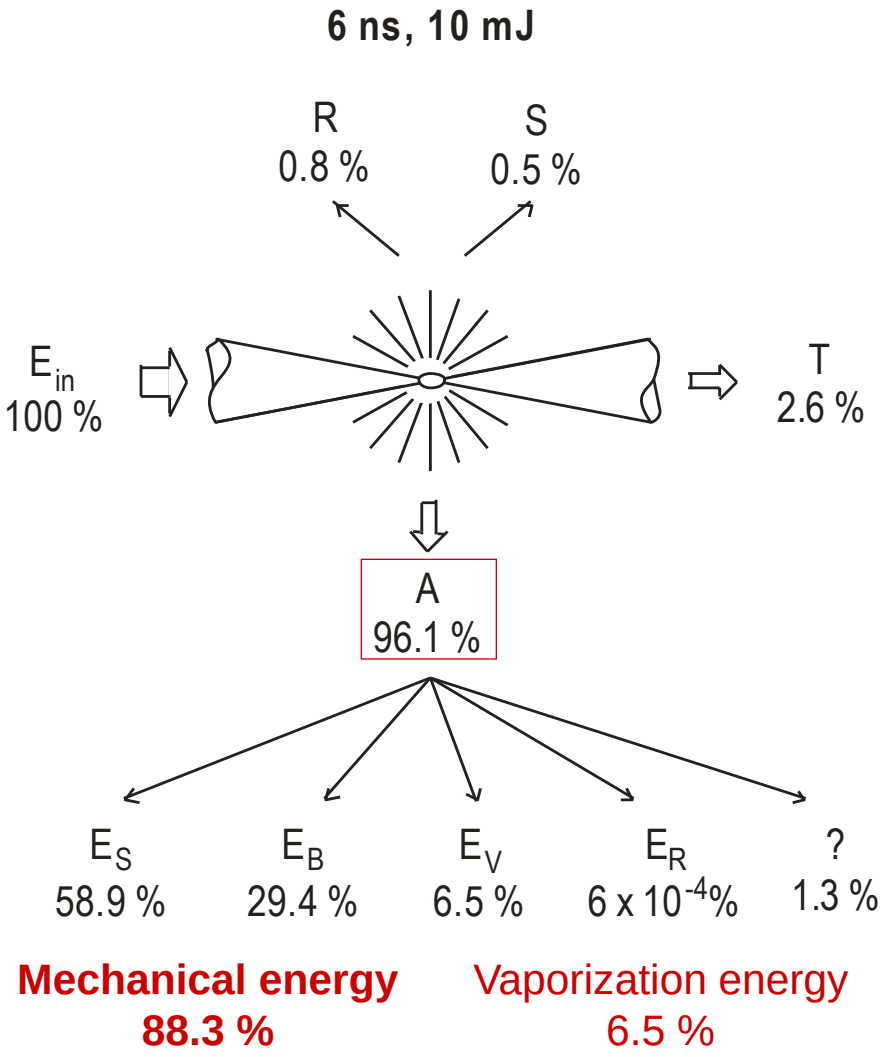

Ns laser pulse focused on corneal endothelium and Descemet's membrane

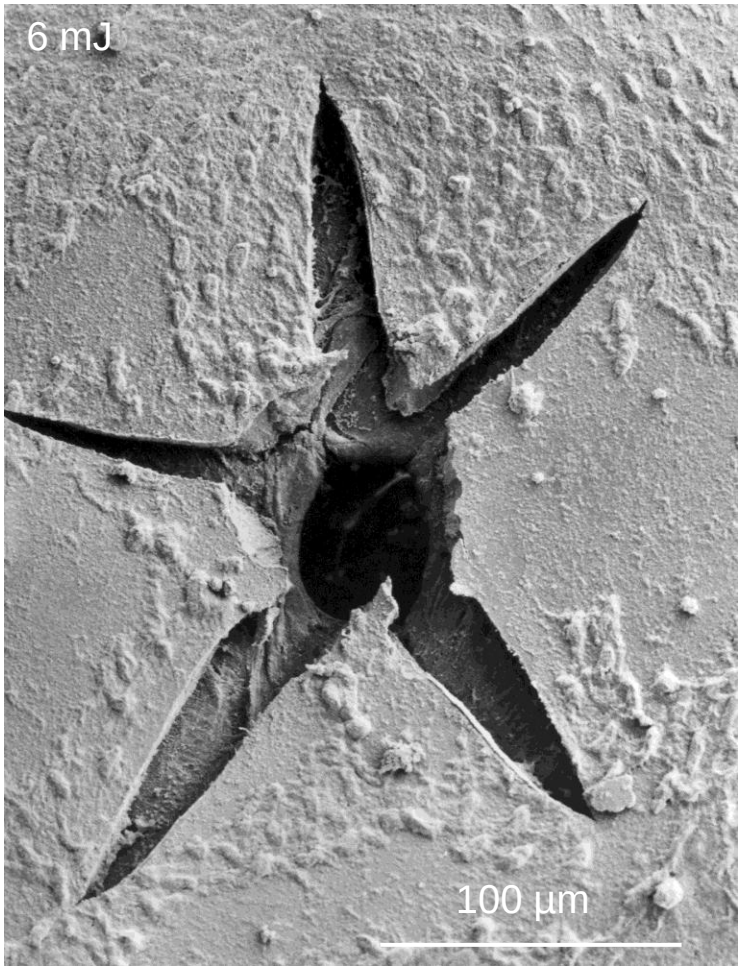

Tissue effects by shock waves

Short duration of shock wave (<20ns)

Elasticity of tissue

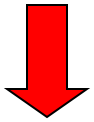

Tissue translations < 5 µm, no gross tissue effects

(They are caused by the cavitation bubbles)

but

possibly damage to cell organelles and membrane

and

Lose to plasma phase transitions at shock front

Tissue effects by plasma and bubbles

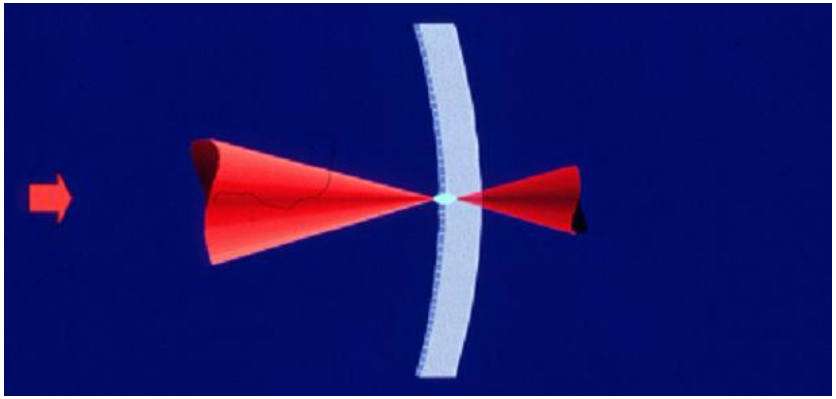

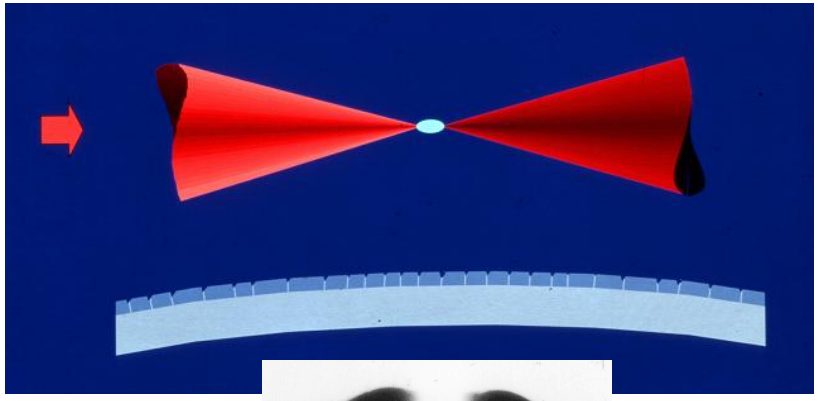

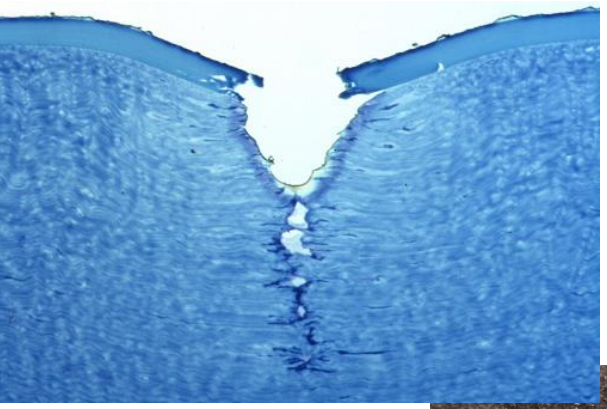

Disintegration of tissue within plasma volume

Jet Impact

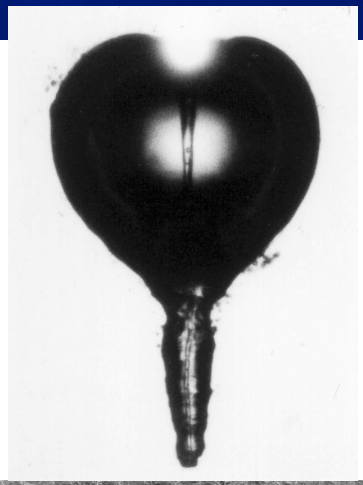

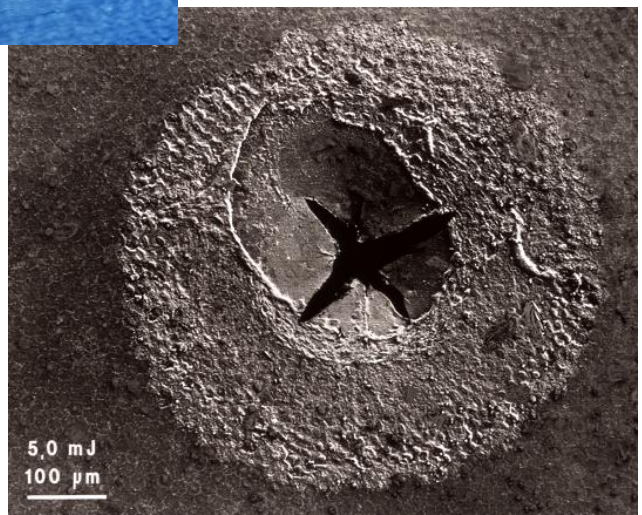

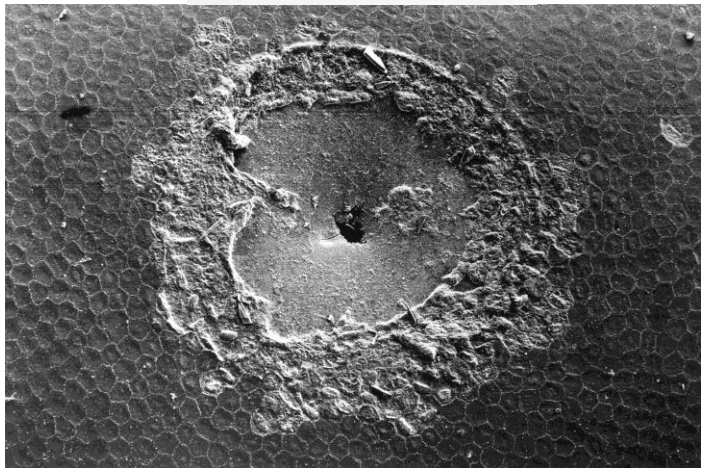

Strategies to minimize side effects

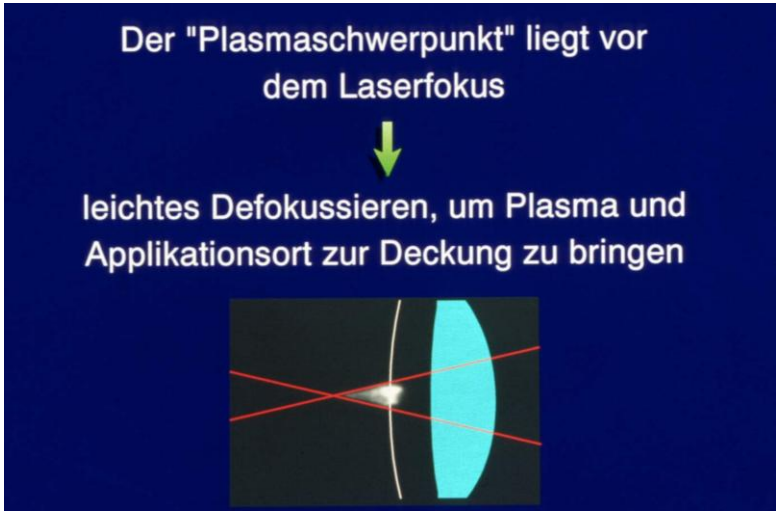

Correct placement of plasma center

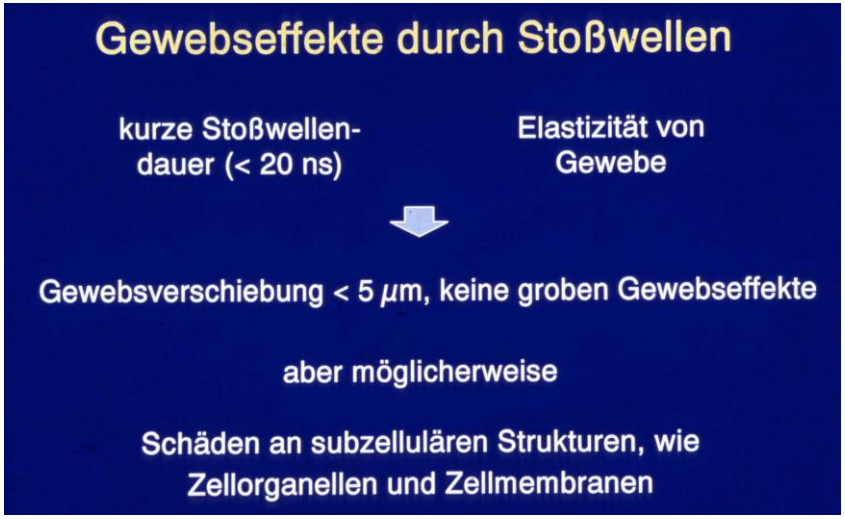

Small pulse energies to minimize collateral damage

Capsulotomy

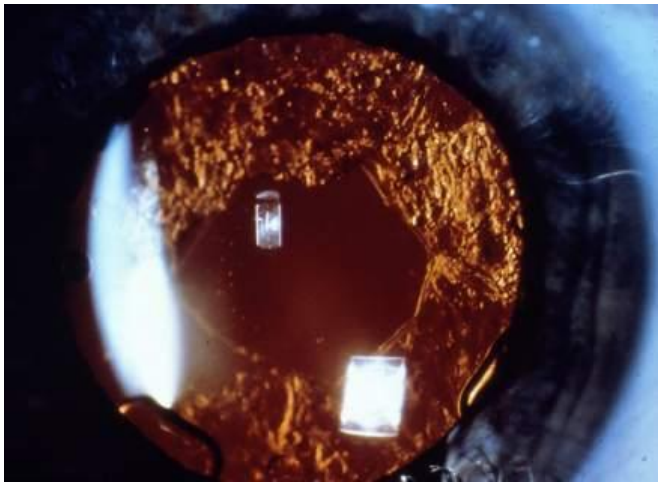

Dissection of vitreoretinal strands

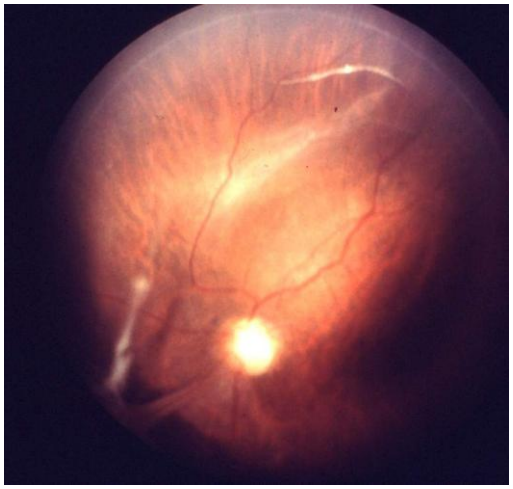

Parameter optimization (1)

Verringerung von Nebenwirkungen

Lokalisierung der Effekte durch

- möglichst kleine Pulsenergie
  (Schadensreichweite ∝ (Laserpulsenergie) $^{1}/_{3}$
- möglichst kompakte Laserplasmen

Parameter

- Fokussierungswinkel
- Lasermode
- Pulsdauer

TEM multimode laser beam

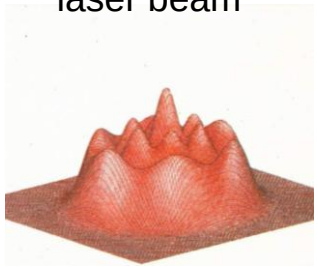

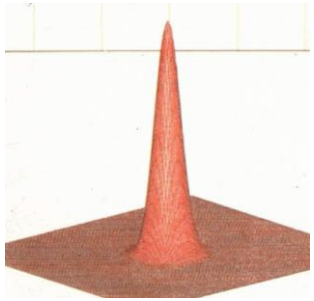

TEM (0/0) single mode laser beam

Multiple plasmas

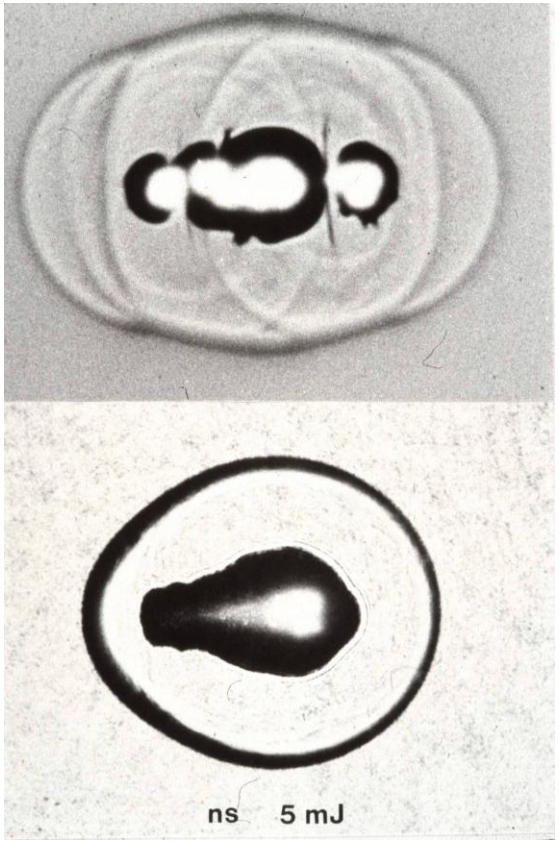

Well localized single plasma

Parameter optimization (2)

Erhöhung der Präzision durch großen Fokussierungswinkel

Vergrößerung des Fokussierungswinkels bewirkt:

- Verkleinerung des Fokusdurchmessers
  ⇒ Plasmabildung bei geringerer Pulsenergie
- kompaktere Plasmen
- geringere Lichtbelastung vor und hinter dem Fokus

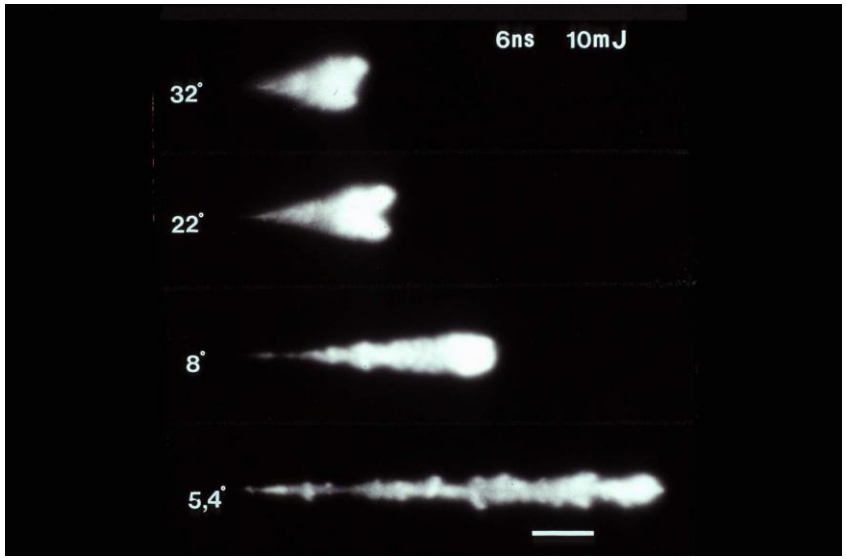

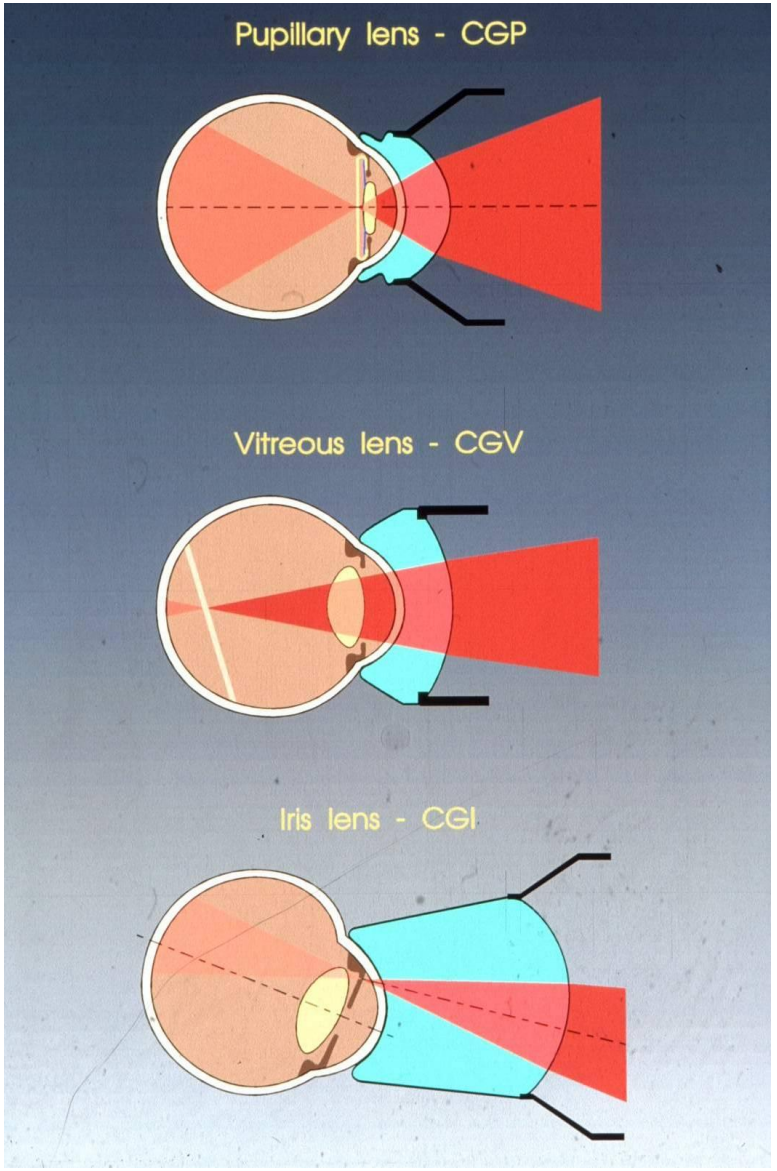

Shorter pulses ⇒ higher precision

Reduction of pulse duration
from ns to fs :

⇒ Lower energy threshold
for optical breakdown

⇒ Finer tissue effects

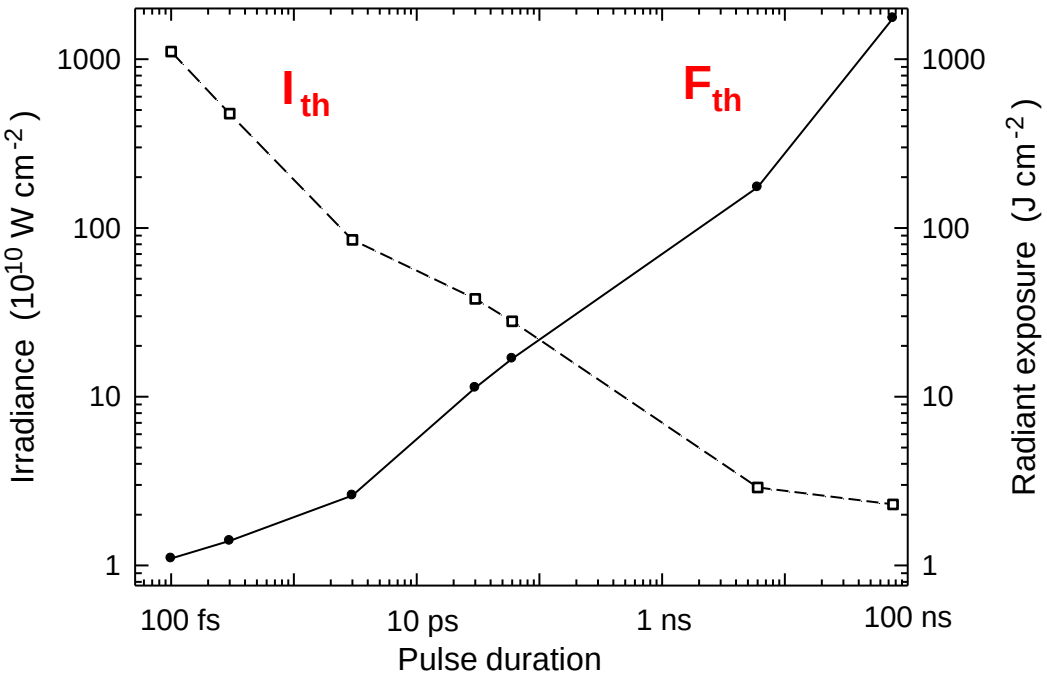

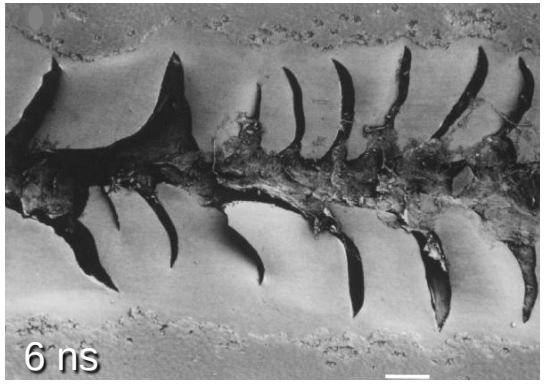

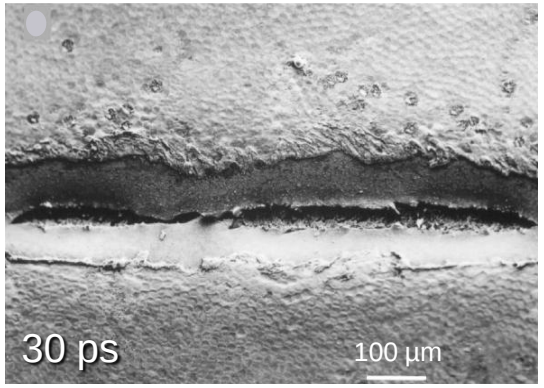

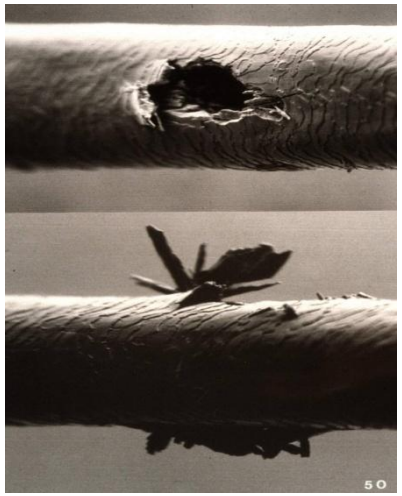

Iridotomies produced using different laser pulse durations

6 ns, single exposure

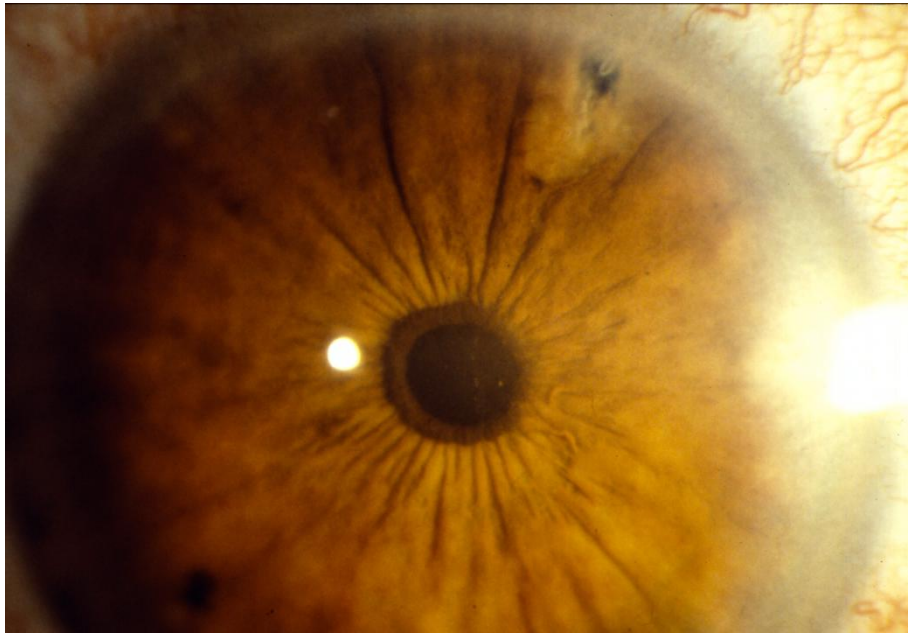

40 ps, many pulses

Flap cutting for corneal refractive surgery

Correction of myopia...

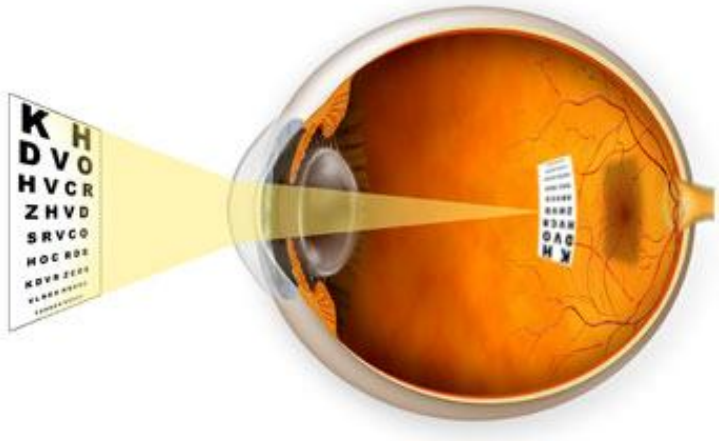

... by ArF excimer laser ablation

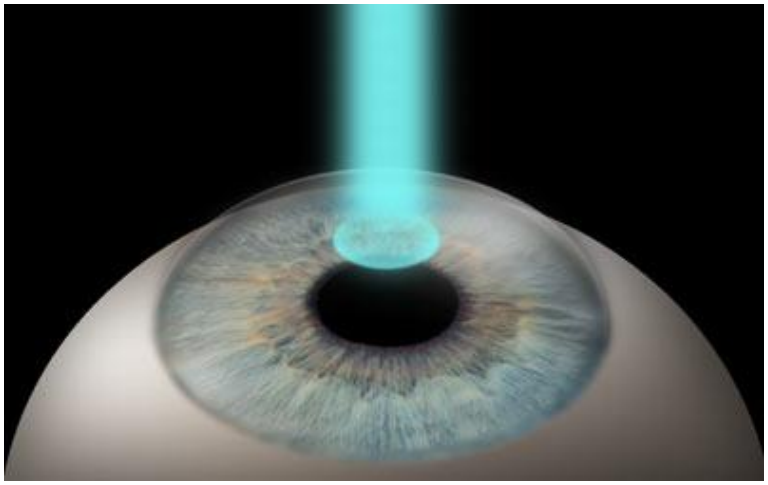

Traditional Flap generation for

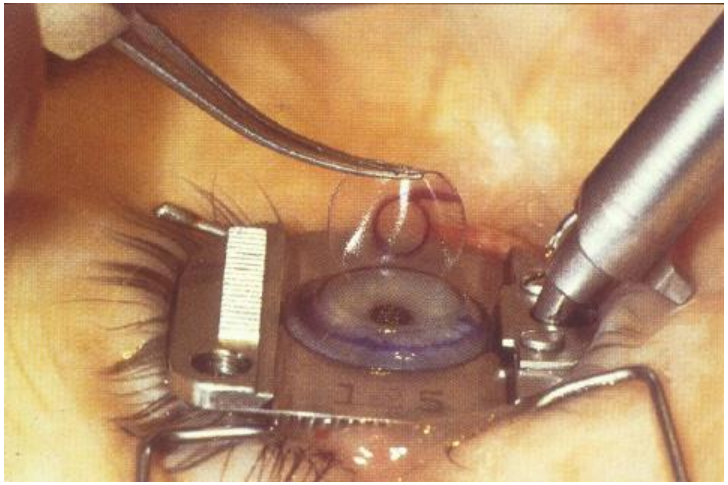

Fs Flap generation (large NA)

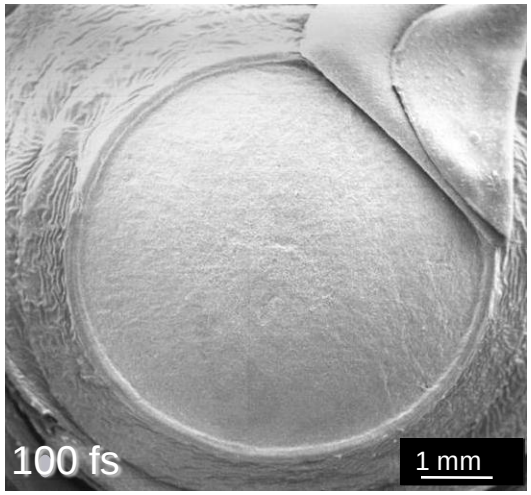

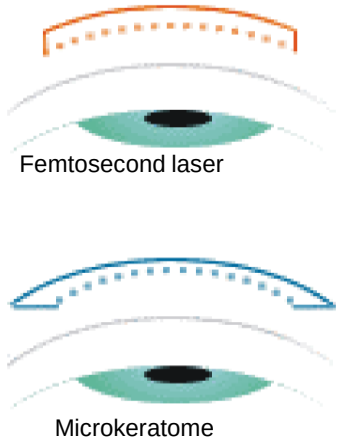

Methods of refractive femtosecond laser surgery

Fs Flap generation for ArF-laser LASIK

Fs-keratome:

Reproducible flap thickness

Freedom in cutting geometry
⇒ flap can be designed for precise re-positioning after ArF laser surgery

! important for wavefront-guided surgery !

Lenticule cutting and removal

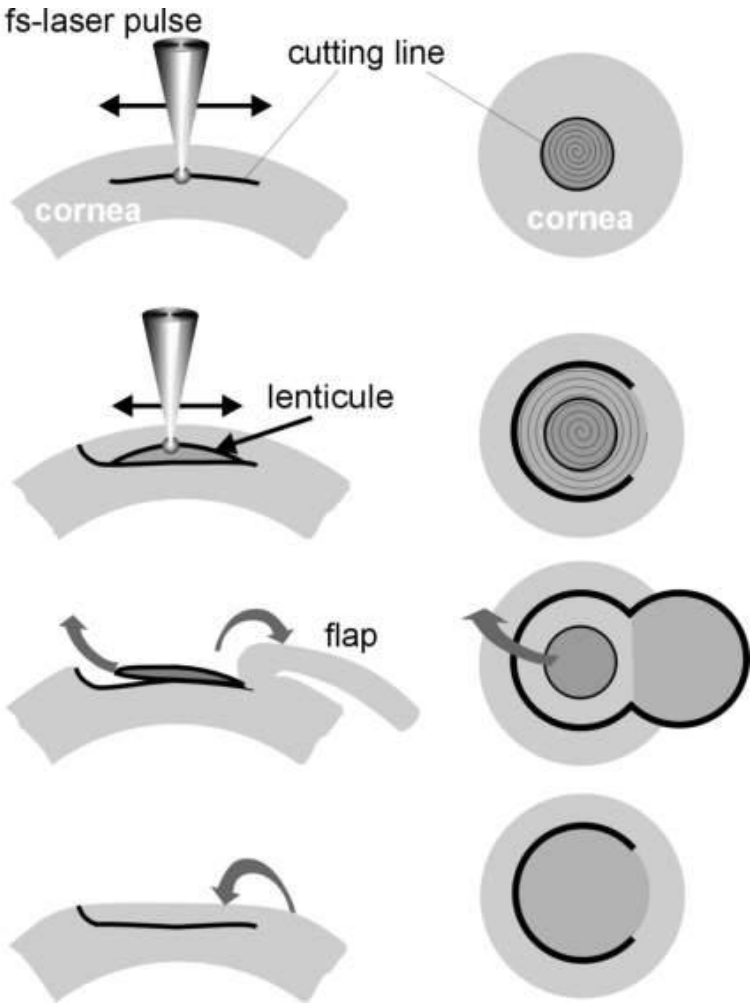

History of LASIK (Video)

Bis hierher klausurrelevant.

Das Folgende ist Zusatzmaterial

Principal requirements for controlling the laser lightning

- Small aberration-free laser focus
- Precise and smooth tunability of deposited energy
- Good pulse-to-pulse reproducability

In which part of the parameter space
of pulse duration and laser wavelength
can these requirements be fulfilled?

Have another careful look (after 40 years of research on optical breakdown),
both on an experimental and a theoretical level !

Experimental requirements

Laser

- Excellent beam quality (temporal and spatial)

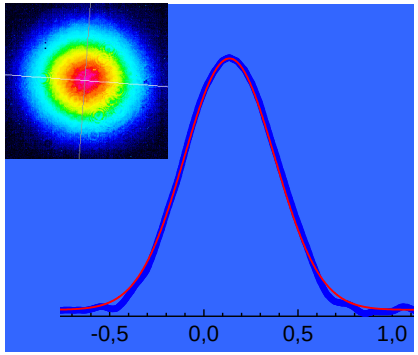

Setup

- Tight focussing (large NA), to achieve a small focus suitable for the creation of nanoeffects
- Aberration-free focussing in spite of large NA (UV-VIS-IR water immersion-objectives)
- Water as breakdown medium (less impurities than in solids)

Breakdown criterion

- Bubble formation instead of plasma luminenscence (sensitive, well defined, easily detectable)

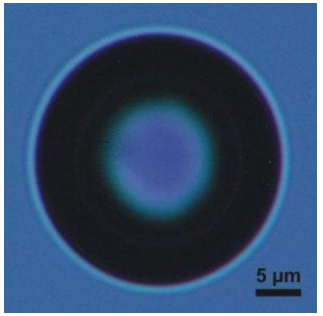

Pulse shapes of Nd:YAG ns-laser pulses

- regular versus Gaussian (slm) pulses -

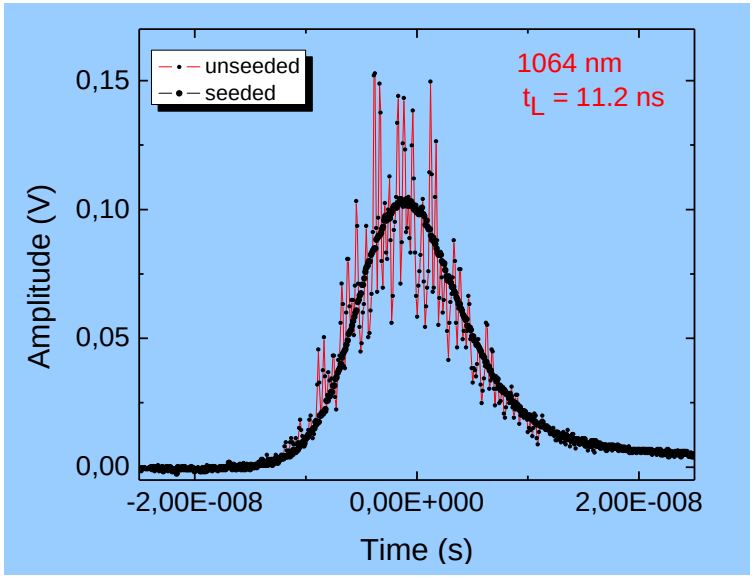

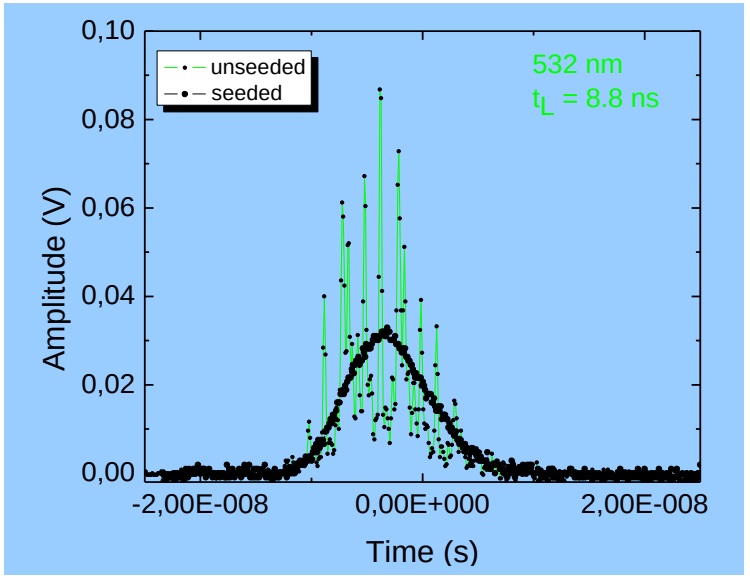

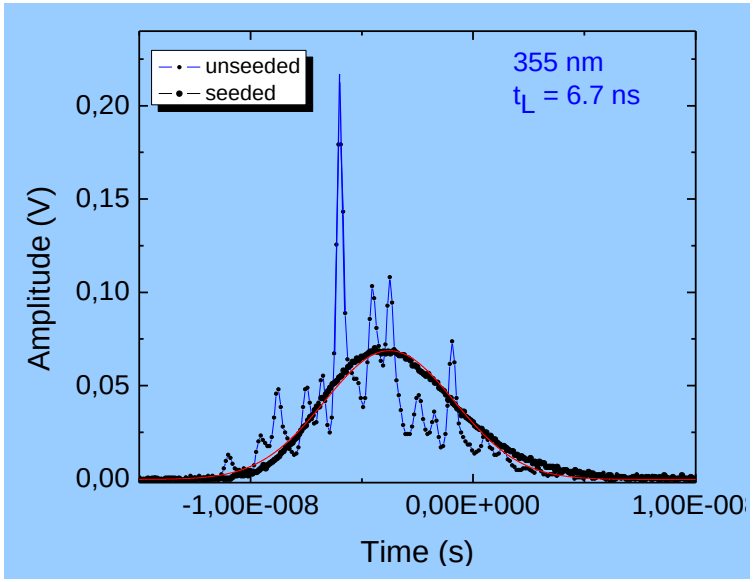

Smooth pulse shape
$\Rightarrow$ good reproducability

Plasma generation by smooth ns pulses is “deterministic”, similar to femtosecond breakdown!

Bubble detection & determination of bubble size

- Theory predicts (at threshold) bubble diameter < 200 nm

  (Appl Phys B 81:1015-1047, 2005)

⇒ Bubble detection via light scattering

(Phys. Rev.Lett. 100:038102, 2008)

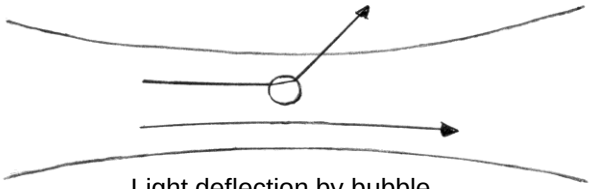

Light deflection by bubble

- Determination of bubble radius R_{max} by measuring the bubble oscillation time T

- Minimum detectable radius

  photographs: ≈ 850 nm

  Scattering technique: < 50 nm

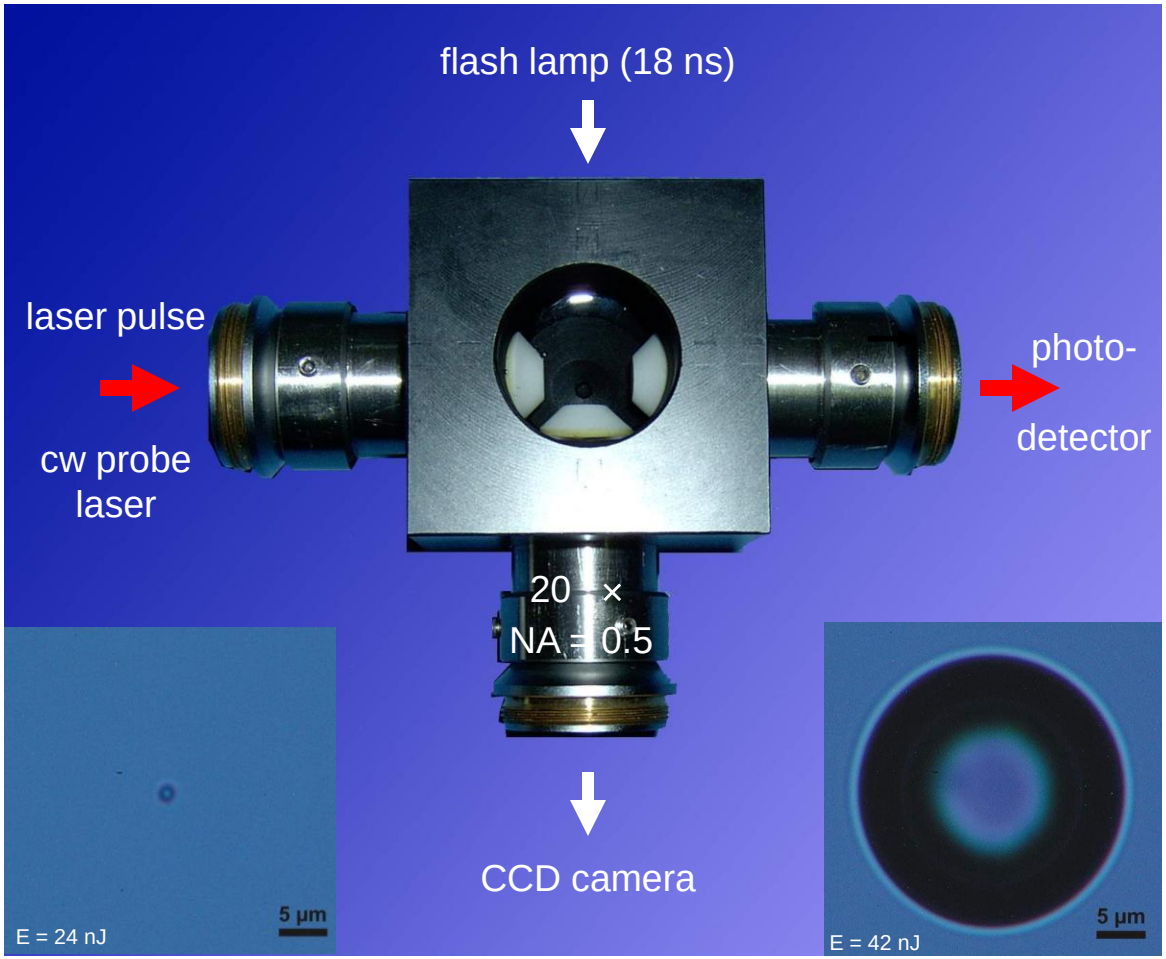

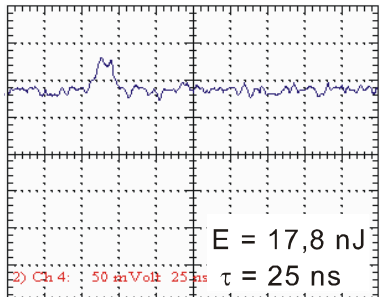

$$R_{max} = \frac{T}{1.83}\sqrt{\frac{p_0 - p_v}{\rho_0}}$$

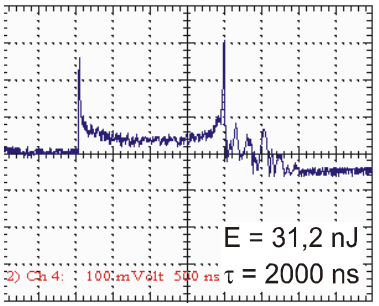

Bubble size for fs pulses and ***regular*** ns pulses

(40x, NA = 0.8)

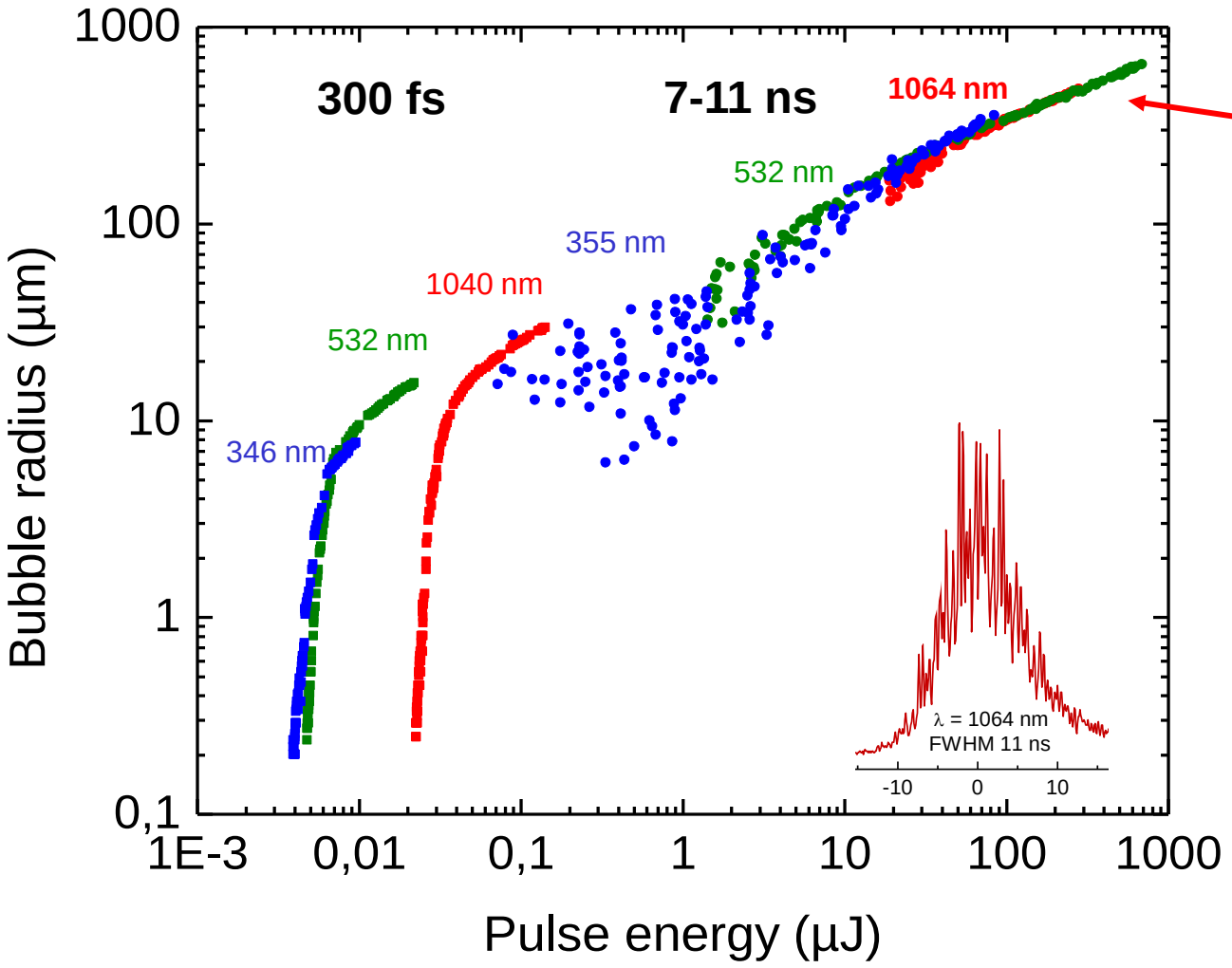

Regime for capsulotomies & iridotomies

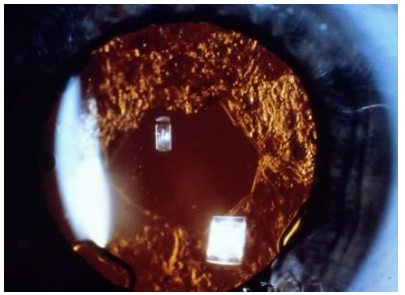

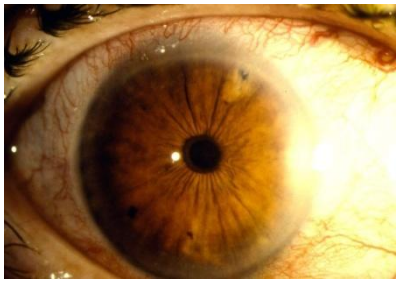

Fine femtosecond-effects ⇔ Gross nanosecond-effects

"deterministic" ⇔ "stochastic"

Stepwise breakdown with ***smooth*** UV ns pulses

355 nm, 6.8 ns, 40x, NA = 0.8

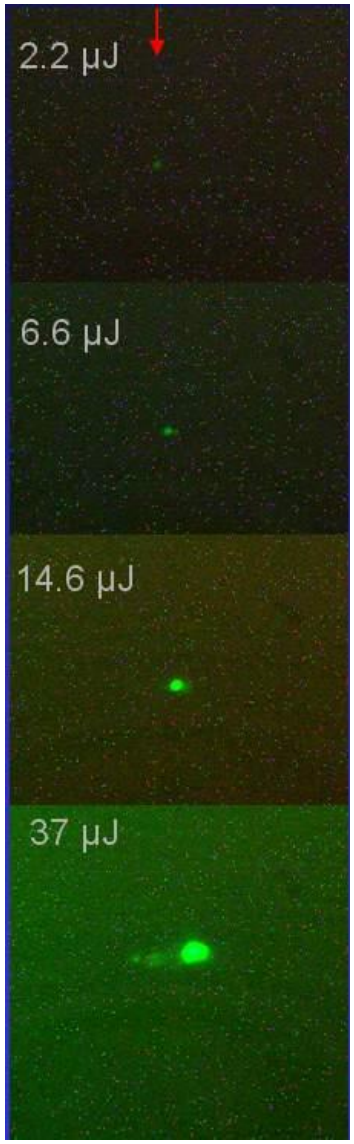

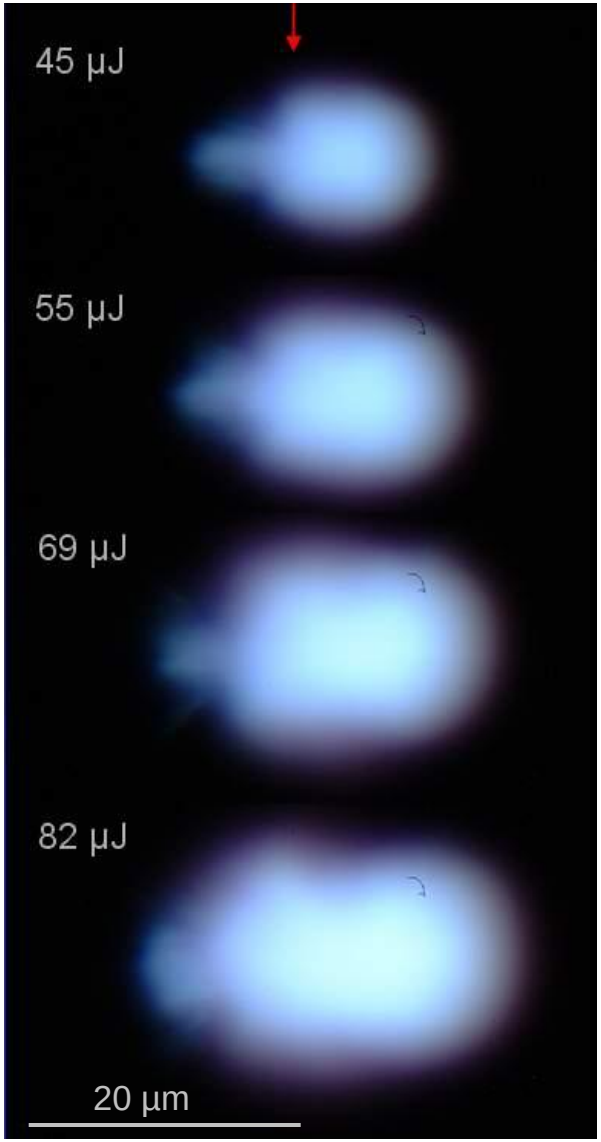

Bubble- and plasma size

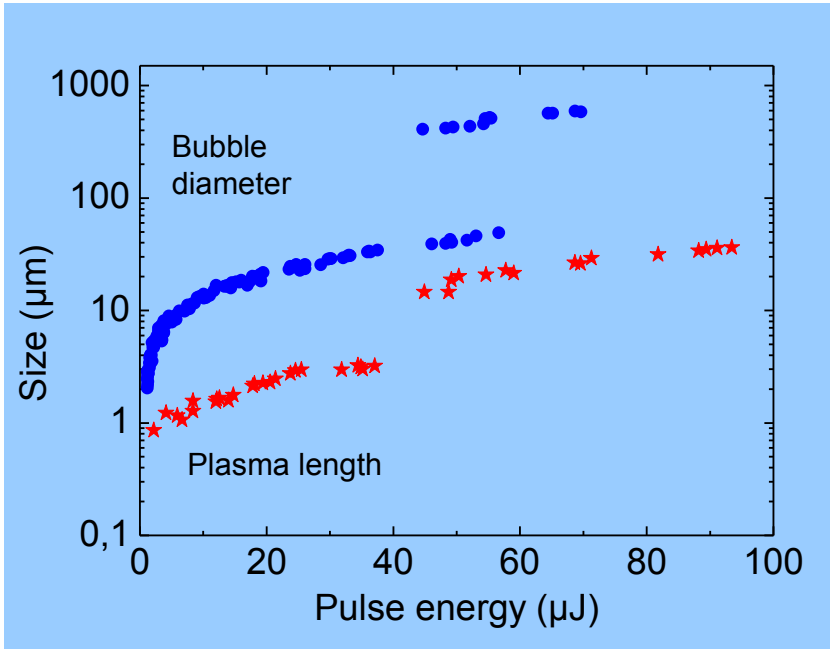

Energy and pulse duration dependence of bubble size

(40x, NA = 0.8, Gaussian ns pulses)

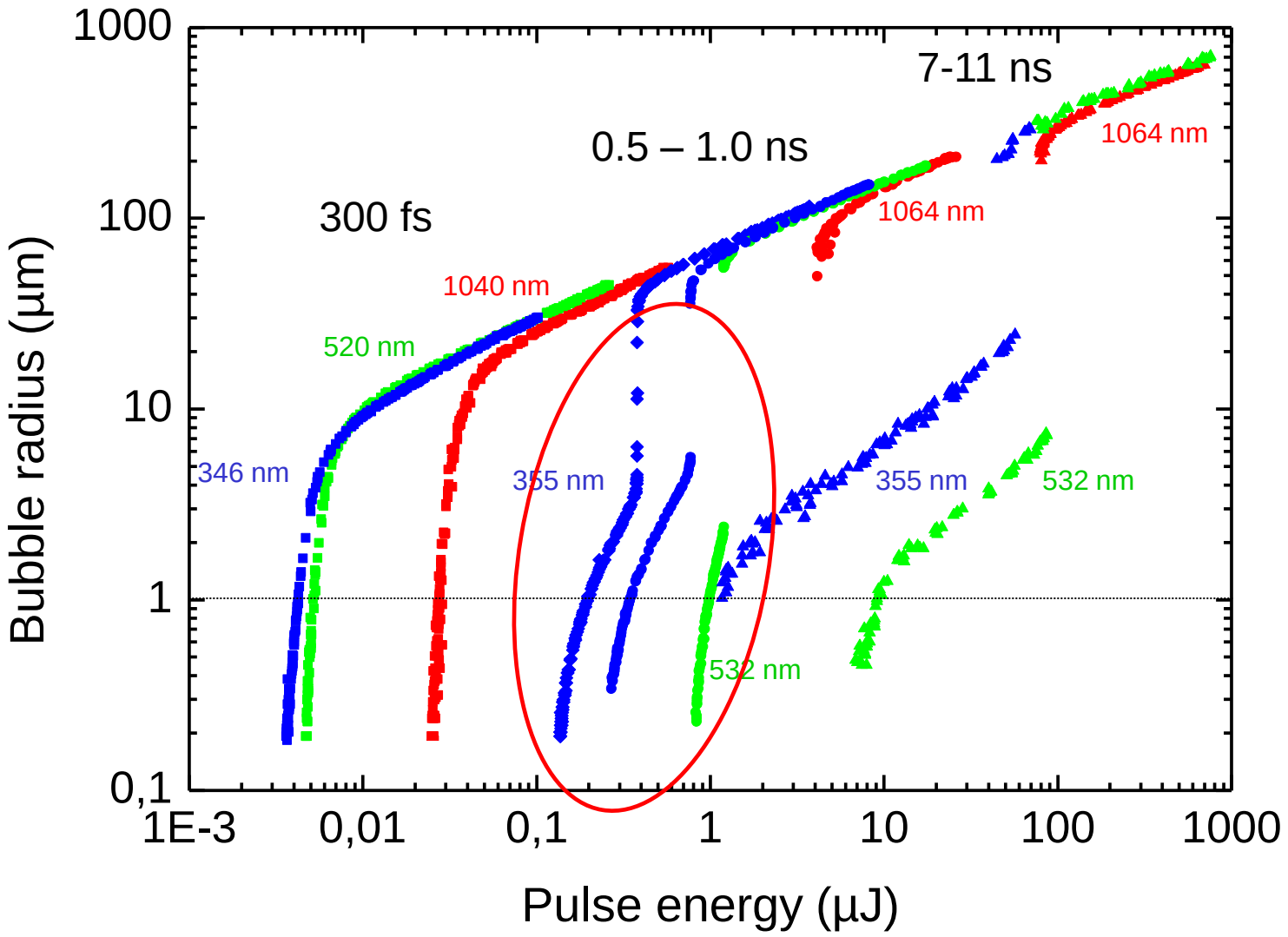

Microchip lasers can do what could previously be achieved only by using expensive femtosecond lasers !

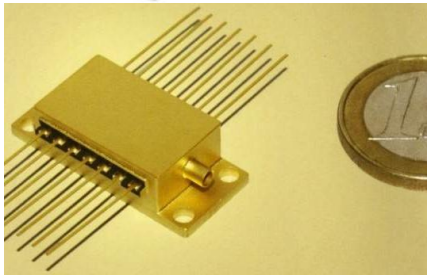

Bundesrepublik Deutschland
Deutsches Patent- und Markenamt

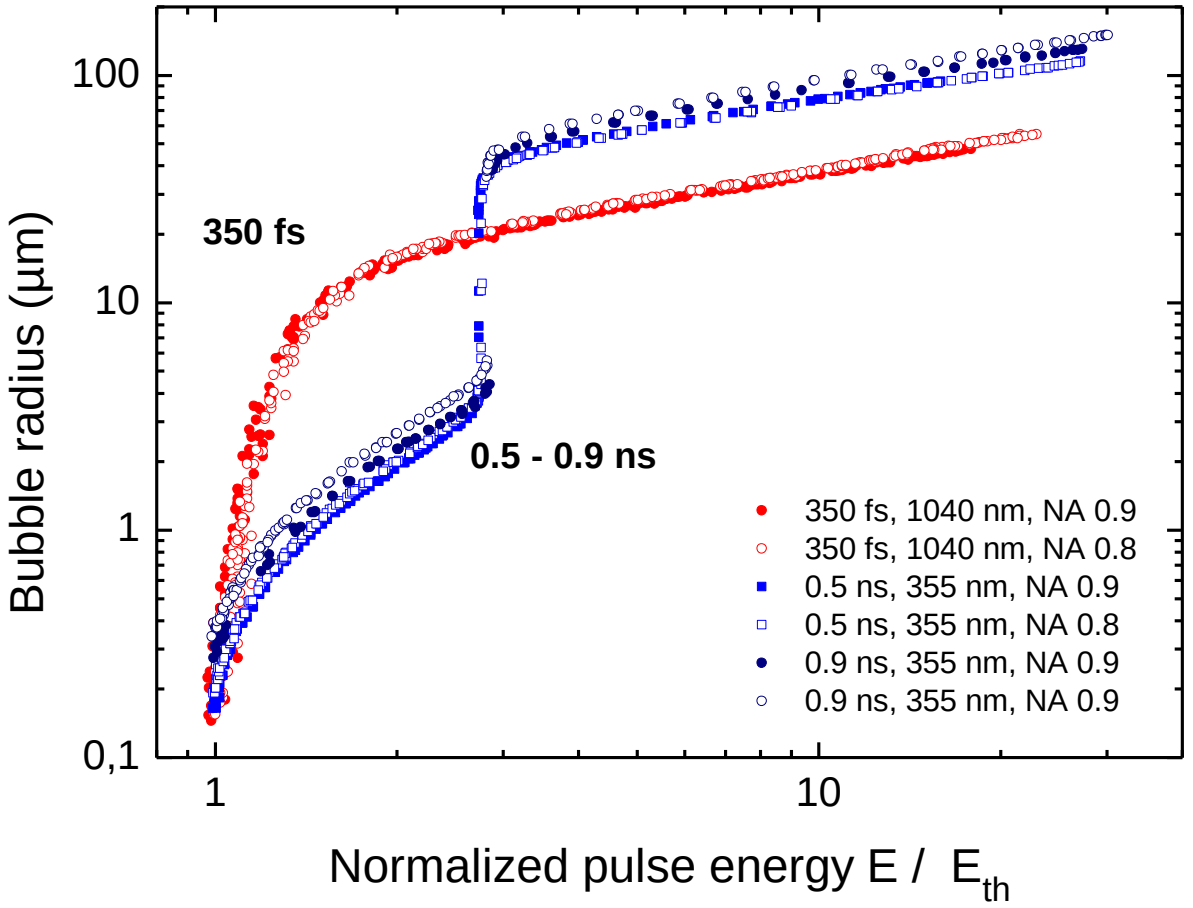

The small-bubble regime is larger with ns pulses than with fs pulses

⇒ Good tunability of laser effects

Can we utilize the new level of understanding
of nonlinear energy deposition
for improving medical technology ?

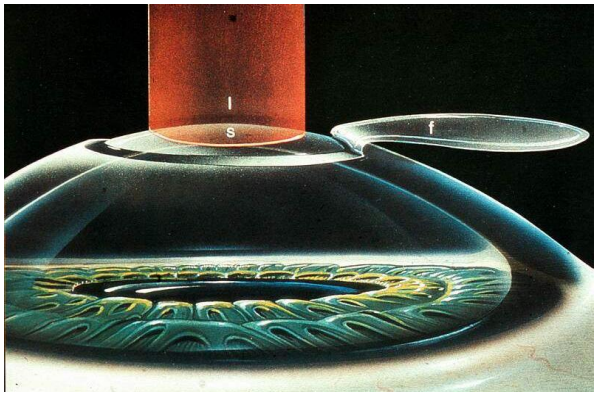

Flap creation in refractive surgery (LASIK)

Mechanical keratome

- one cutting pattern
- precision & complication rate depends on surgeon's skills
- small
- cost-effective

Femtosecond laser

- various cutting patterns
- high precision & reproducability
- few complications
- bulky
- expensive

New approach for flap creation

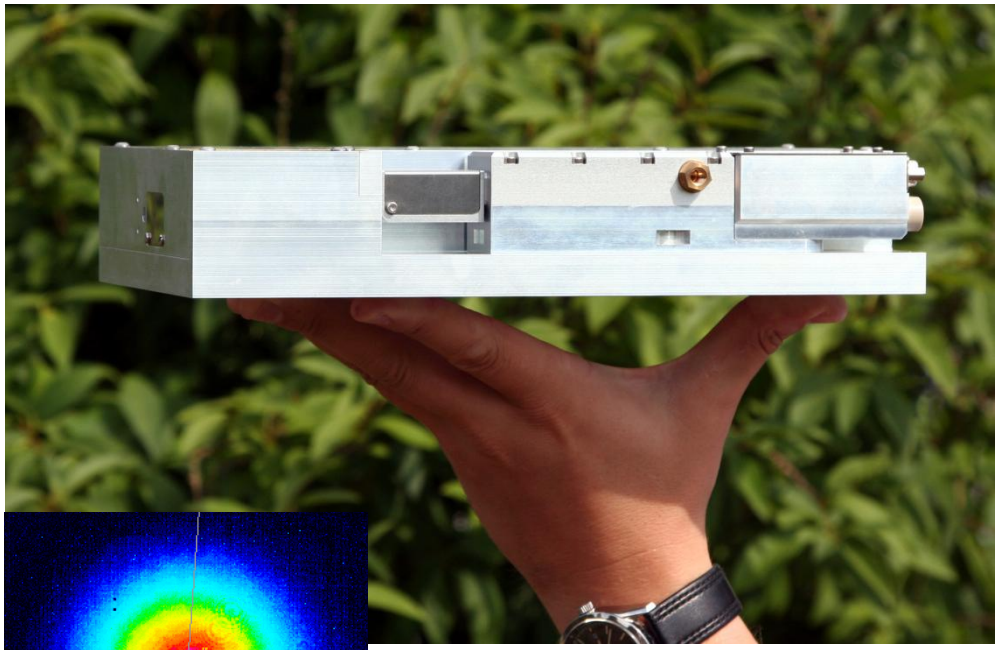

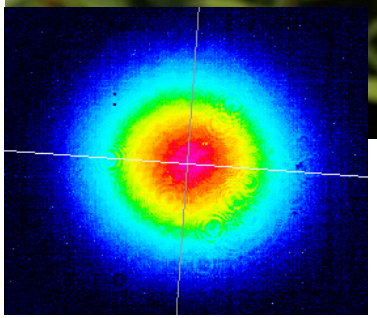

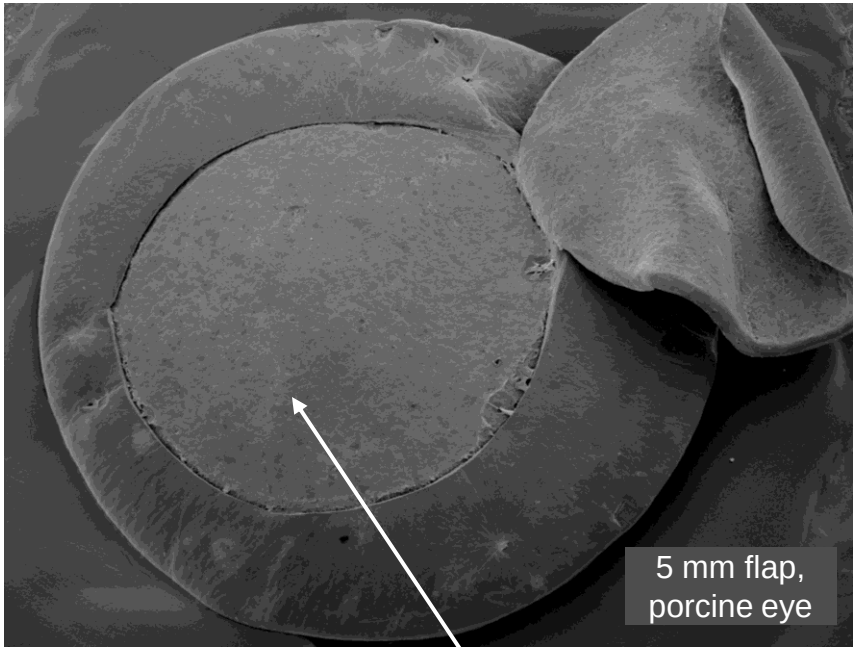

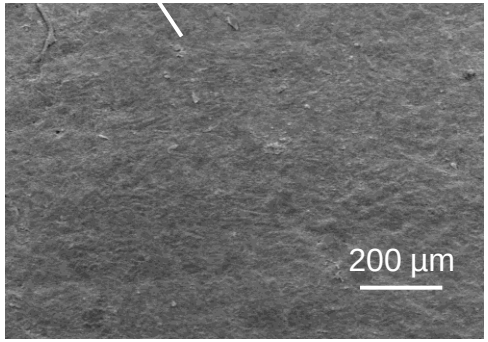

- UV-laser (355 nm, 600 ps)
- 150 kHz pulse repetition rate
- good beam quality
- compact
- cost effective

Development of a commercial product
together with an industrial partner

Precision gain by UV-laser

Femto

(IR, 1040 nm)

Focus 3.3 µm

at NA = 0.4

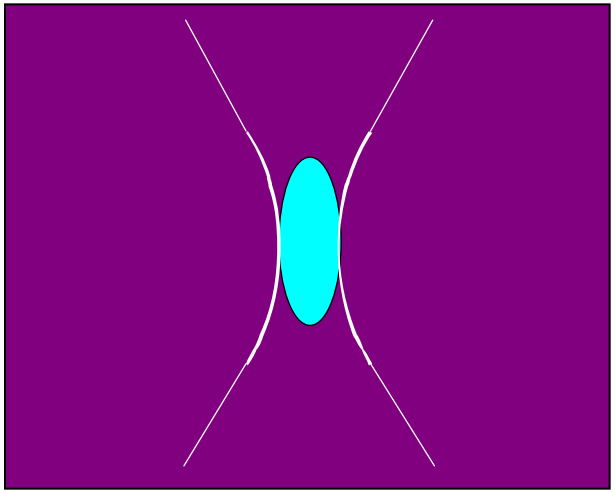

Nano

(UV, 355 nm)

Focus 1.1 µm

at NA = 0.4

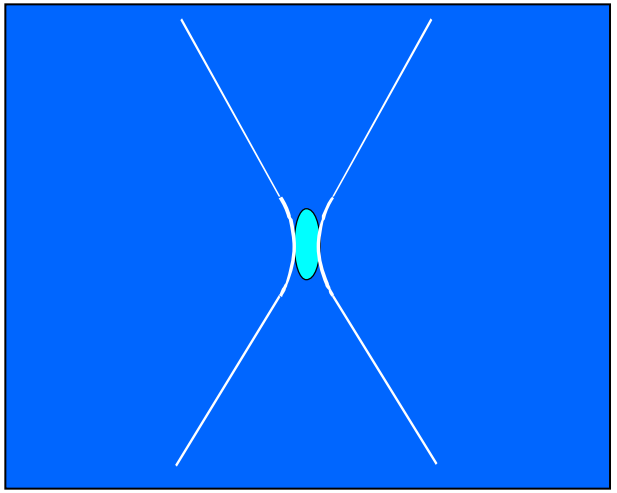

UV focal diameter and length are merely 1/3 of IR values

⇓

Better precision when using UV pulses

Quality of cuts with the new technique

(355 nm, 0.7 ns pulse duration)

Side cut

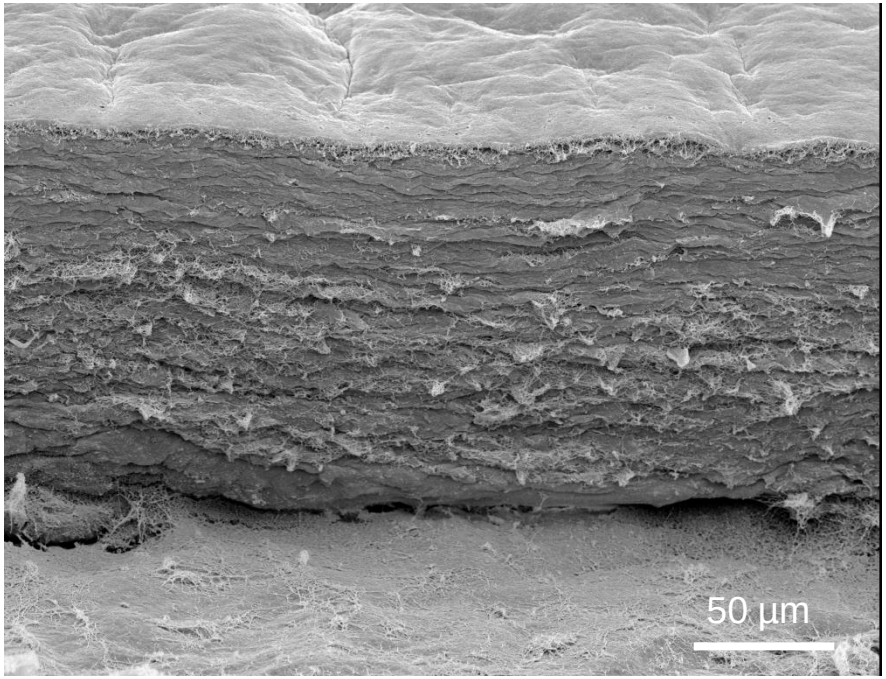

Flap-bed

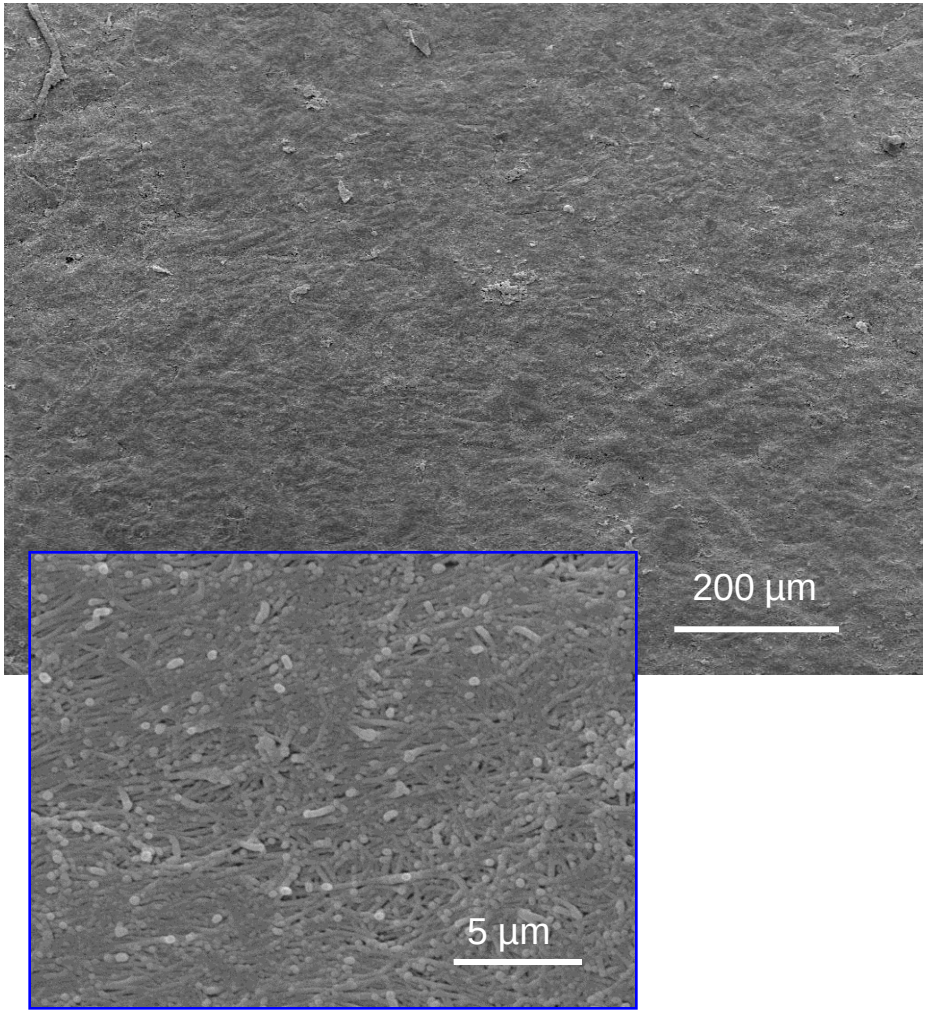

Flaps in porcine cornea

Flap lifting on porcine eyes

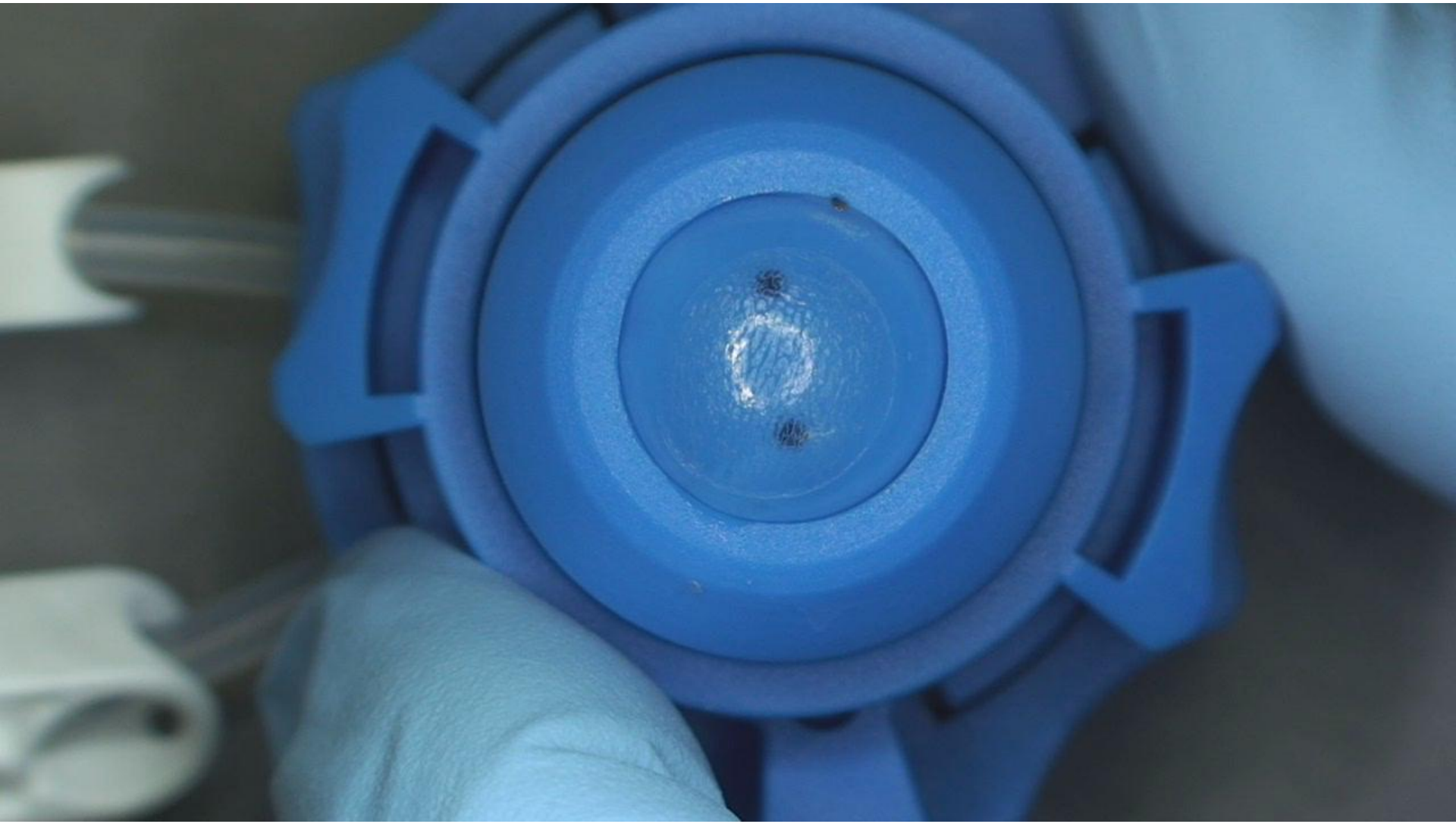

SCHWIND „Smart Tech“ Laser

Technical Features

λ= 355 nm

τ= 700 ps

150 kHz

Small footprint

No water cooling

No climatization

Stable operation

Cost effective

Applications

LASIK
(7.5 – 10.5 mm flaps)

Variable cutting angle
(45° - 105°)

Intra-corneal
rings and inlays

Incisions for
correction of
astigmatism

BMO

Experimental Discovery

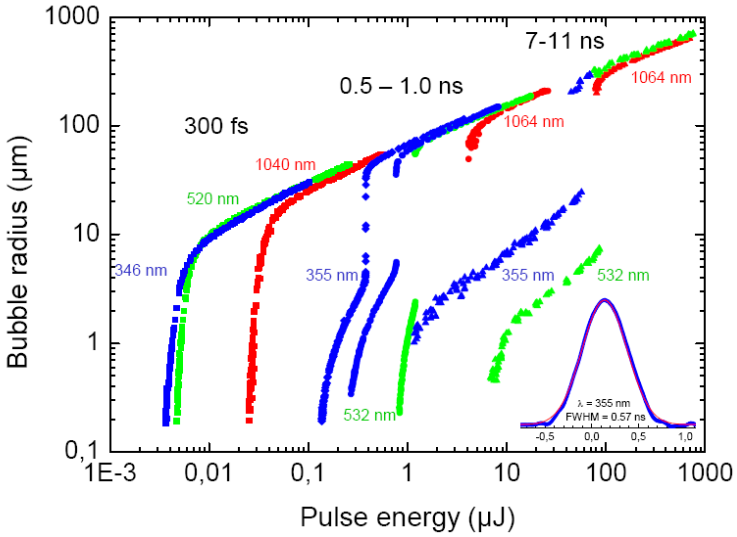

⇓

Theoretical Understanding

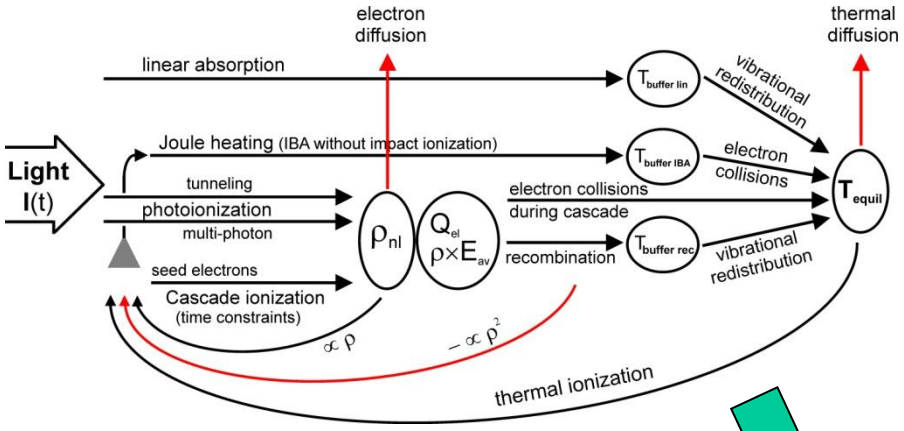

⇓

MLL

Technical realization

other applications

Laser lithotripsy

Nieren- und Harnleitersteine

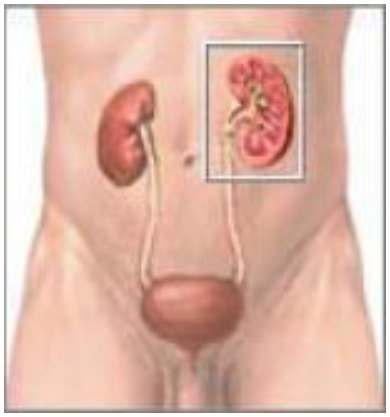

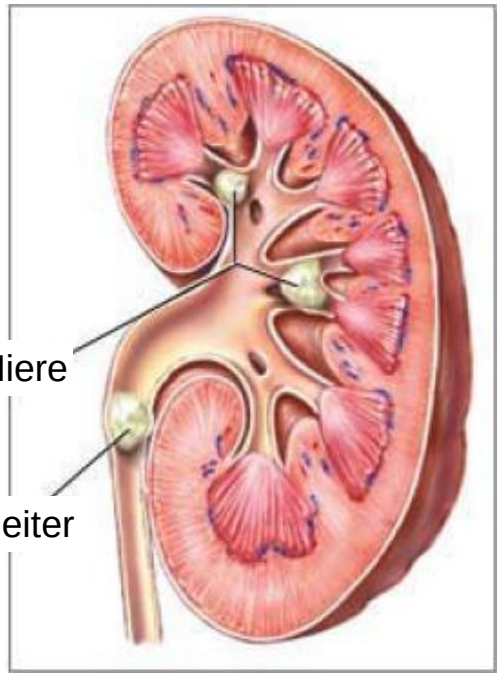

Nieren- und Harnleitersteine

Harnleiterstein mit Harnstau
(visualisiert durch Kontrastmittel)

Harnleiterstein
(vergrößert)

Shock wave effects in tissue and on stone

Stoßwellenwirkung

Stein: Rißbildung, Fragmentierung

Gewebe: elastische Verformung,
Schäden auf subzellulärer Ebene

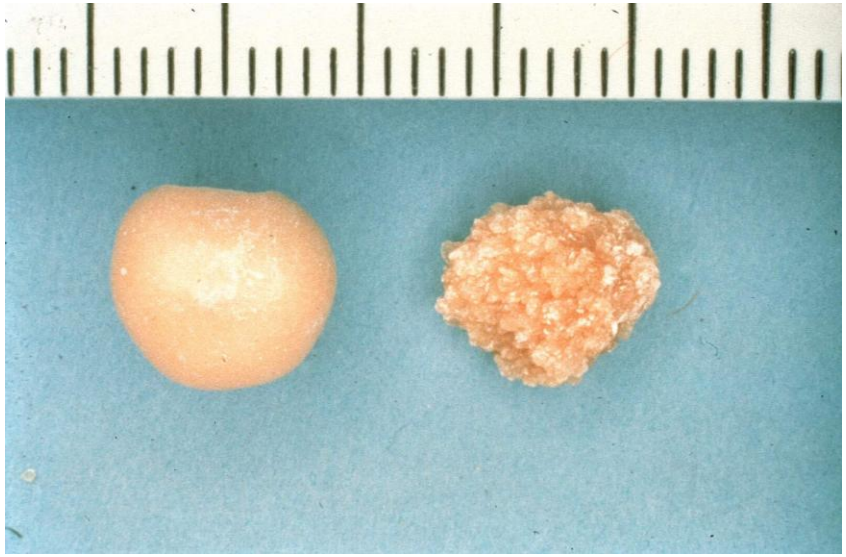

⇒

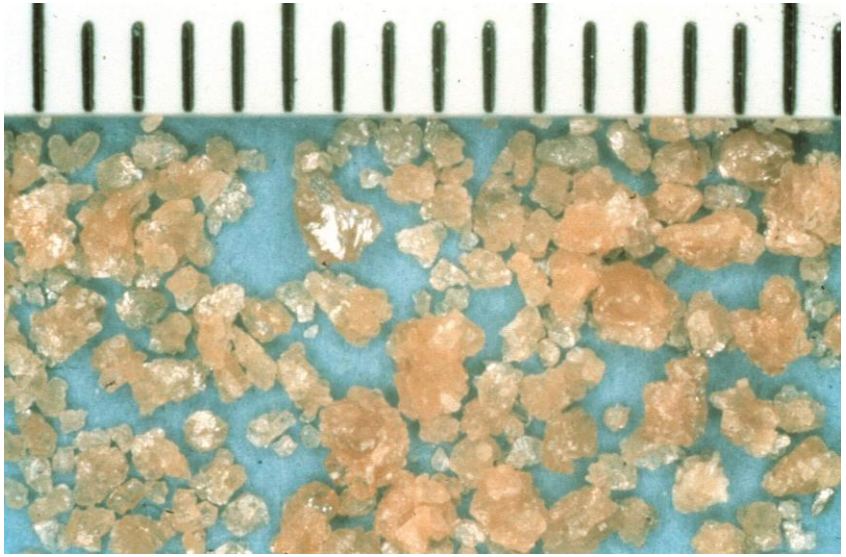

ESWL and laser lithotripsy

ESWL

Stoßwellenerzeugung extrakorporal
Fokussierung in den Körper.

Laserlithotripsie

Stoßwellenerzeugung durch Plasmabildung
direkt auf dem Stein.

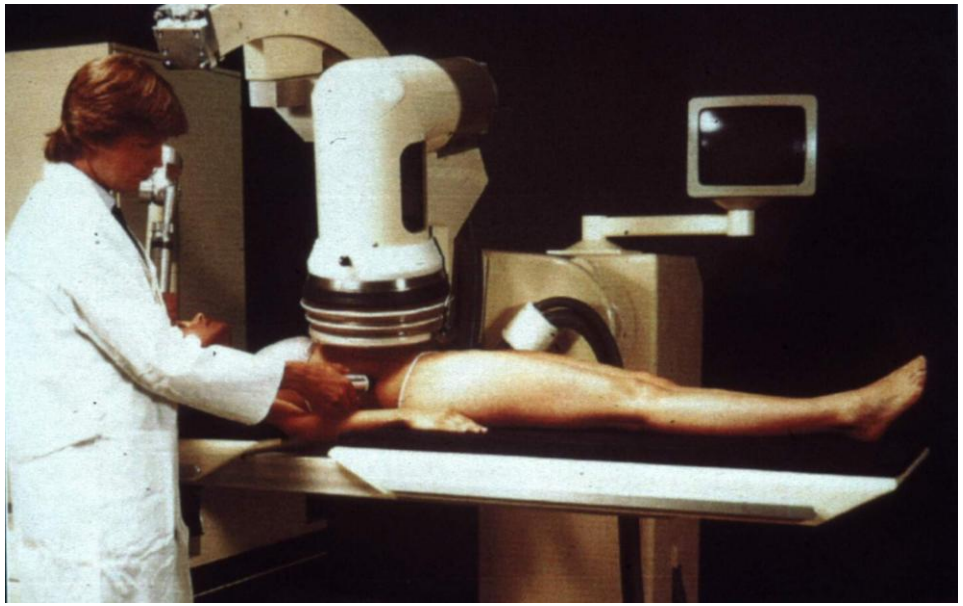

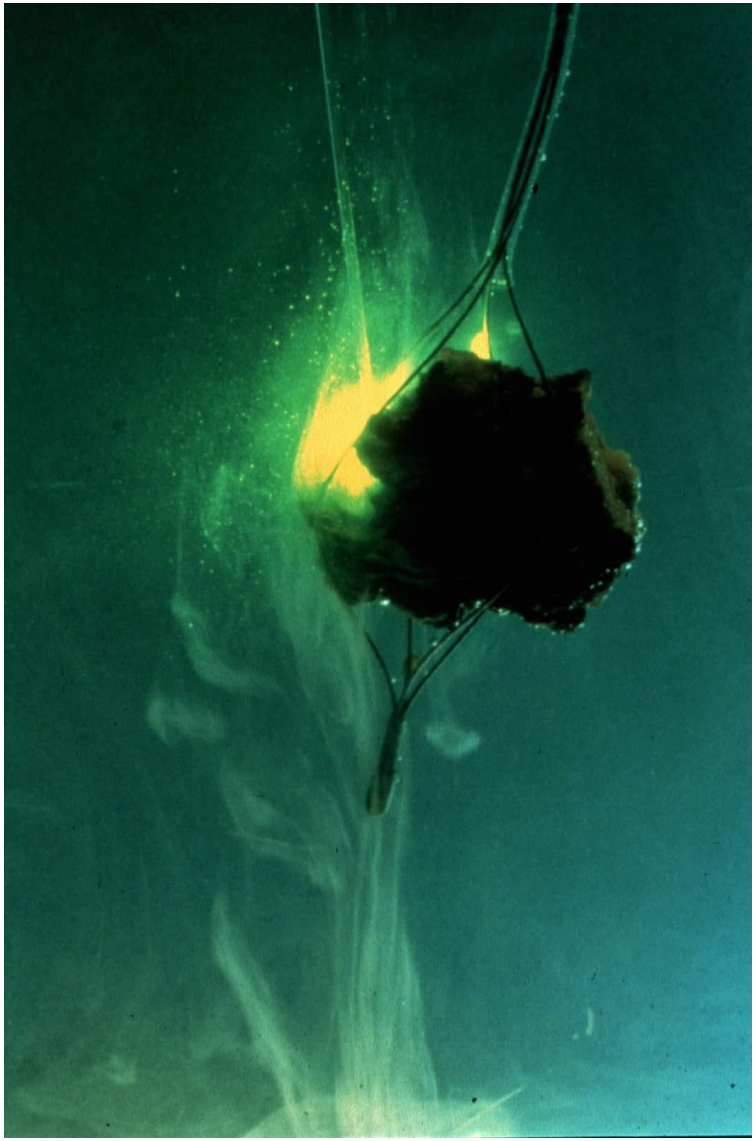

Shock wave focusing in ESWL

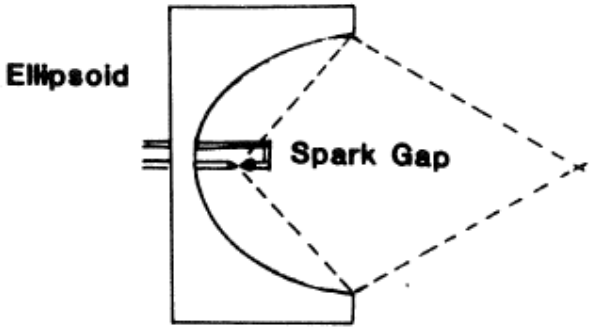

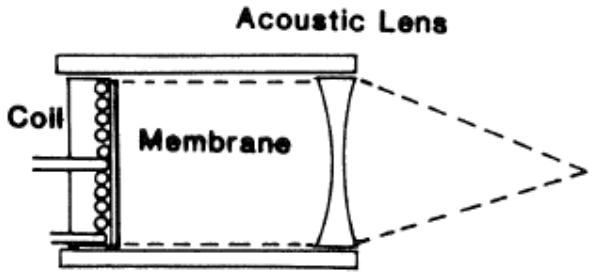

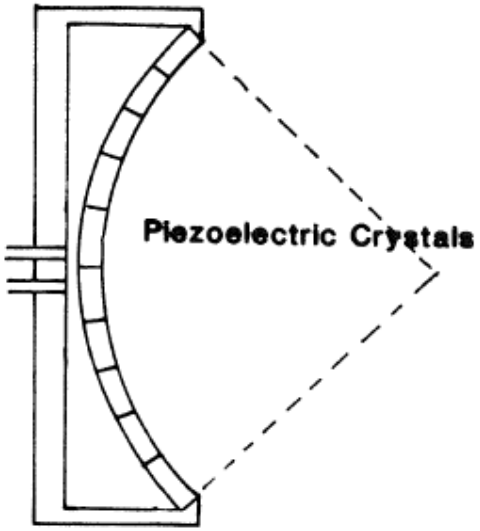

Acoustic impedance matching in the early days

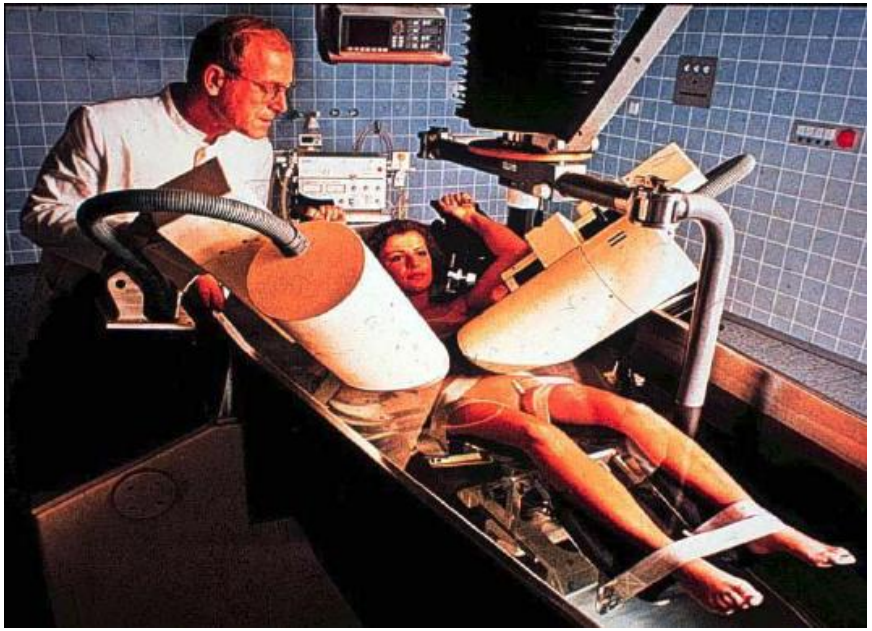

Typical temporal shock wave profile

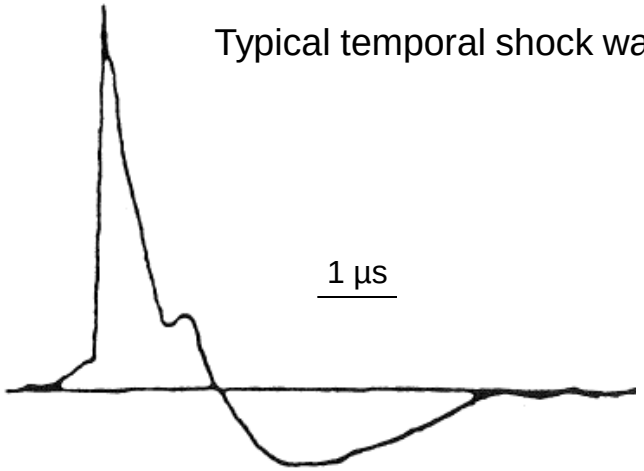

Shattering mechanism

Materialparameter

	Nierensteine	Gallensteine
statische Druckfestigkeit	40 - 80 bar	22 - 32 bar
statische Zugfestigkeit	6 - 11 bar	3 - 10 bar

Quelle: Diss. B. Ihler (1992)

Umwandlungsgrad von Laserlichtenergie in Stoßwellenenergie im Stein

(1,5 µs Puls, 400 µm Faser)

Primärstoßwelle: 0,6 % bei 100mJ

Sekundärstoßwelle: 0,6 - 1,4 % bei 100mJ

ESWL: Energie im Fokus (Ø11mm): 15 - 20mJ

Quelle: Ihler (1992), Müller (1990)

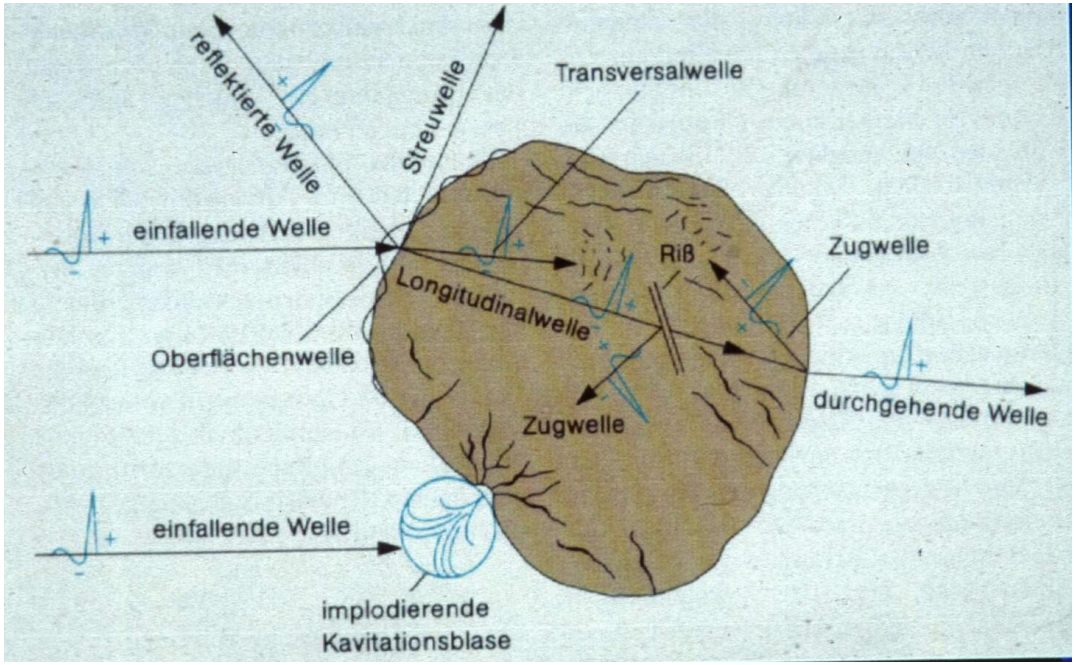

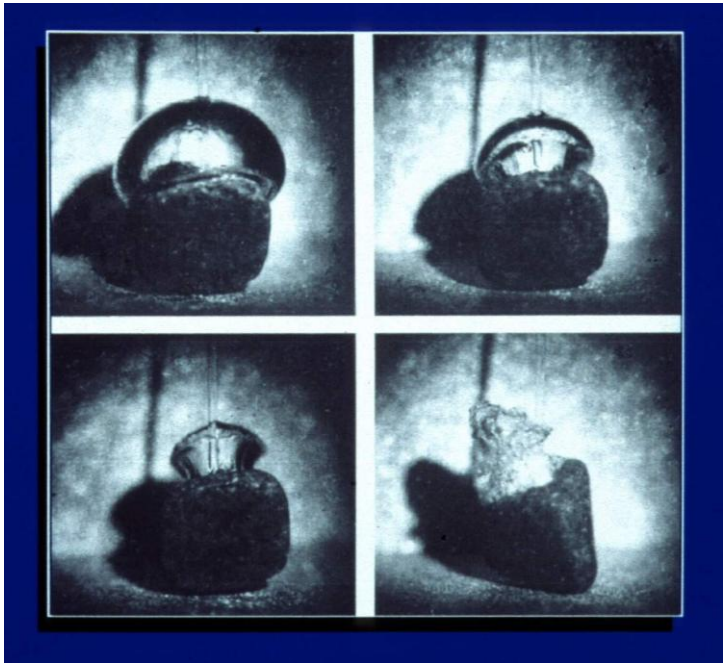

Stone fragmentation in ESWL with large focus

W. Eisenmenger, Ultrasound in Med. Biol. 28:769-774 (2002)

For some time, manufacturers tried to achieve a small shock wave focus to mimimize side effects in ESWL

Then it was discovered that a focus larger than the stone was more effective for stone fragmentation and required fewer pulses with lower pressure ⇒ less side effects

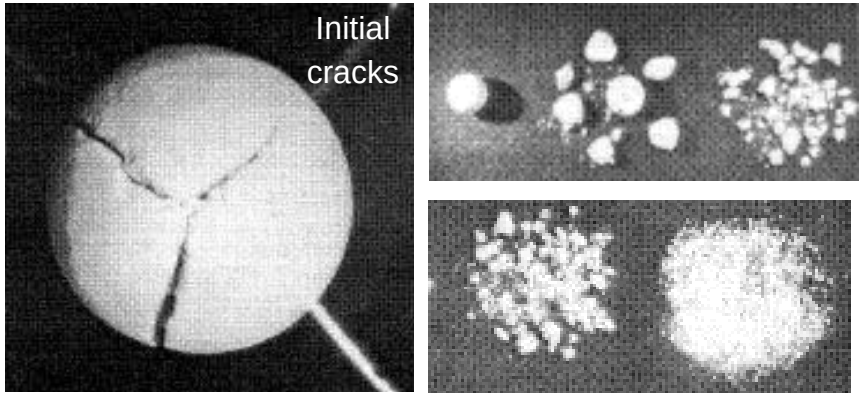

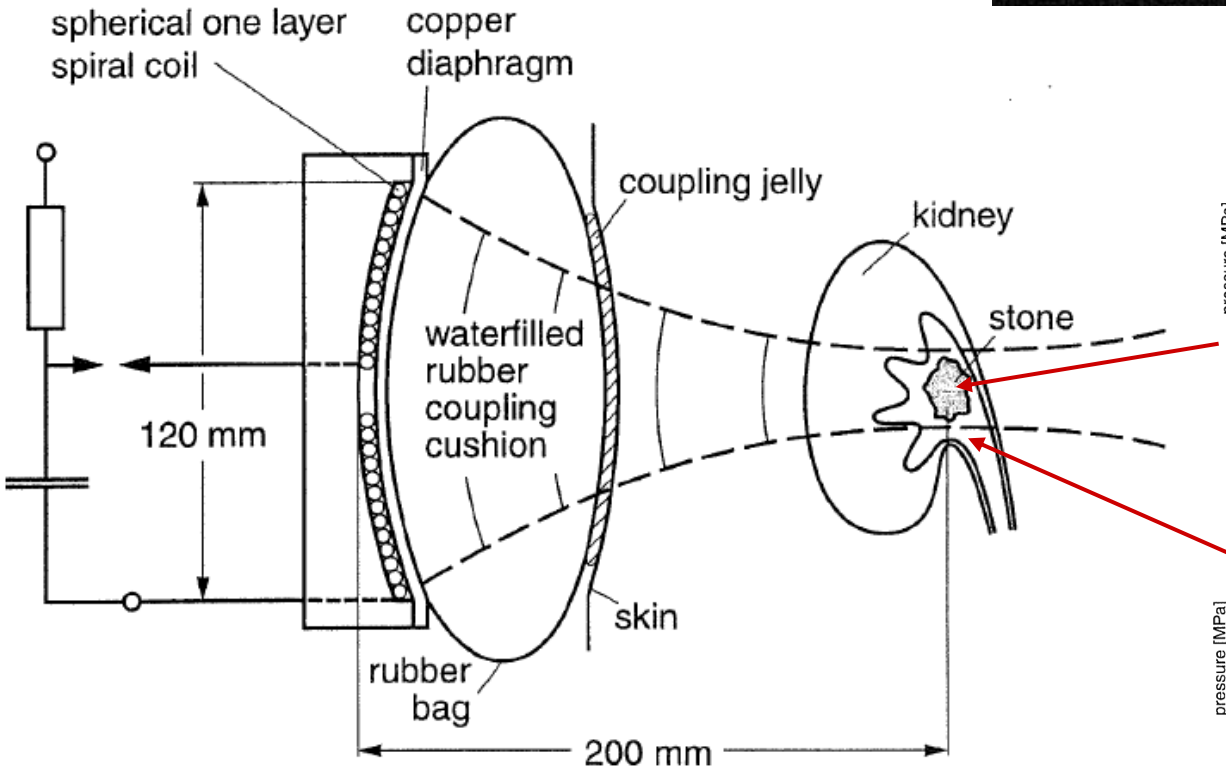

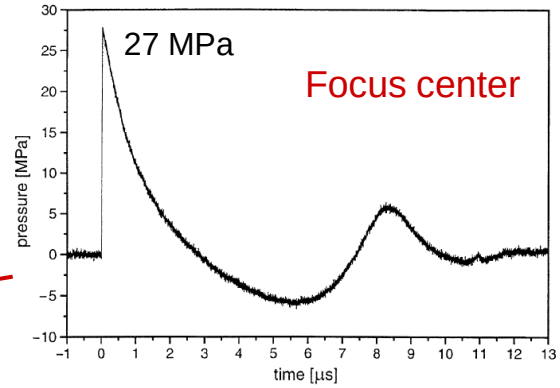

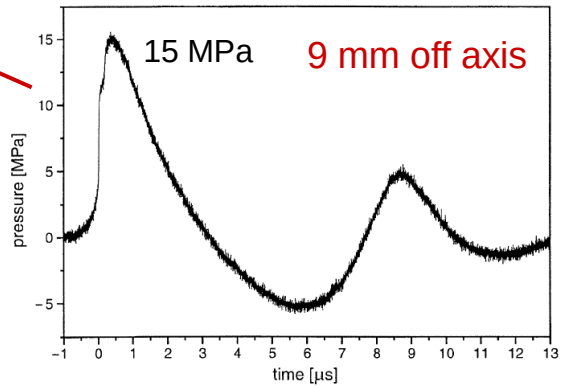

Fragmentation mechanism in ESWL (2)

W. Eisenmenger, Ultrasound in Med. Biol. 27:683-693 (2001)

Sharply focused pressure wave

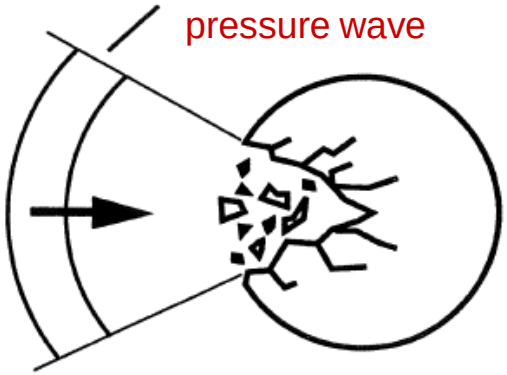

„Squeezing“ by the pressure pulse propagating in the *surrounding* liquid or tissue

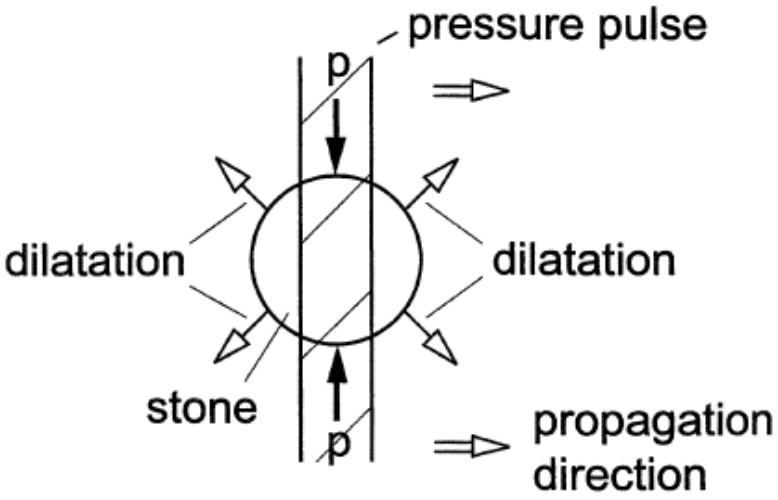

Orientation of cleavage planes resulting from „squeezing“

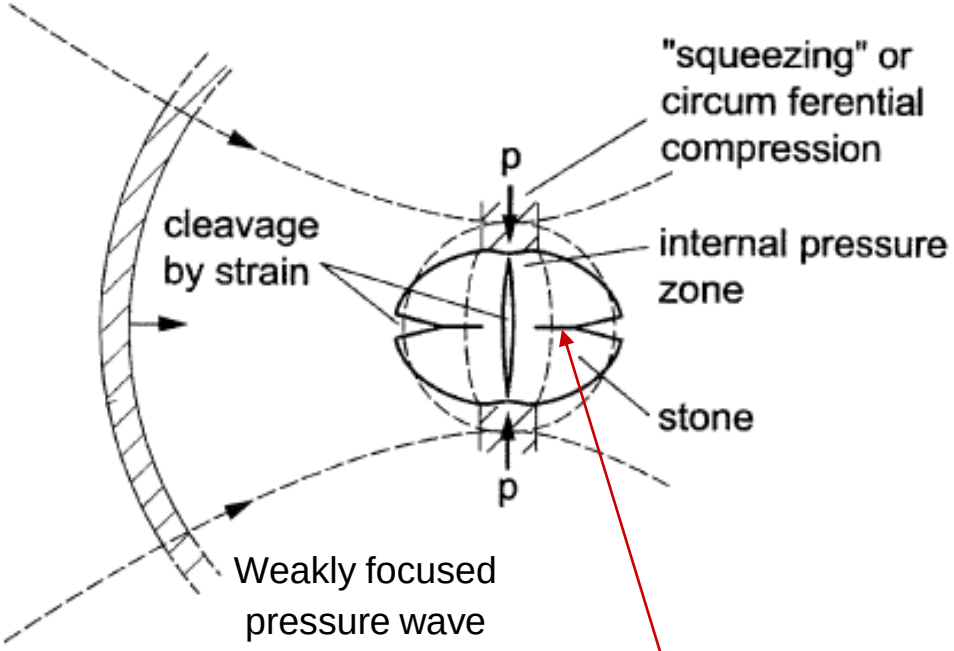

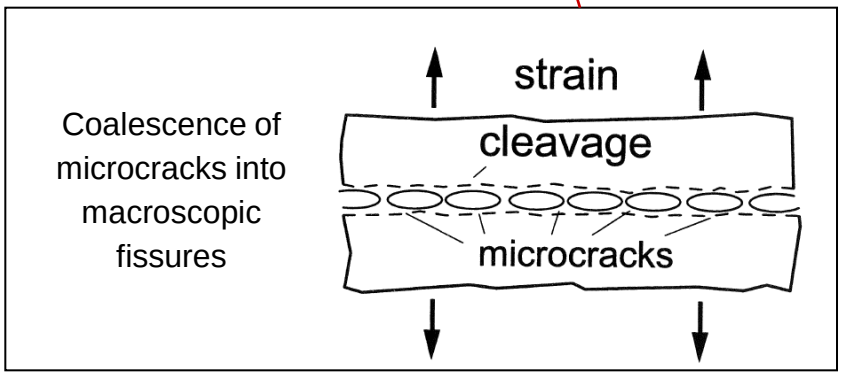

Fiber fragmentation

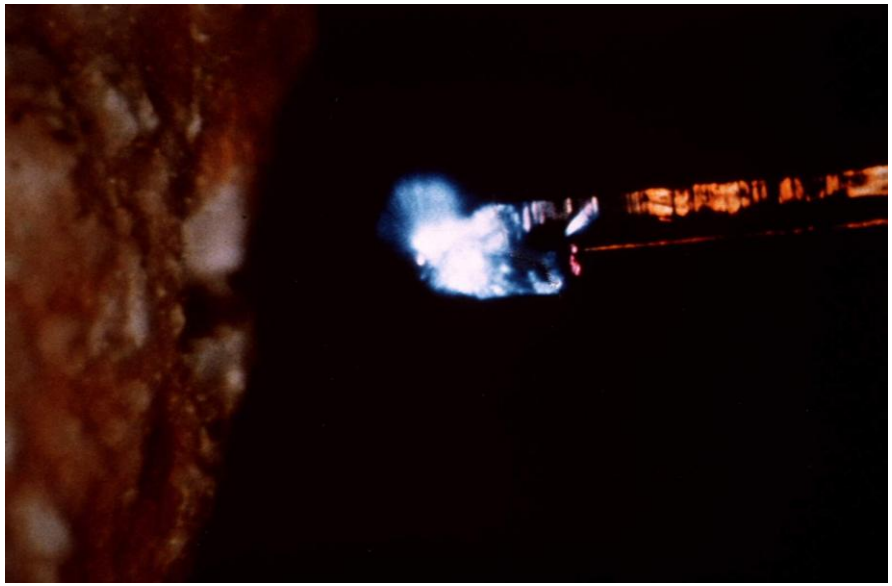

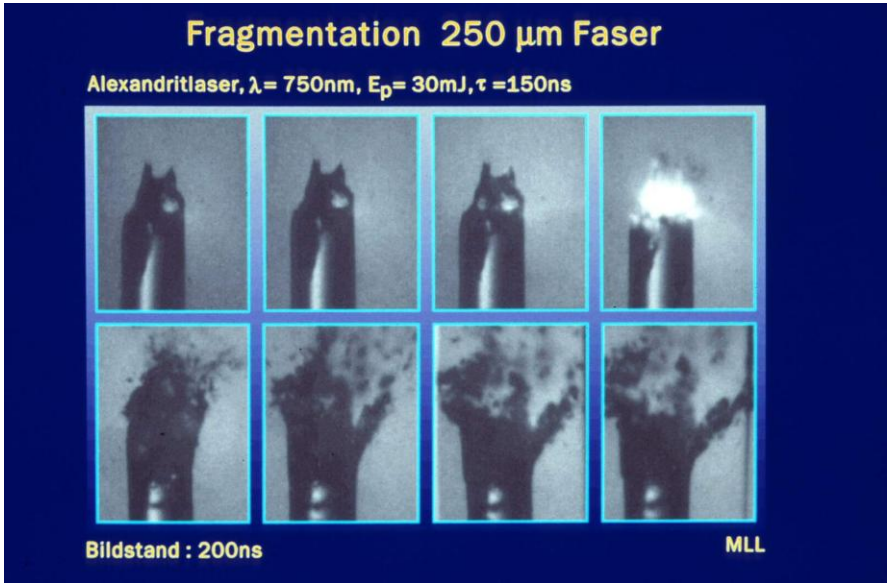

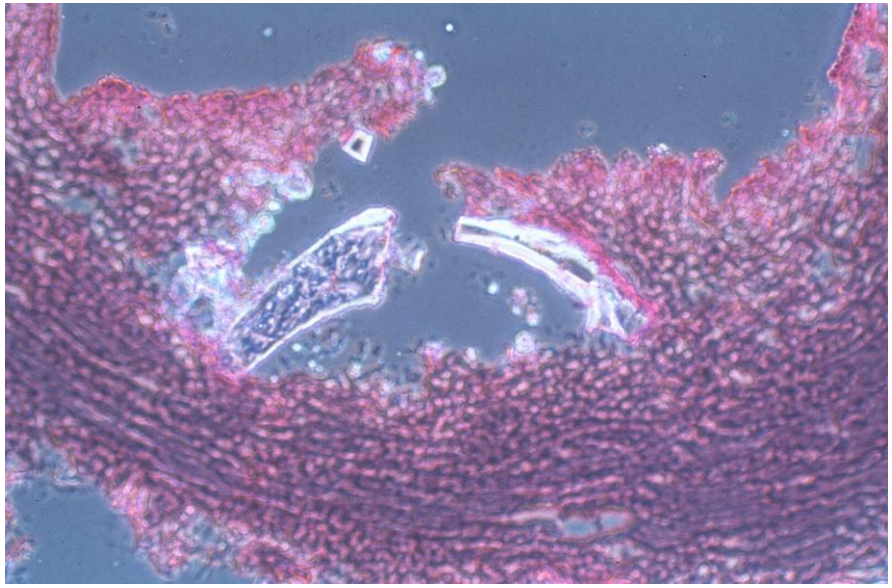

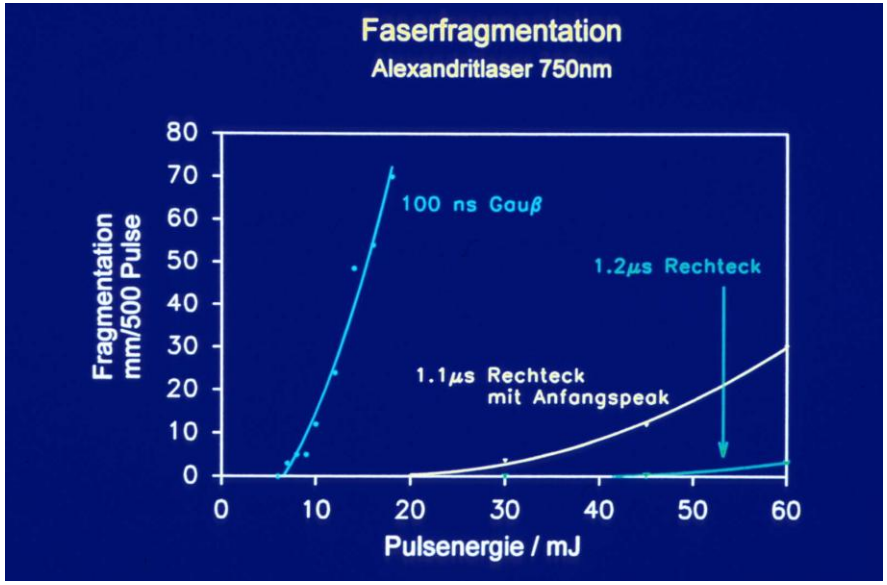

Minimization of tissue damage (1)

Optimale Wellenlänge ?

- Gewebeabsorption *und* Steinabsorption sinken mit zunehmender Wellenlänge
- hohe differentielle Absorption bei $\lambda = 504nm$, $620 < \lambda < 800nm$
- Bei Verwendung der wellenlängenabhängigen Arbeitsenergie und Faserkontakt sind immer Gewebeschäden möglich

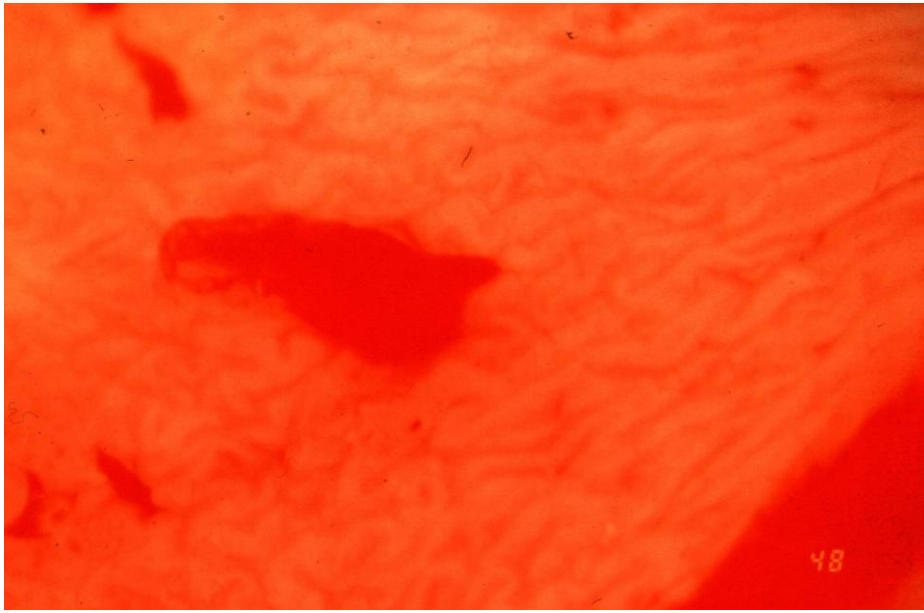

No easy way to avoid tissue damage at pulse energies used for stone fragmentation

Vermeidung von Gewebeschäden

- optische Kontrolle (Katheter ca. 2mm)
- Fluoreszenzmessung + optoelektronische Rückkopplung (200 µm Faser)

Minimization of tissue damage (2)

- Fluorescence/plasma luminescence monitoring -

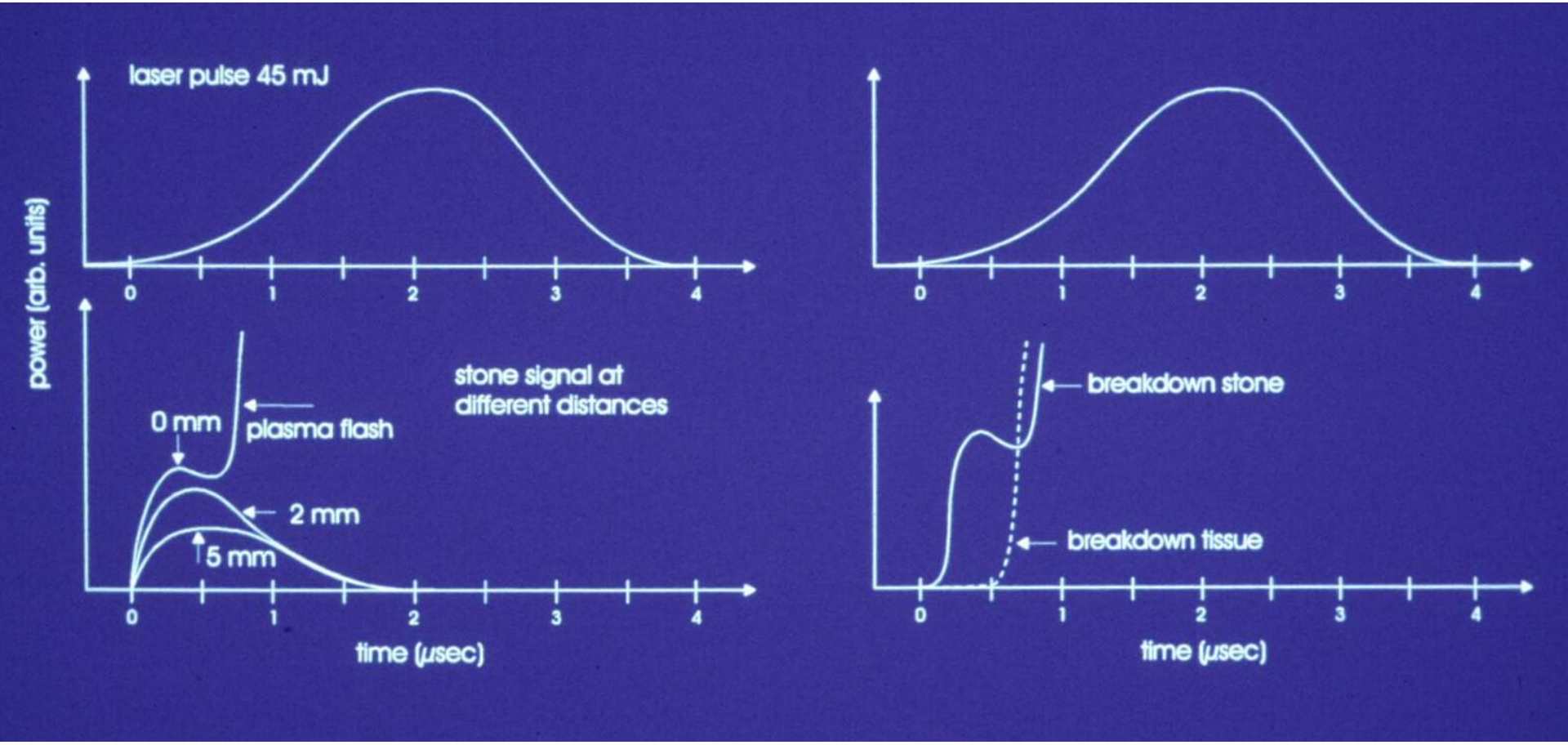

Plasma luminescence starts earlier and is brighter on stone than on tissue (ureter wall)

⇓

Measure plasma luminescence and switch laser pulse off when no luminescence is detected in due time

Feedback control for minimization of tissue damage

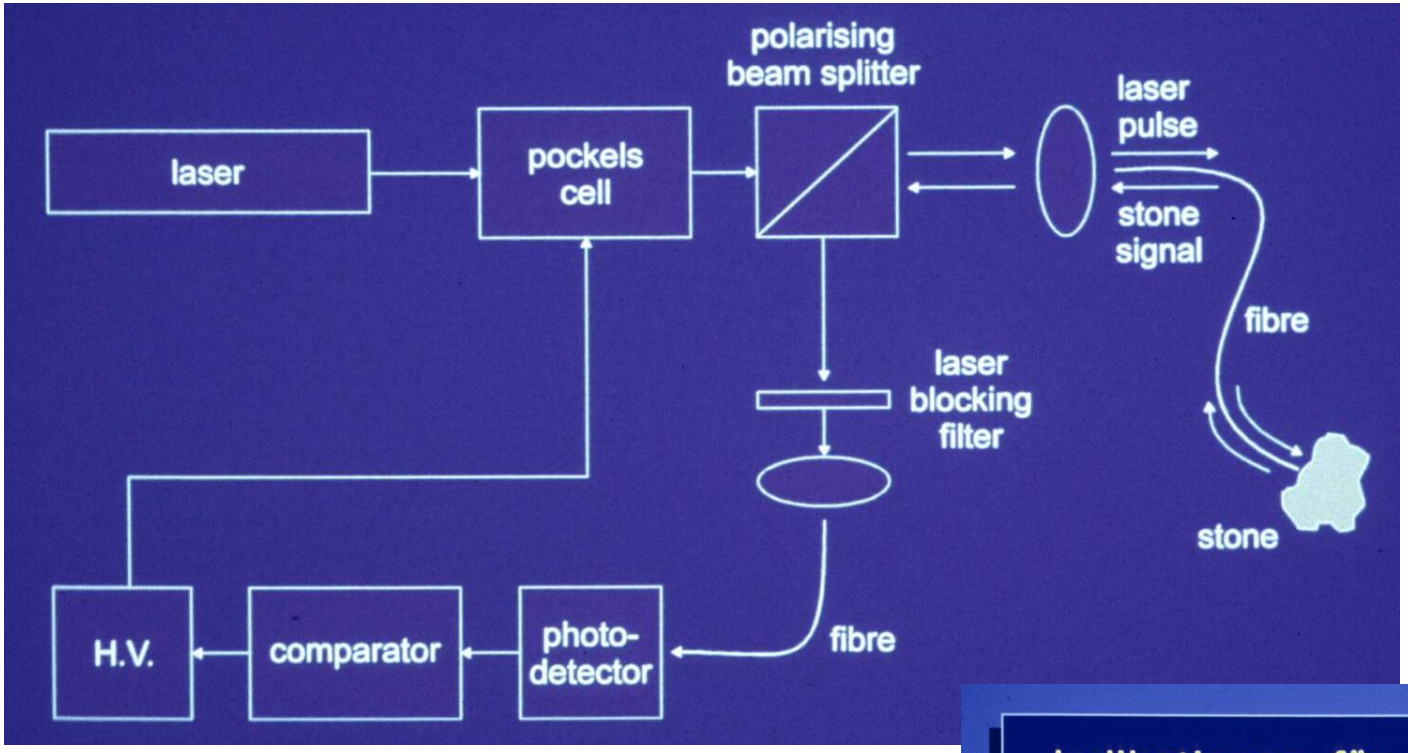

Plasma luminescence is measured, and, when necessary, laser pulse switched off using a Pockels cell and a polarizing beam splitter

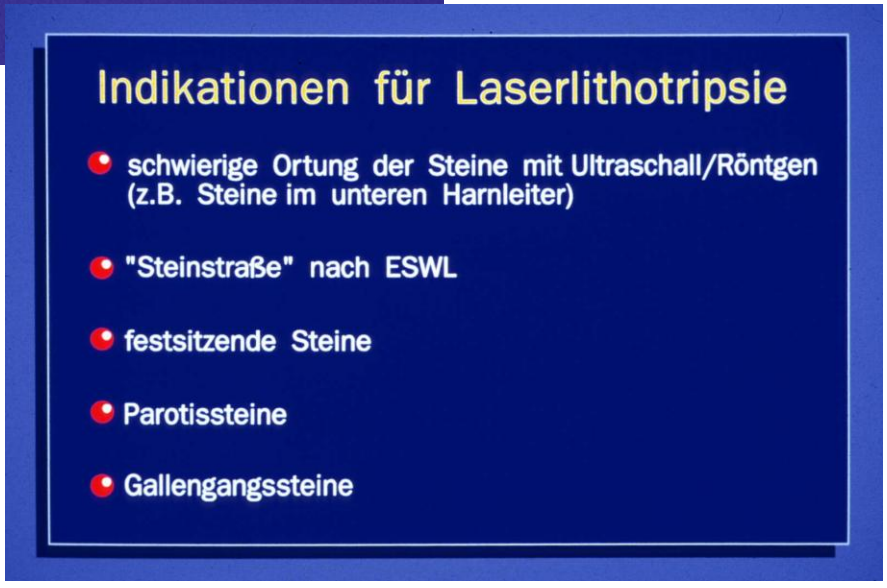

Femtosecond cell surgery:

Applications,

mechanisms,

Fs-laser cell surgery @ 80 MHz repetition rate

Intranuclear chromosome dissection

König et al. Cell. Mol. Biol 45:195-201 (1999)

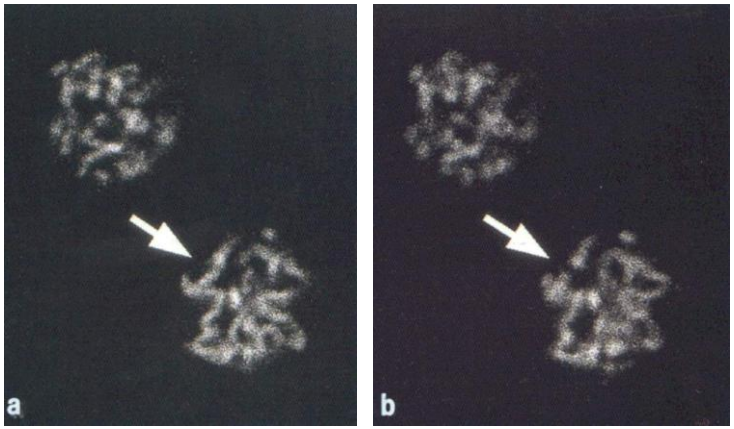

170 fs, 780 nm, NA = 1.3

40 000 pulses of **0.4 nJ**

Total energy: 15 µJ

Transfection of cells with DNA encoding Green Fluorescent Protein (GFP)

Tirlapur & König, Nature 418:290-291 (2002)

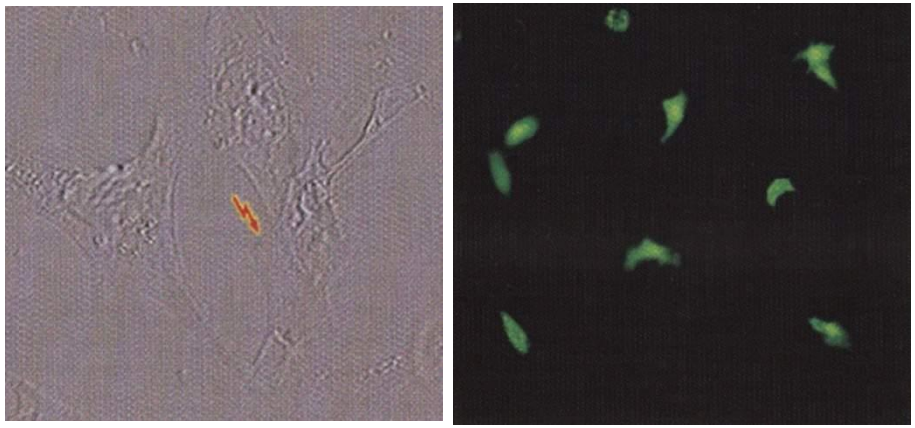

170 fs, 800 nm, NA = 1.3

960 000 pulses of **0.6 – 1.2 nJ**

Total energy: 570 – 1150 µJ

Fs-laser cell surgery @ 1 kHz repetition rate

Selective destruction of a mitochondrion

Shen, Mazur & Ingber, Harvard University, 2003

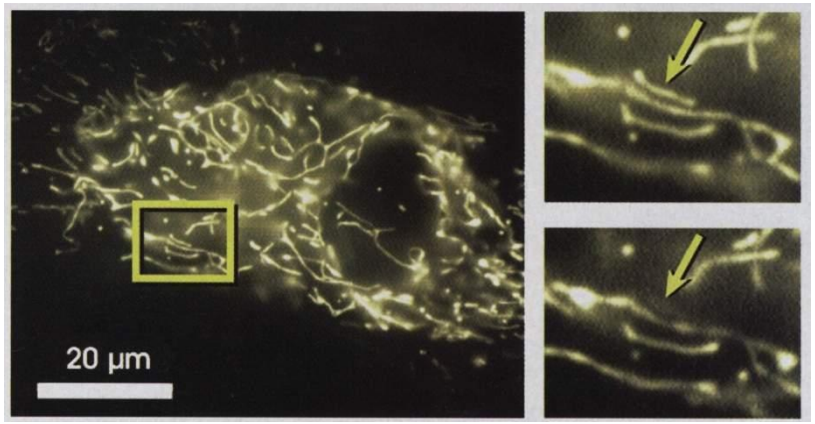

100 fs, 800 nm, NA = 1.4,

Several hundred pulses of **2 nJ**

Total energy ≈ 1 µJ

Dissection of an axon in a C. elegans worm to study nerve regrowth

Yanik, Ben-Yakar et al. 2003

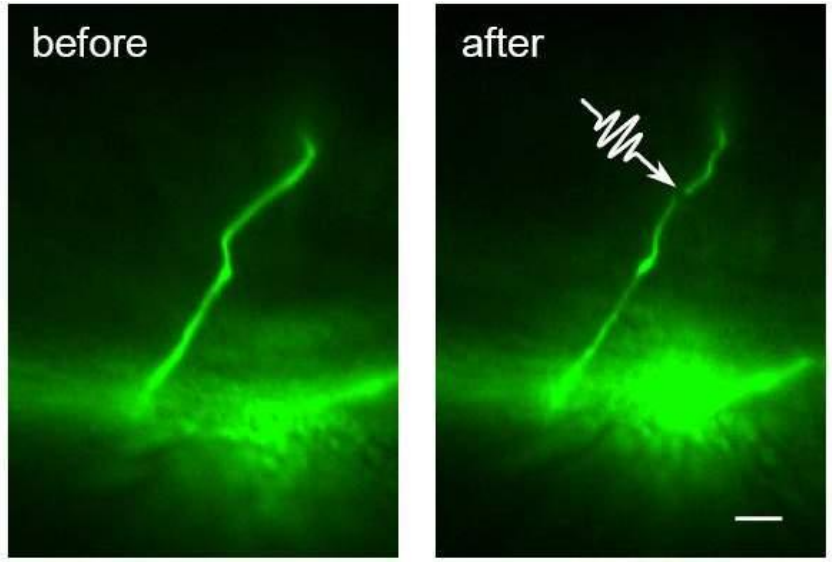

200 fs, 800 nm, NA = 1.4,

400 pulses of **10 nJ**

Total energy: 4 µJ

Application example:
Cell transfection

Goals of membrane permeabilisation

Gene transfer for cell transformation

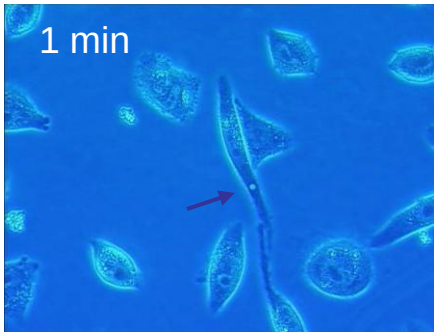

Hole in cell membrane

(phase contrast microscopy)

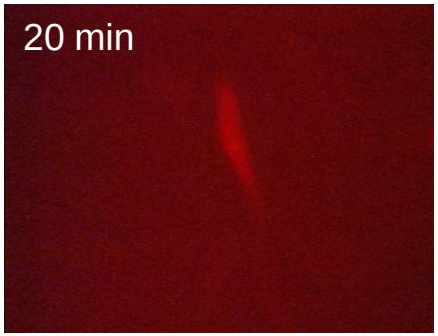

Proof of permeabilisation

(propidium iodine fluorescence)

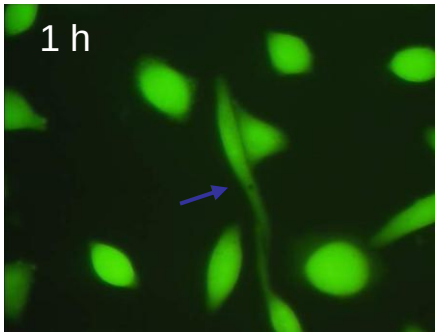

Proof of cell vitality

(Calcein-AM-Fluorescence)

Transfer of nanoparticles for protein inactivation

Fokussed irradiation

+

Linear or nonlinear energy deposition

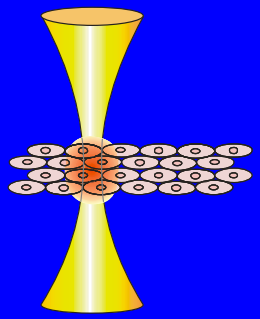

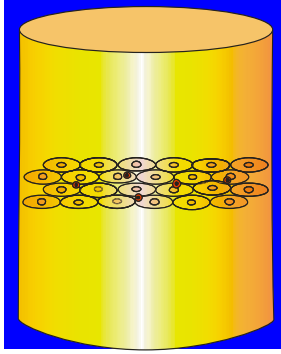

Irradiation of entire cells

+

Targeting via nanoparticles attached to antibodies that bind to the target proteins

Mechanisms of membrane permeabilisation by fs pulses

100-200 fs,
800 nm,
NA = 1.3

Repetition rates >> 1 MHz

≈ 1 Mill. pulses of ≈ 1nJ each
from a fs oscillator

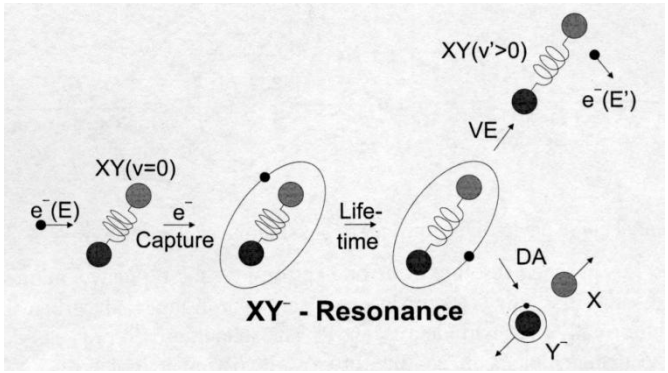

Low-density plasma $\rho \leq 2\times10^{19}$ cm^{-3}

$\Delta T << 100°C$

Breaking of chemical bonds
by low-energy electrons (3-20 eV)

⇓

Dissection results from
accumulative bond breaking

Repetition rates ≤ 1 MHz

Hundreds of pulses of ≈ 10-100 nJ
from an amplified or cavity-
dumped fs laser system

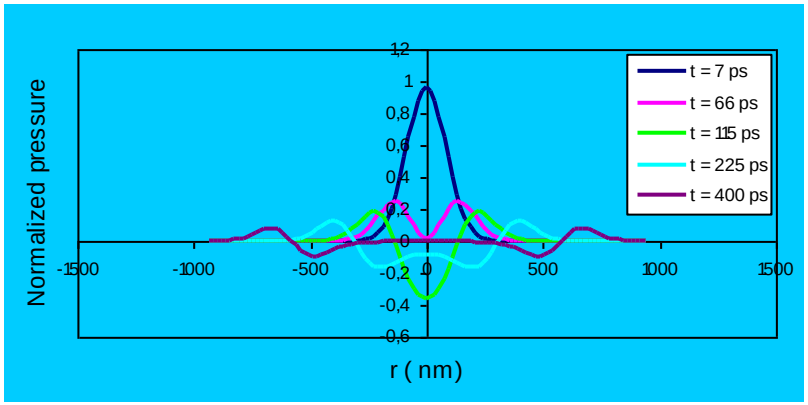

Plasma density $\rho \geq 2\times10^{20}$ cm^{-3}

$\Delta T \geq 132°C$, $\Delta p \geq 132°C$

Formation of minute cavitation bubbles
by heating and thermoelastic stretching

⇓

Mechanical disruption

Bubble formation and membrane permeabilisation

Problem

- Membrane permeabilisation in single shot regime requires bubble formation
- Bubble oscillation will damage the cell if the bubble is too large

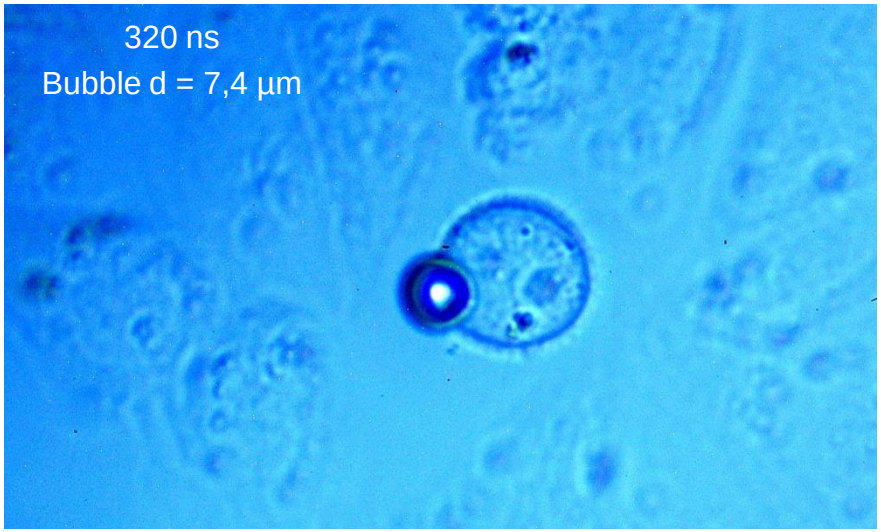

CHO-cell, N_2 ns-Laser (337 nm) 63x objective

Solutions

- Short pulses, small focus
  $\Rightarrow$ small bubbles
- Online-dosimetry of laser energy by online detection of bubble size

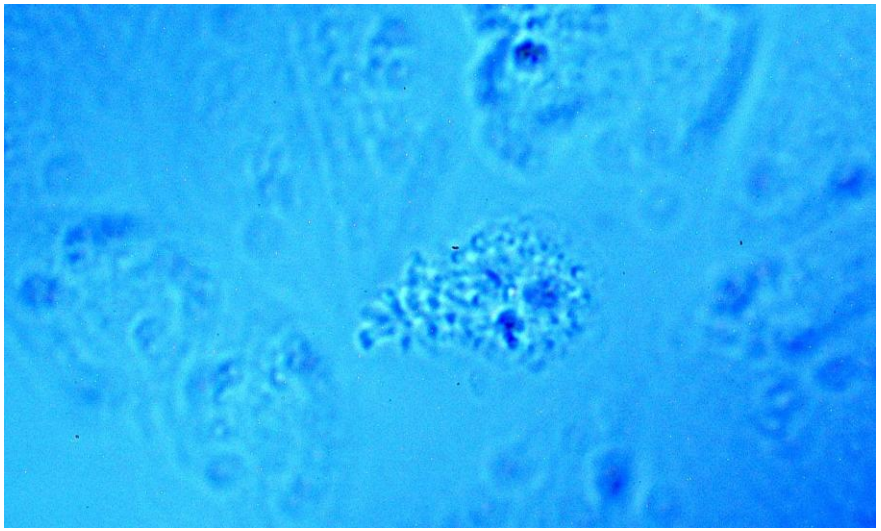

30 s after attempted optoperforation

Experimental bubble detection & photography

- Theory predicts minimum bubble diameters of < 200 nm

  (Appl Phys B 81: (2005))

⇒ Bubble detection via probe beam scattering

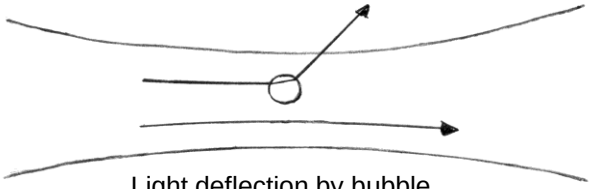

Light deflection by bubble

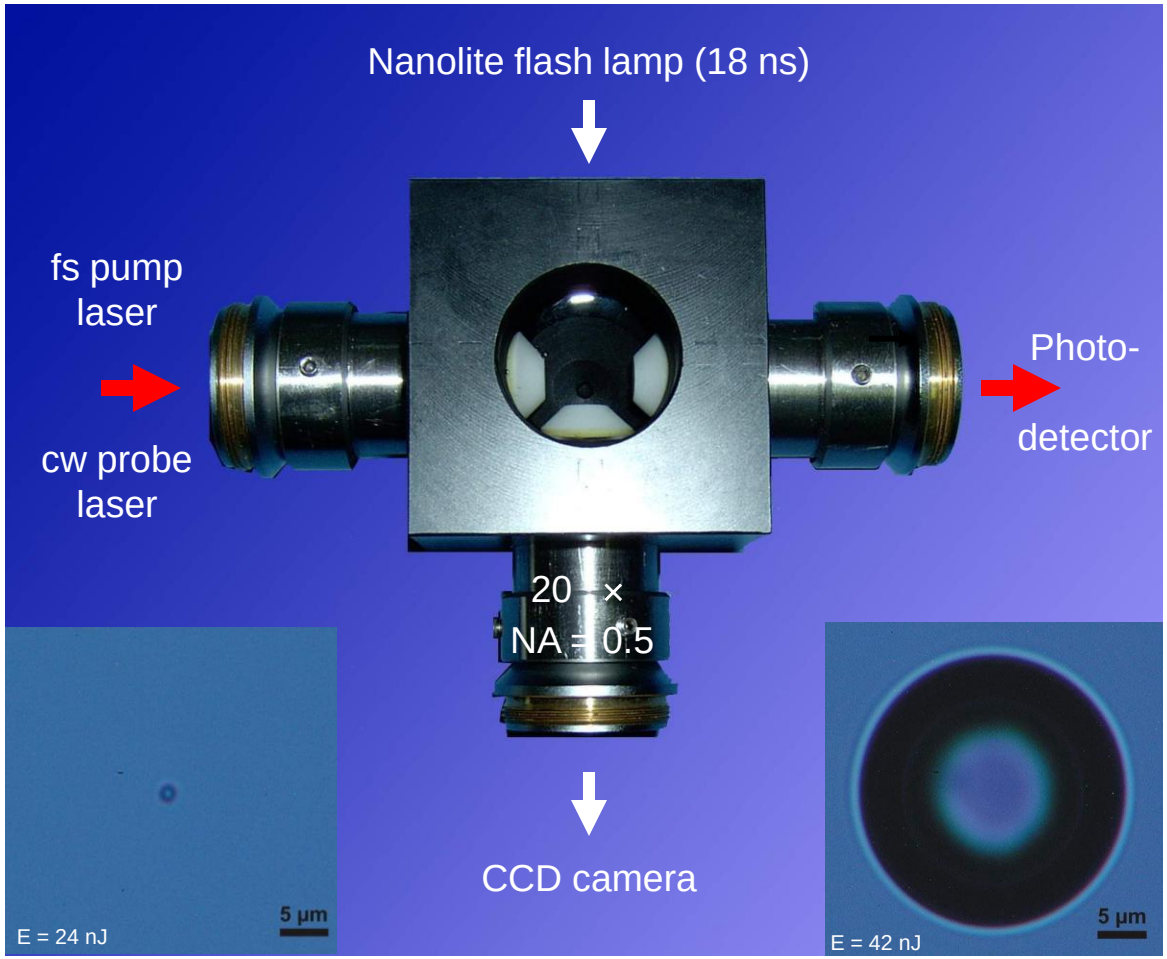

- Determination of bubble radius R_{max} through detection of bubble oscillation time T

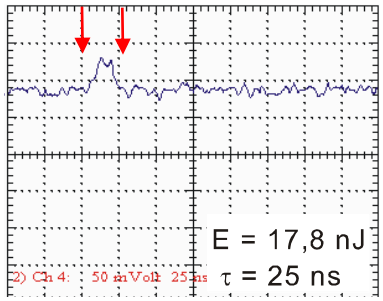

$$R_{max} = \frac{T}{1.83}\sqrt{\frac{p_0 - p_v}{\rho_0}}$$

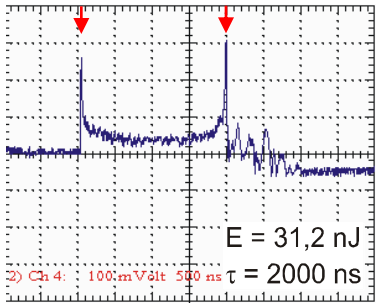

Bubble sizes from scattering signals and flash photography

(1040 nm, 315 fs, NA = 0.8)

R_{max} at threshold:

325 nm for 1040 nm

190 nm for 347 nm

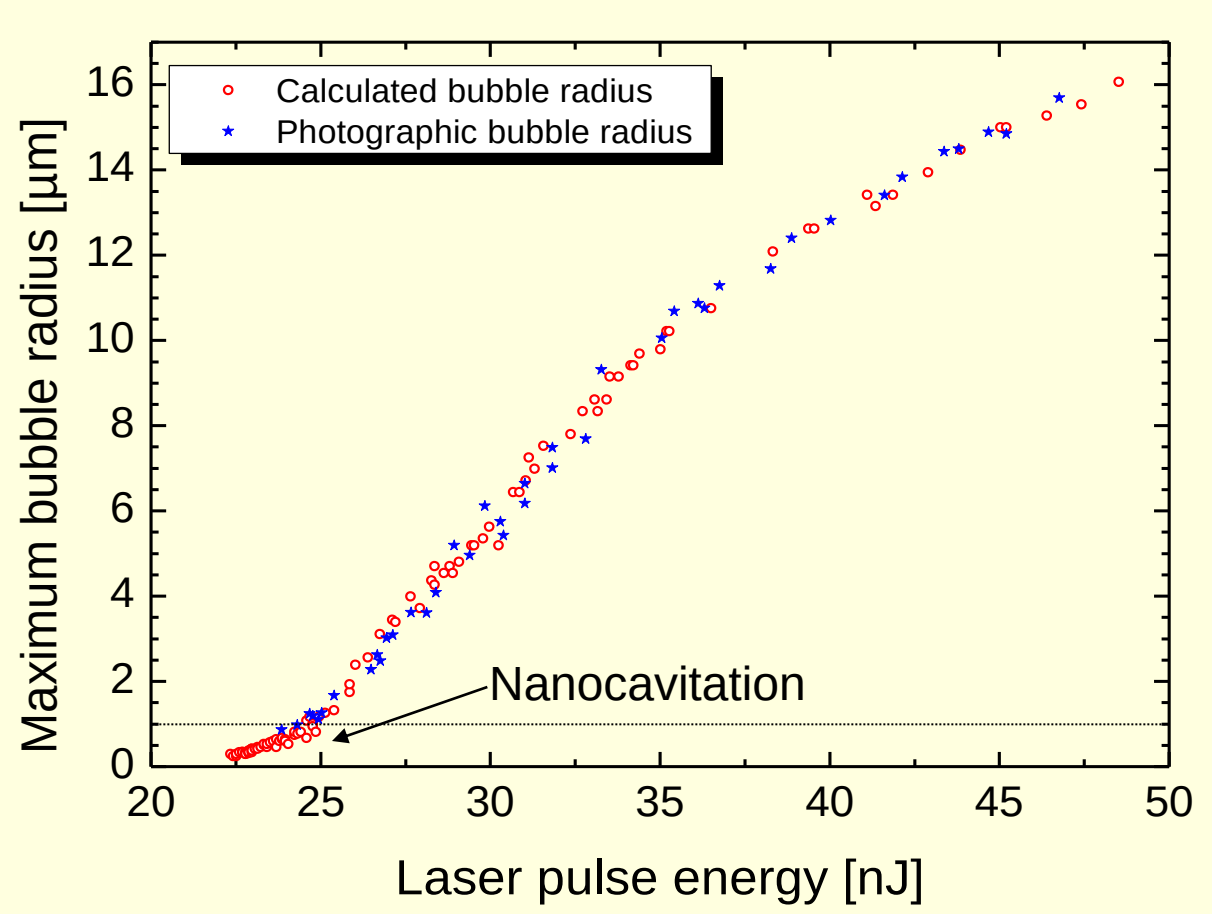

Bubble radius at threshold (325 nm) is much smaller than the focal spot radius (790 nm)

⇒ Nanocavitation is well compatible with nano-surgery

Dosimetry and online control of optoperforation

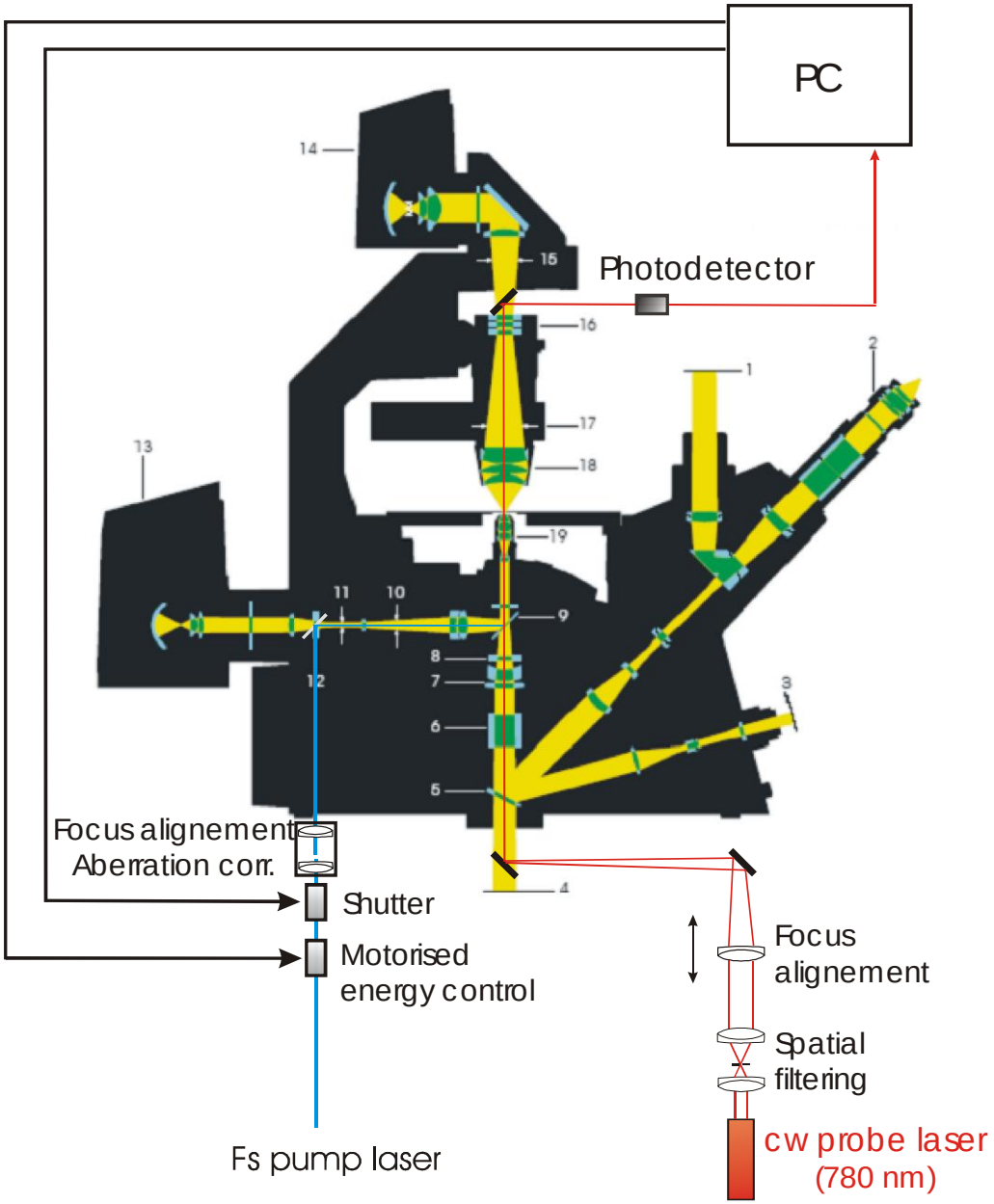

- Bubble detection via cw probe beam
- Determination of bubble size from bubble oscillation time
- Energy used for optoperforation corresponds to appropriate bubble size

⇒ Reliable and gentle perforation of the cell membrane

Computer controlled optoperforation

315 fs, 347 nm, NA = 0.6

Signals just above bubble formation threshold

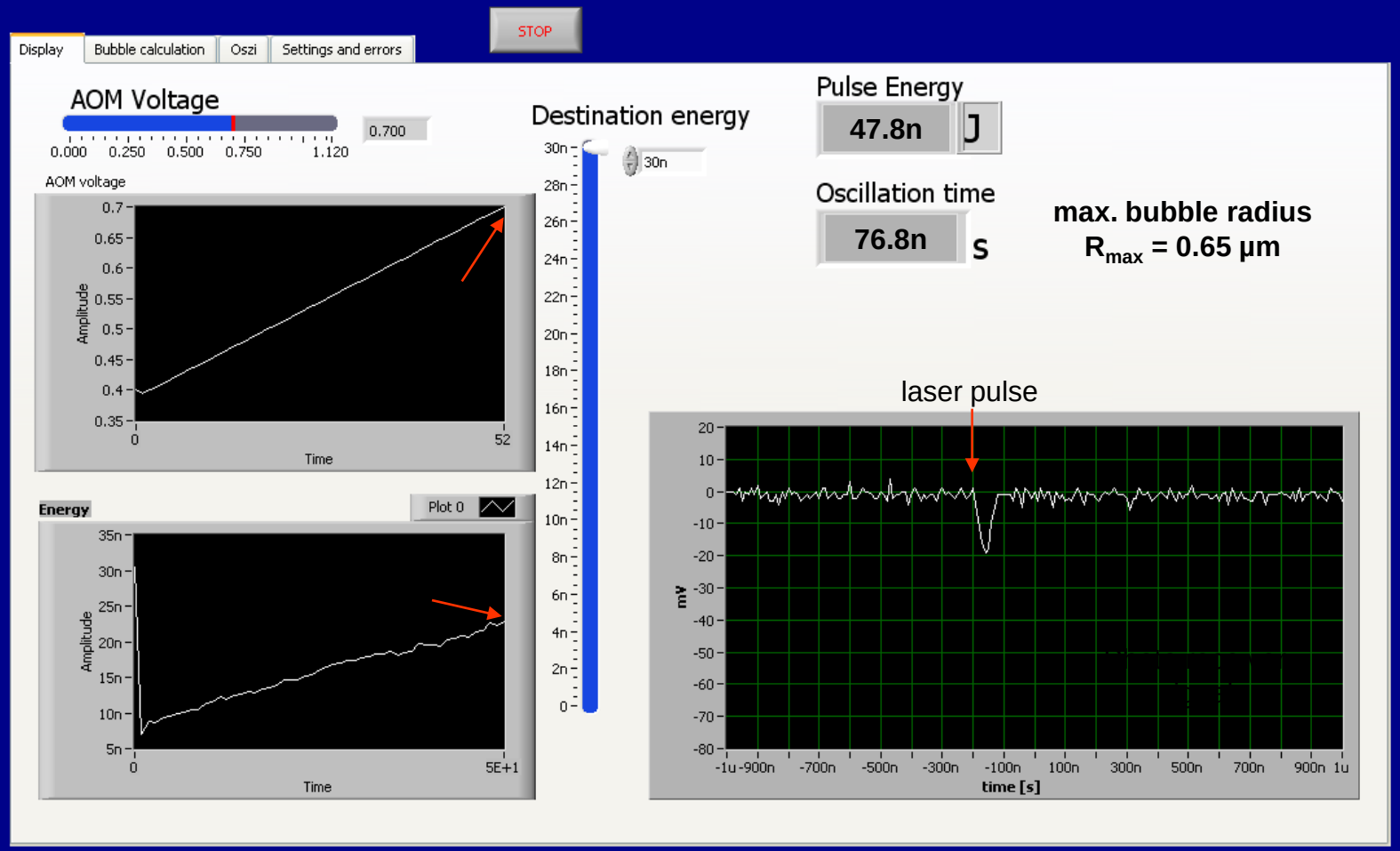

Automatic evaluation of Mie forward-scattering signals

(Bubbles produced by 315-fs pulses, λ = 1040 nm, NA = 0.9)

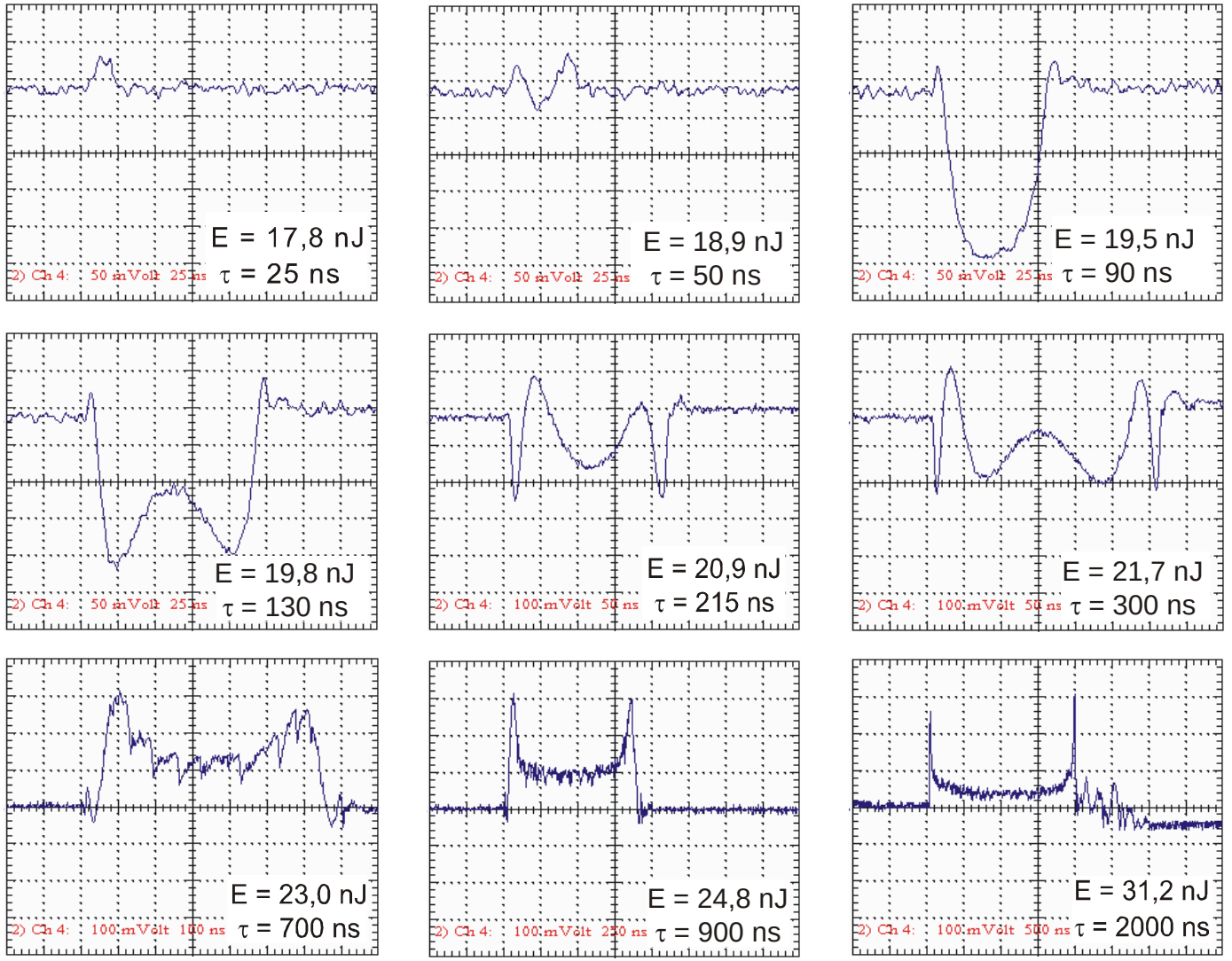

Automatic identification of oscillation time is challenging !

Evaluation using large gradients

- Differentiation -

Small bubble

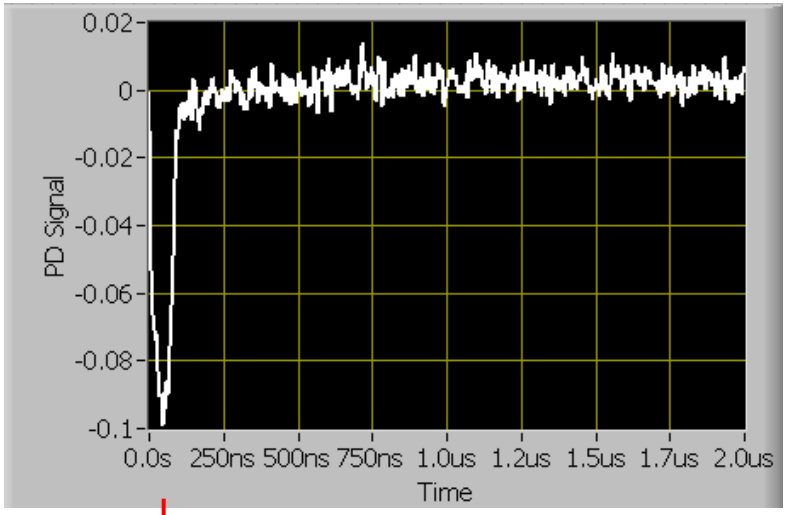

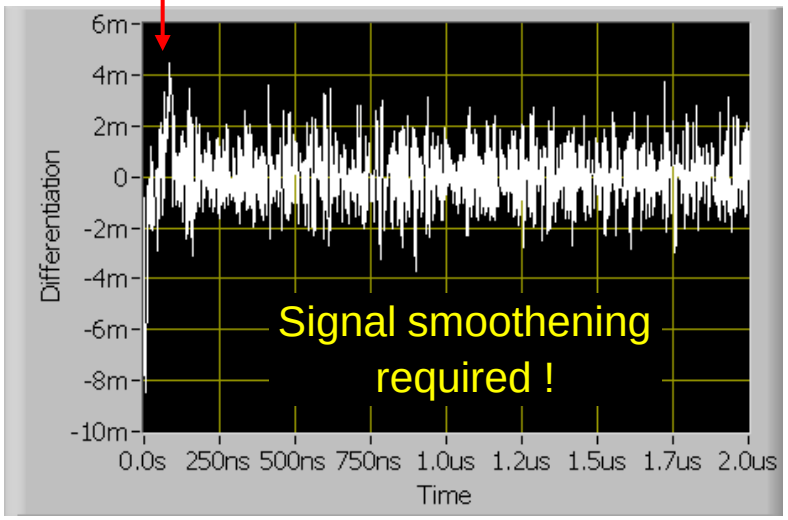

Big bubble

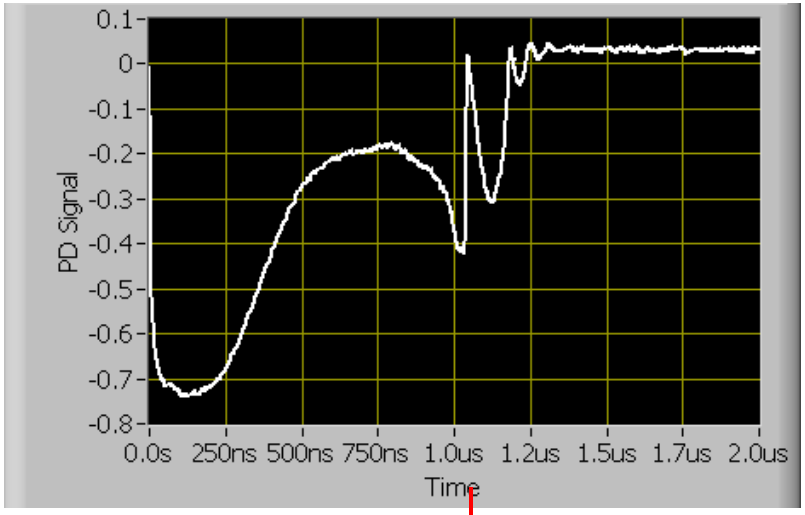

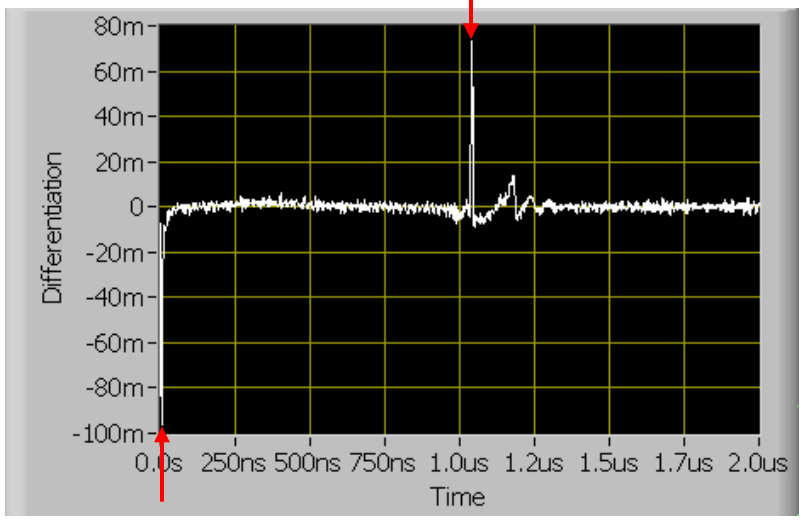

Automatic bubble size detection during pulse series with increasing energy

Every 10th signal is displayed

Total number of evaluated signals:

2500

Bubble radius increases from 600 nm to 6.5 µm

Real-time evaluation presently up to 300 Hz laser repetition rate

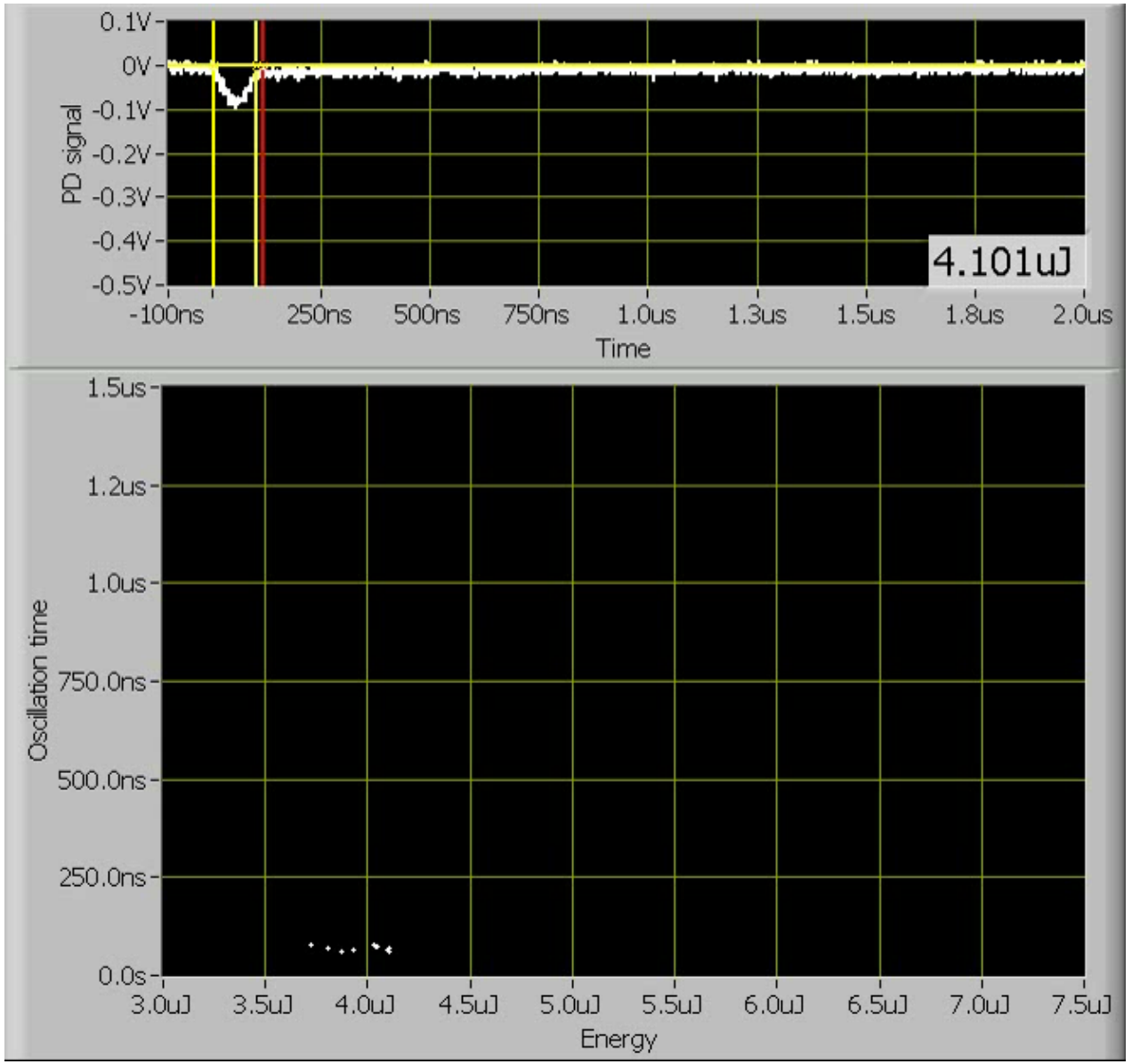

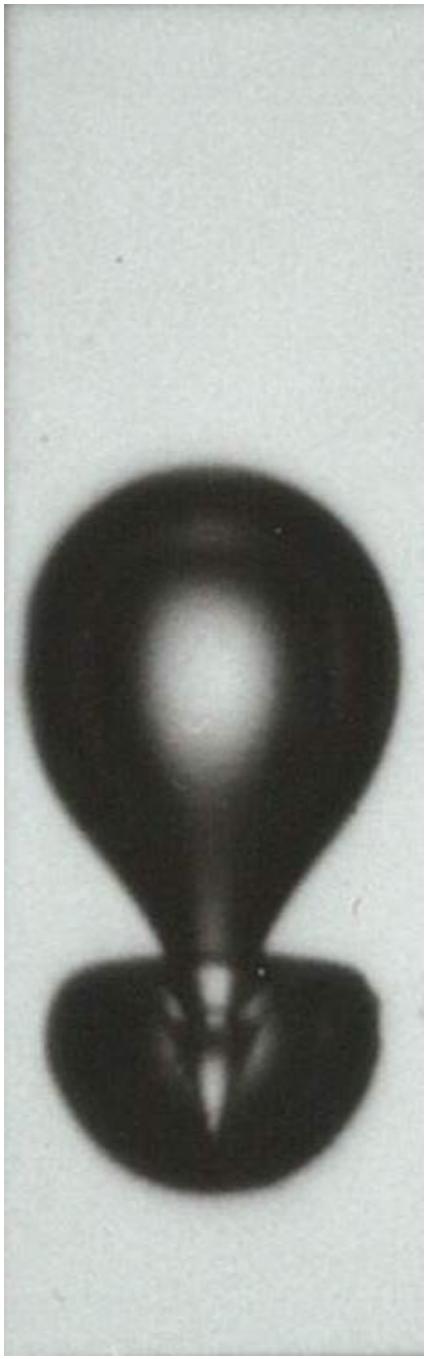

Perspectives

Test *accumulative* UV ns effects
at laser repetition rates > 100 kHz

Look at opto-*injection*

Opto-injection by jetting may

- Ehance the amount of delivered material
- reduce cell damage
- relax focusing requirements in z direction

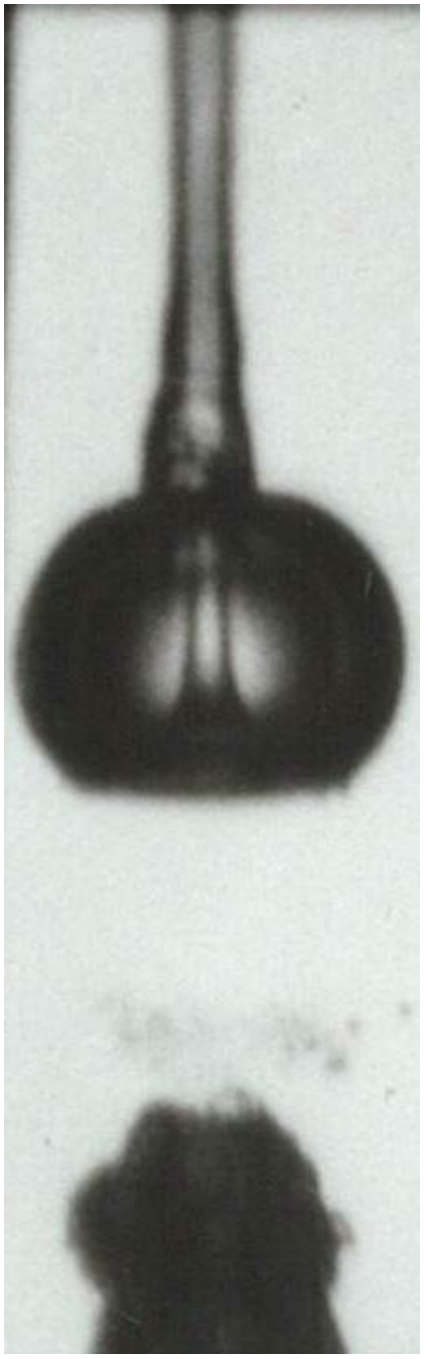

Ablation, Dissection, and Transport of Biomaterials using Fs and Ns Laser Pulses

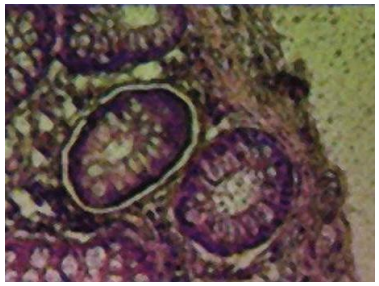

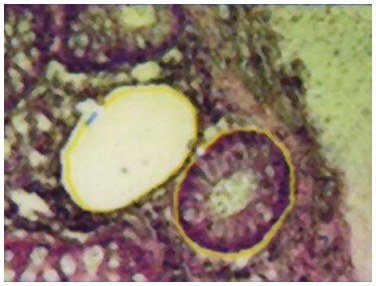

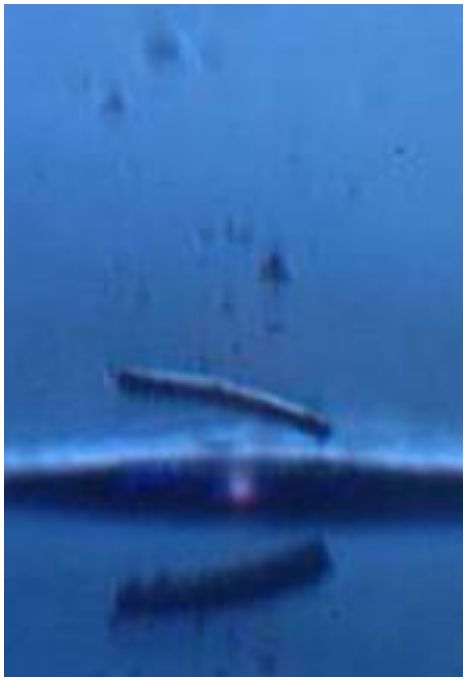

Background

Goal of microdissection and ‚catapulting‘

Separation of small amounts of biomaterial

- from histologic sections with heterogeneous cell populations for genomic or proteomic analysis
- from heterogeneous live cell populations, e.g. for seperation of differentiated cells from pluripotent ‚precurser‘ stem cells

Commercial system used in this study

N_2 laser (λ = 337 nm) coupled into microscope
+ computer-controlled stage
(PALM-Zeiss Microbeam)

Step 1: Laser dissection of specimens (LMD)

Step 2: Laser pressure ‚catapulting‘ (LPC)

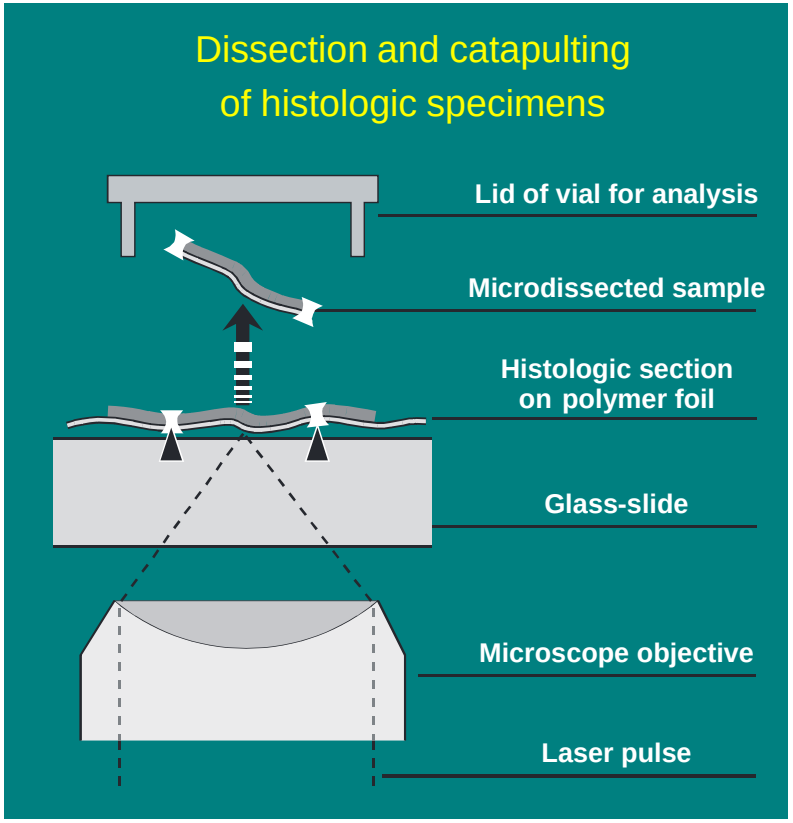

Techniques for separation of histologic specimens

Conventional mechanical preparation

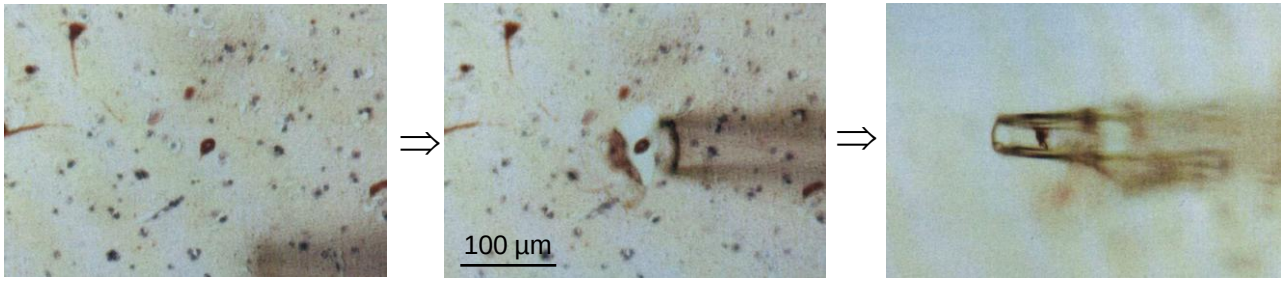

Laser dissection and catapulting

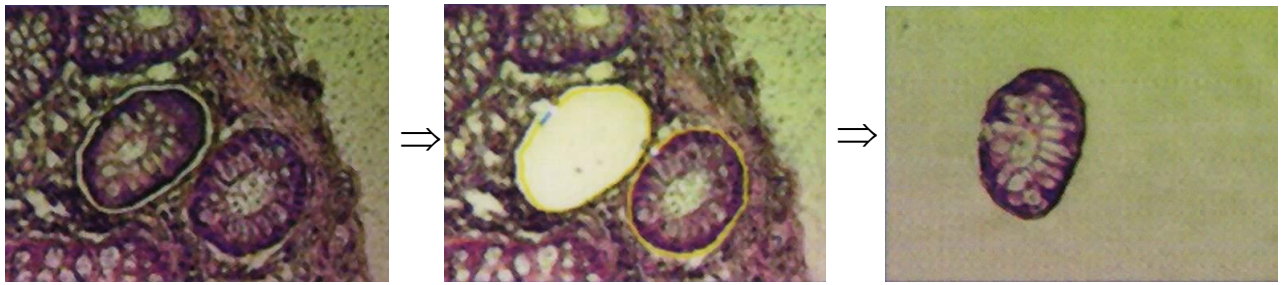

Application example

Proteomic and genomic analysis of tumor cells in an early cancer stage to identify „tumor markers“ enabling a tumor and patient specific treatment

⇒ Quantitative analysis requires isolation of single cells from heterogeneous cell populations, without parts of neigbouring cells.

Mechanism of microdissection at 337 nm

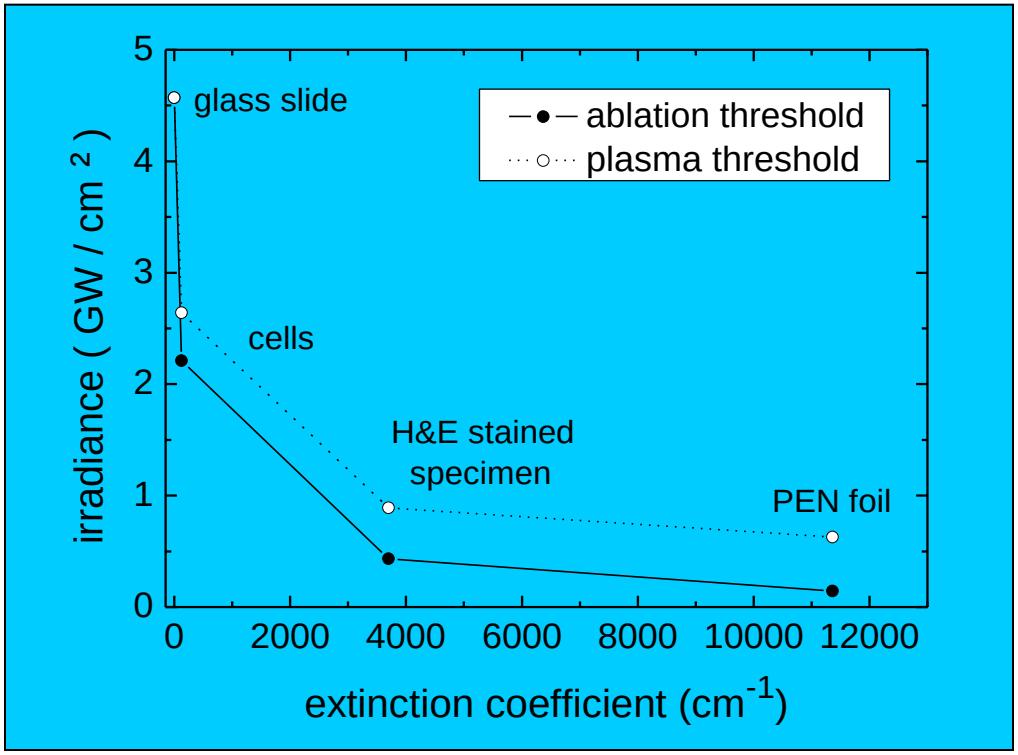

Ablation of PEN-foil + histology

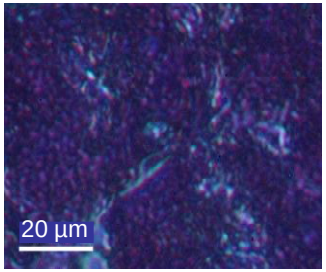

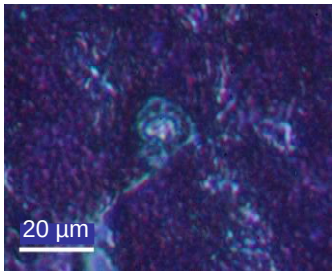

500 nJ 5 µJ

Plasma formation on PEN-foil + histology
5 µJ pulse energy, multiple exposures

- Energies commonly used for dissection (40x, NA = 0.6) : 0.5 µJ
- Thresholds for ablation: 0.15 µJ
  for plasma formation: 0.3 µJ

⇒ Dissection relies on plasma formation supported by linear absorption

Dynamics of catapulting

Paraffin sections (4 µm) on PEN foil (1.3 µm),
40x Objective, NA = 0.6, E = 10 µJ, r = 40 µm

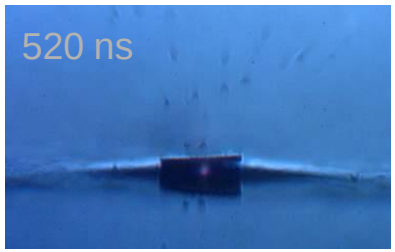

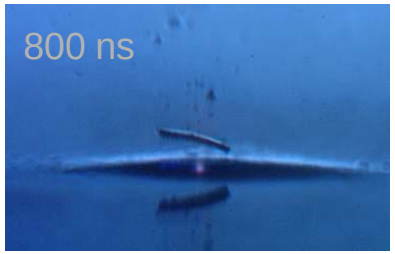

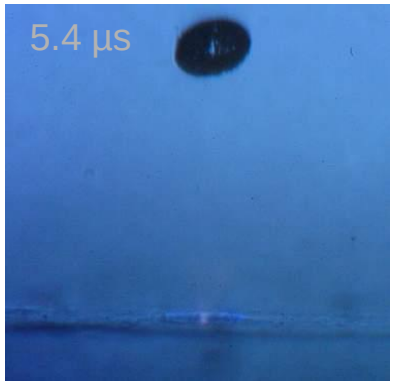

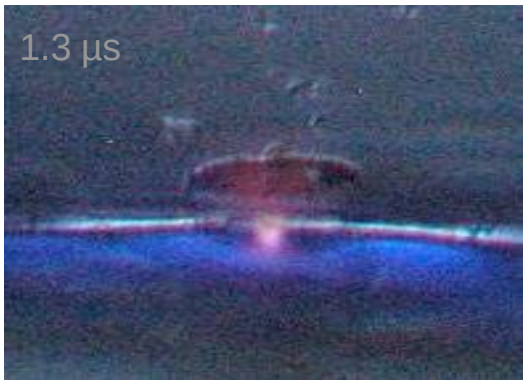

Initial velocity: 200 m/s, Acceleration: $\approx 10^8$ g

Laser catapulting relies on confined ablation and plasma formation

Can radiation pressure explain laser pressure catapulting ?

- Radiation pressure: $p = I / c$

  The force exerted by the radiation pressure during the laser pulse can accelerate the specimen to a velocity of 0.9 mm/s

  (calculated for E = 6.5 µJ, τ = 3 ns, specimen radius 40 µm, and specimen thickness 5 µm)

- Measured velocity of specimen: 200 m/s

  (220 000 × larger than achieved by radiation pressure)

  ⇒ Radiation pressure hardly contributes, confined ablation/plasma formation dominates

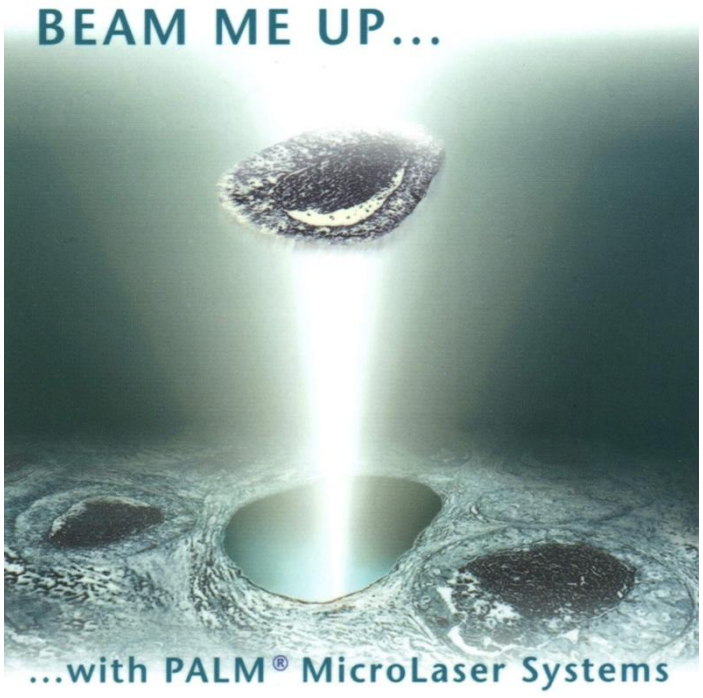

Plasma-driven shock wave propagation

(40x objective, NA = 0.6, E = 10 μJ, r = 40 μm)

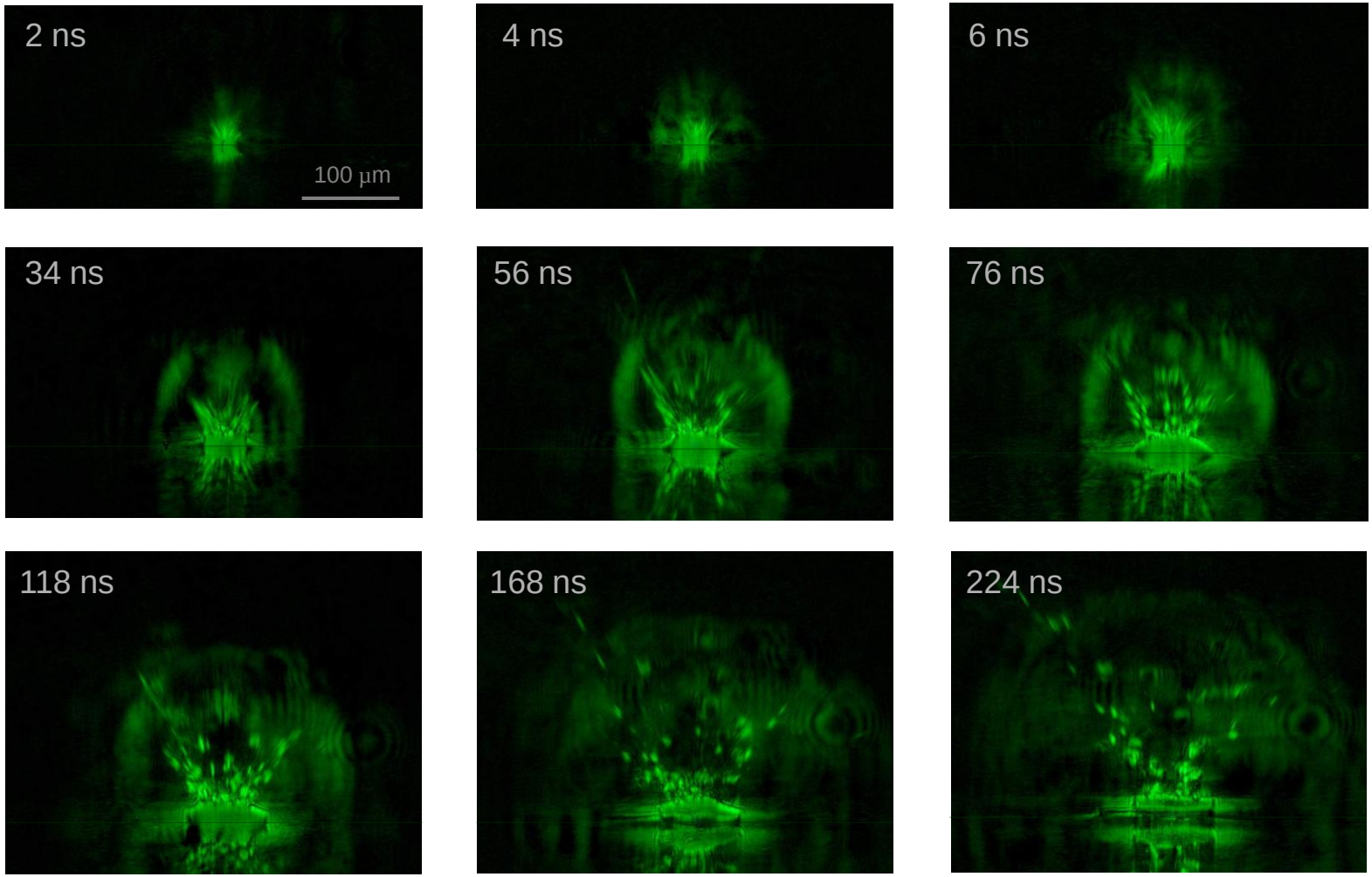

Initial shock wave velocity: 26 000 m/s

Initial pressure: 670 MPa

$$p = \left[\frac{7}{6}\left(\frac{v_s}{c_0}\right)^2 - \frac{1}{6}\right] p_0$$

$c_0 = 345\ \mathrm{m/s},\ p_0 = 0.1\ \mathrm{MPa}$

Problems of PEN carrier foil

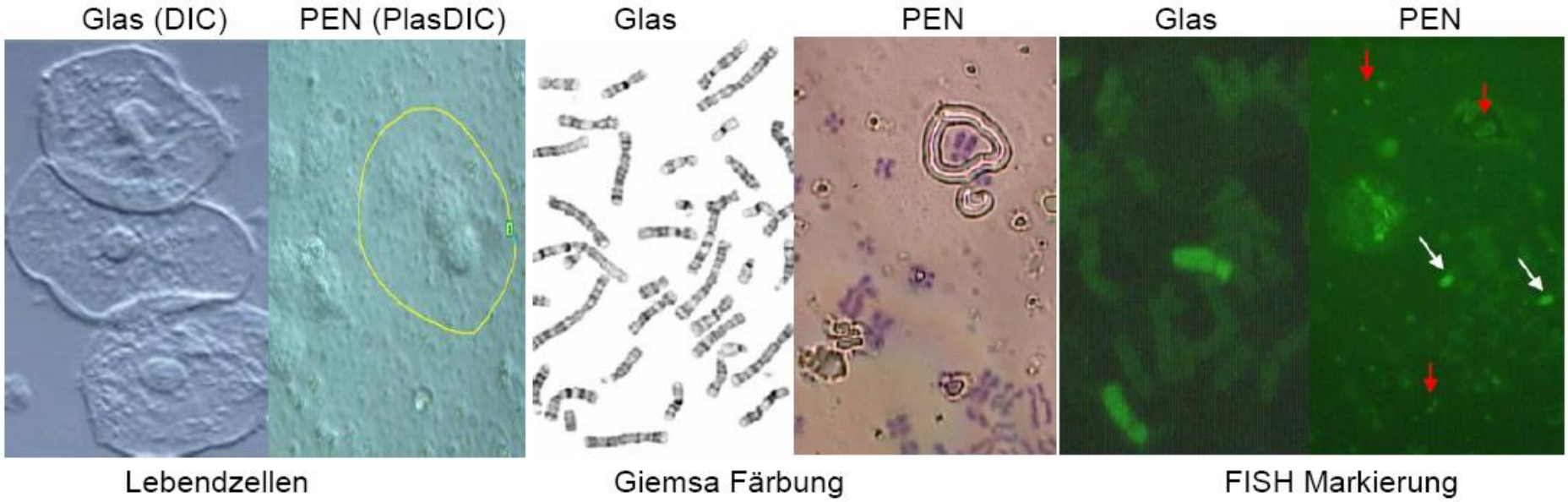

Foil scatters light and has stron autofluorescence

New weakly adhesive carrier system

- Absorber (sputtered ZnO)
- Accelerator that undegoes phase transition (PEM – Polyelectrolyte multilayer*)

  Control of thickness by number of layers

  Addition of salt controls water content and adhesion
- Carrier (Polyacrylate nanocomposite laquer)

  UV-Absorber is added to increase cutting efficieny

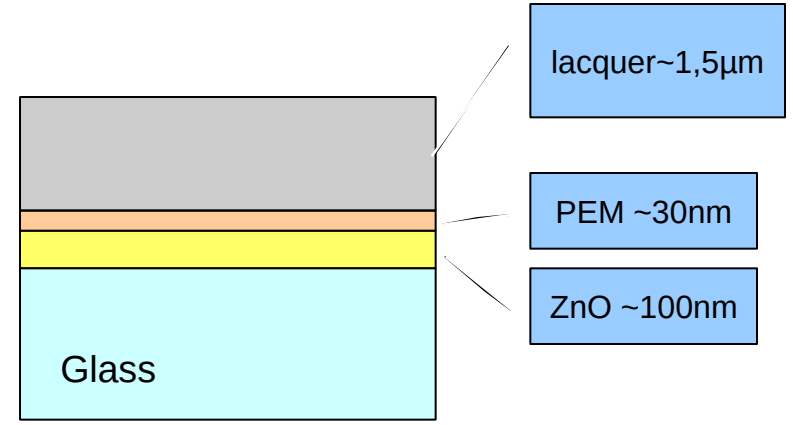

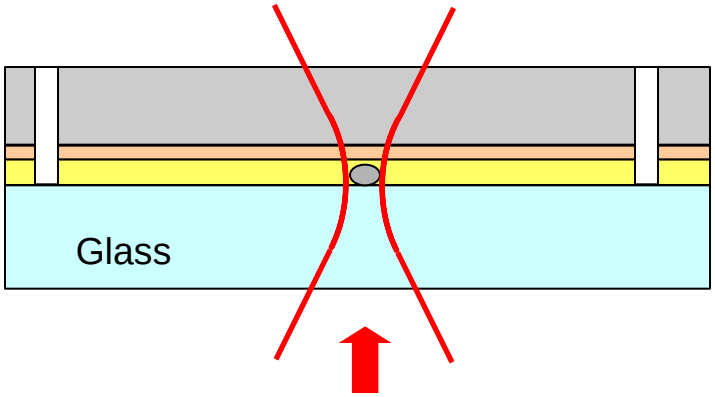

Seperation of functions into different layers makes it easier to adjust the properties of the entire system

* Poly(diallyldimethylammonium chloride) PDADMAC + poly(sodium 4-styrenesulfonate) PSS

Optical properties of the new carrier system

- Good UV absorption and transmission in the visible range
  - Band gap of ZnO 3.3eV
  - Better transmission in the visible range than PEN
- Autofluorescence up to a factor 5 lower than for PEN

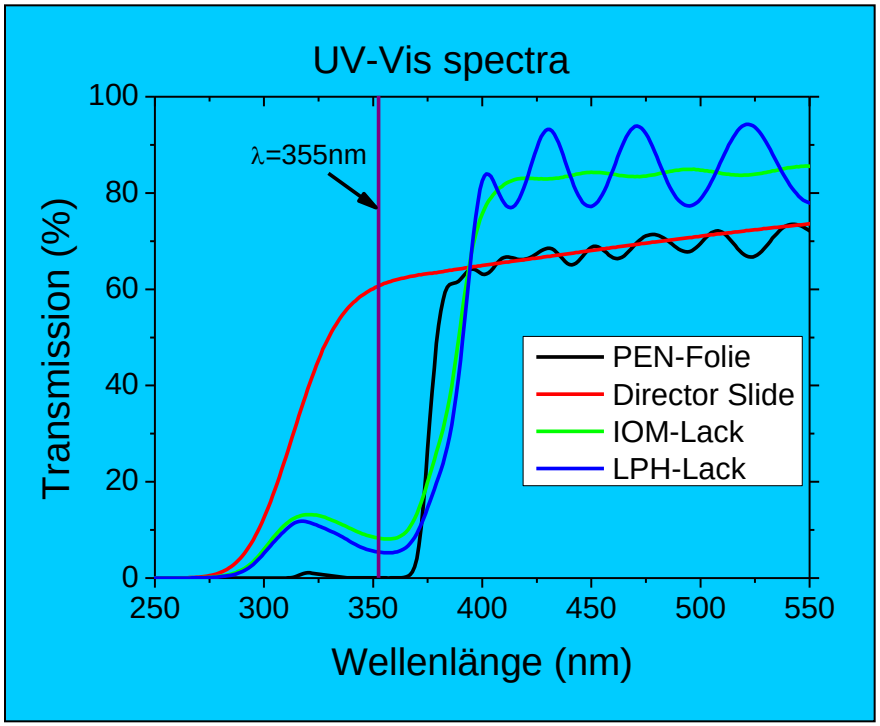

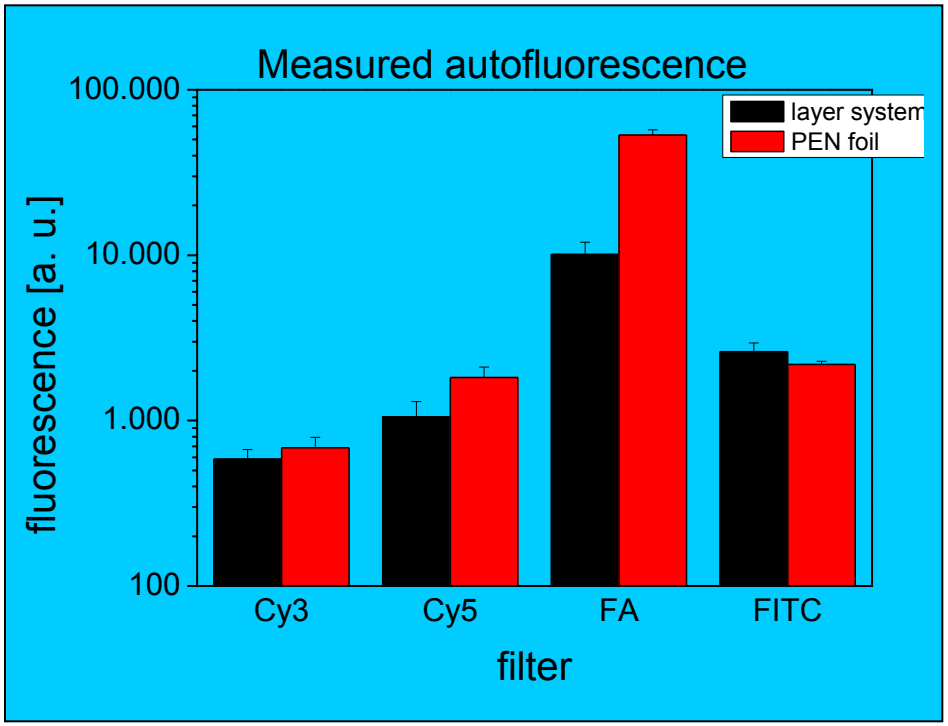

Optical properties of the new carrier system

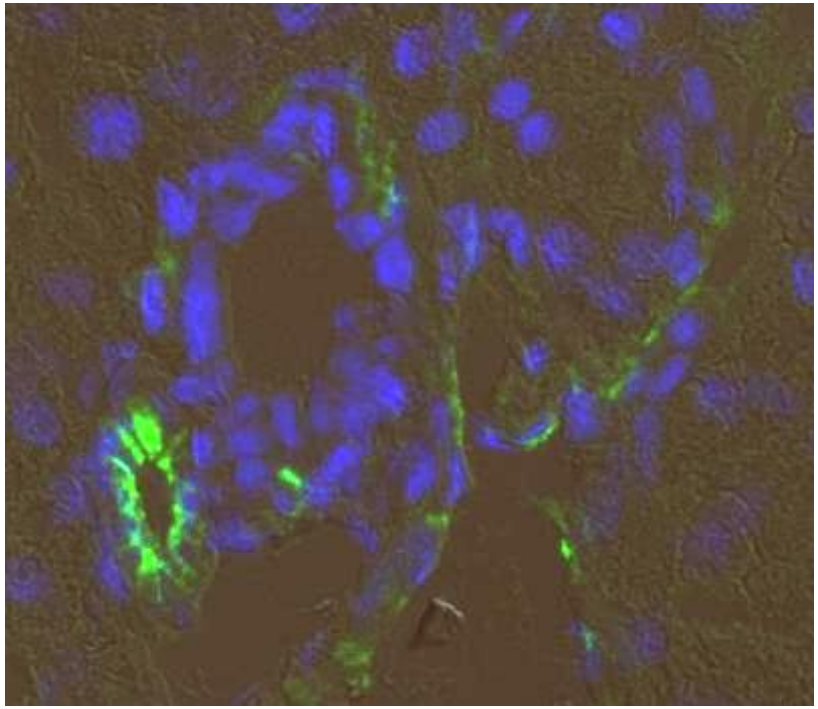

Immunmarkierung für CD31 (grün) an Lebergewebe der Maus. Auf IOM-beschichteten Objektträgern wurden Kryostatschnitte aufgebracht, eine verkürzte indirekte Immunmarkierung mit dem grünen Fluoreszenzfarbstoff Alexa 488 durchgeführt und DNA mit Hoechst 33258 (1:1000) gegengefärbt (blau). Zur zusätzlichen optischen Darstellung der Gewebsmorphologie wurde der Interferenzkontrast nach Nomarski (DIC) eingesetzt (braungrauer Hintergrund). Die Beschichtungen der Objektträger (hier IOM-Lack) erlaubten es erstmals, blaue Fluoreszenz und optische Kontrastierungsverfahren auf LPC-Material anzuwenden.

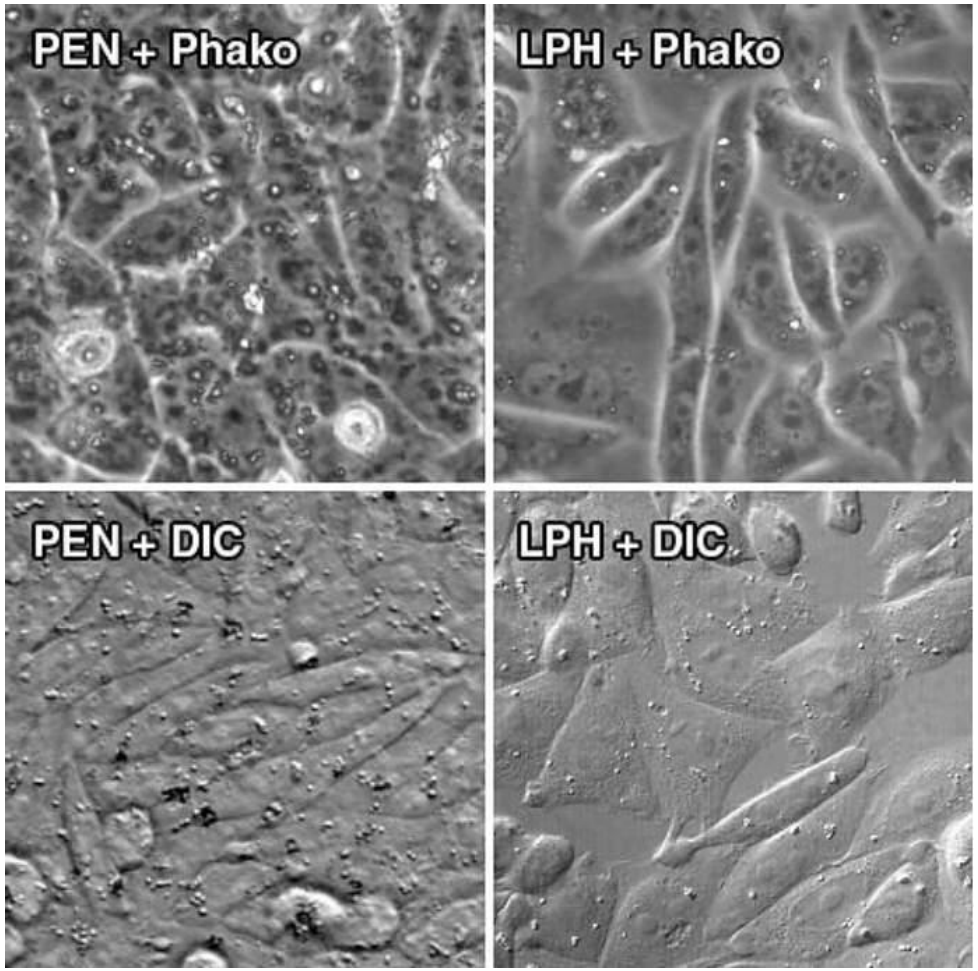

Optische Kontrastierung von CHO-Kulturzellen auf PEN Folie und dem neuen Trägersystem durch das Phasenkontrastverfahren (Phako) und durch den Differenziellen Interferenzkontrast nach Nomarski (DIC).

Femtosecond laser nanosurgery and catapulting

Dissection and catapulting by 346-nm fs-laser pulses

N2 ns laser:

Cutting width ≈ 4 µm

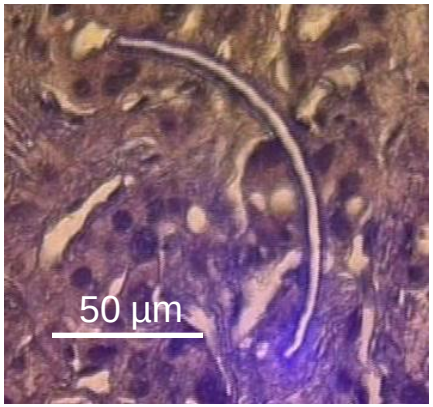

FS-laser:

Cutting width << 1 µm

⇓

Cell nuclei can be dissected and catapulted !

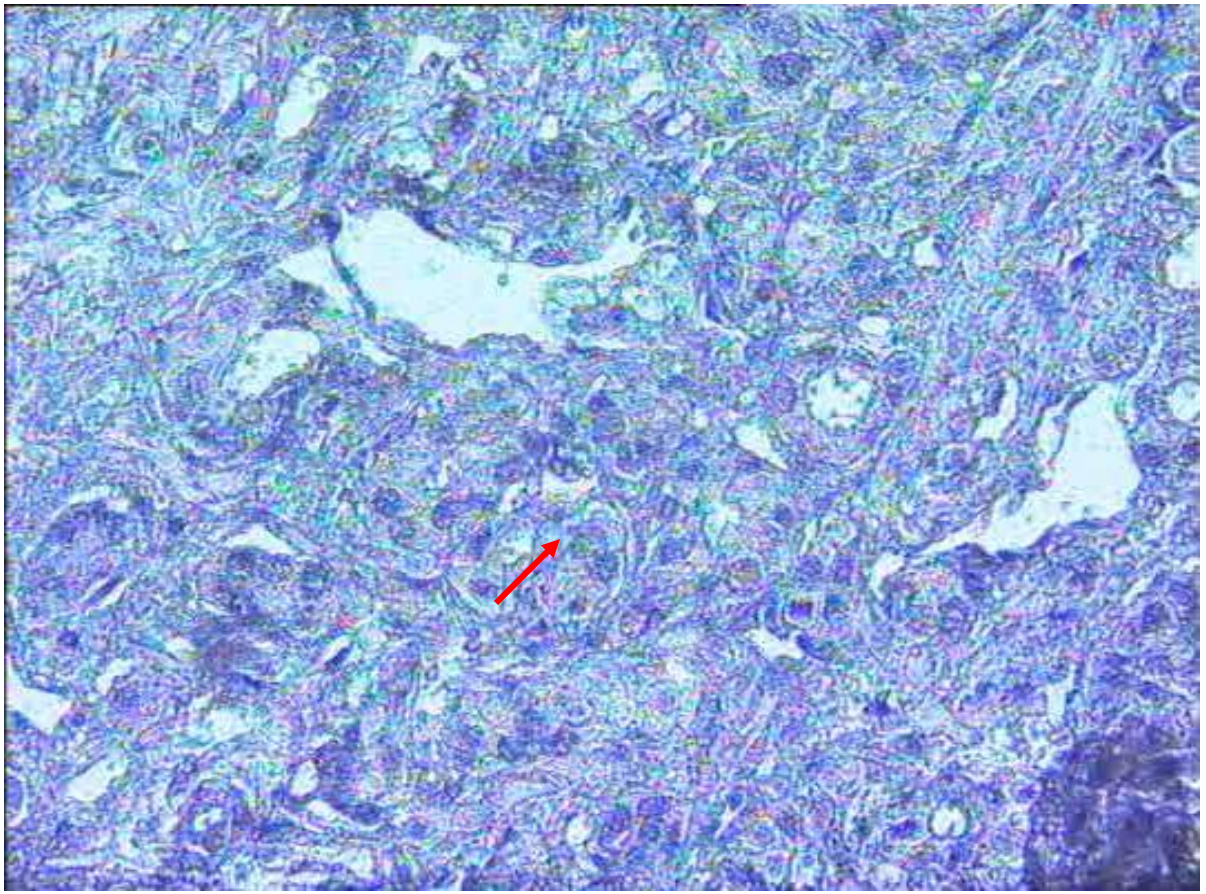

Energy used for dissection: 60 nJ / pulse

Energy used for catapulting: 340 nJ

100 µm

Paraffin section of humane prostate (HE, 5 µm) on 1.3 µm polymer foil

Objective: 40x, NA 0.6, specimen diameter: ≈ 10 µm

Procurement of cell nucleus by 346-nm fs-laser pulses

FS-laser:

Cutting width << 1 µm

⇓

Cell nuclei can be dissected and catapulted !

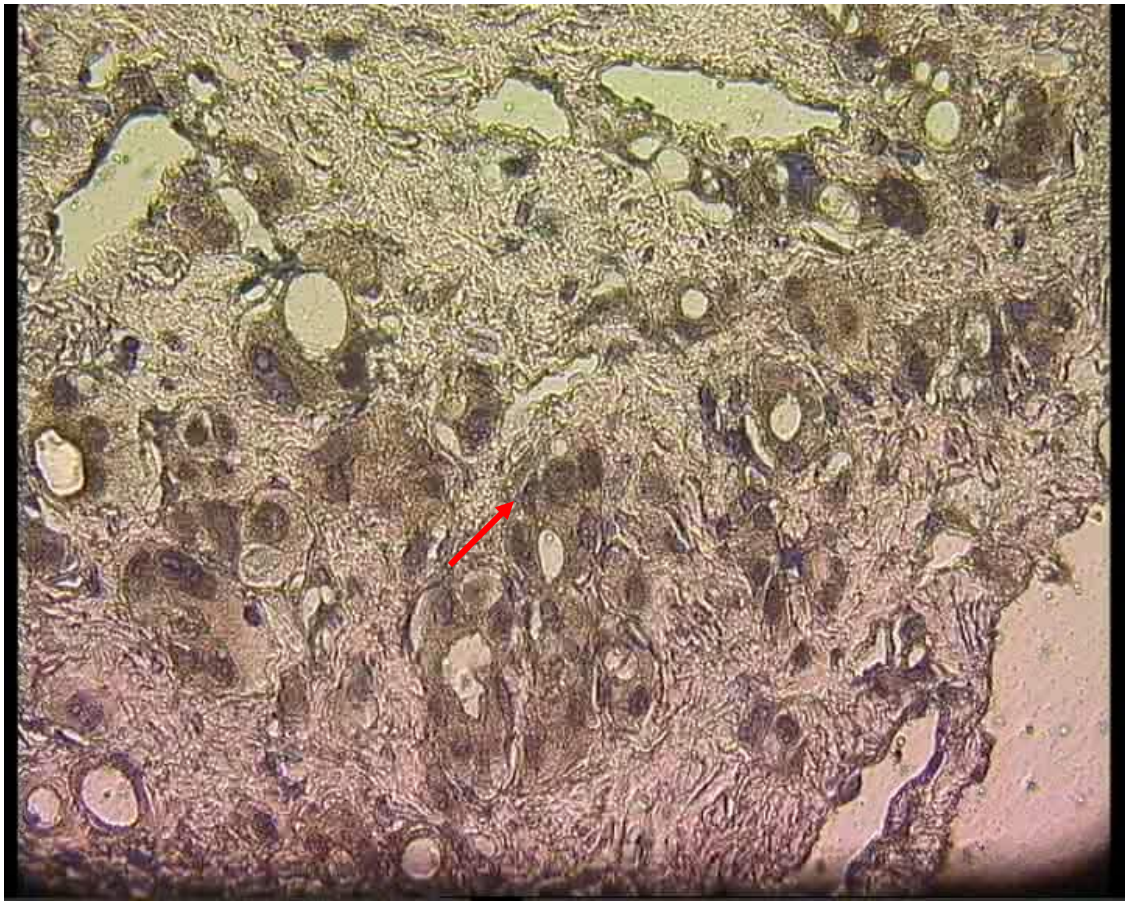

Energy used for dissection: 28 nJ / pulse

Energy used for catapulting: 130 nJ

100 µm

Paraffin section of humane prostate (HE, 5 µm) on 1.3 µm polymer foil

Objective: 40x, NA 0.6

Procurement of large specimens using 1040 nm fs-laser pulses

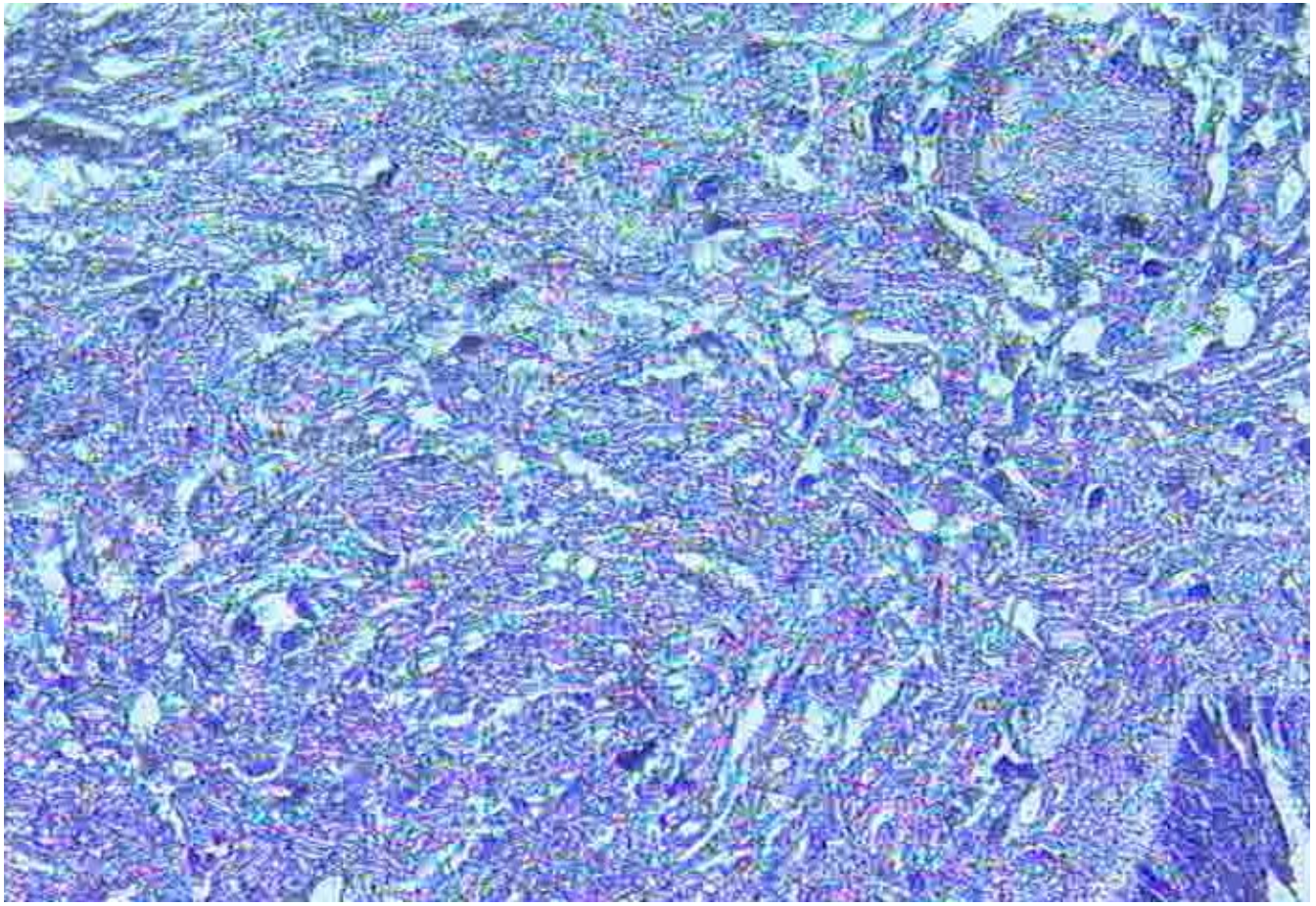

50 µm

Energy used for dissection: 140 nJ
Energy used for Catapulting: 1,2 µJ

Paraffin section of human prostate (HE, 5 µm) on 1.3 µm PEN foil
objective: 40x, NA 0,6, specimen diameter: 80 µm

Vogel et al. Methods Cell Biol. 82:153-205 (2007)

Vogel et al. Biophys. J. 93 : 4481-4500 (2007)

Horneffer et al. J Biomed Opt. 12:054016 (2007)

Nonlinear beam propagation distorts localized energy deposition

- Self-focusing and plasma defocusing result in filamentation during optical breakdown.
- Self-focusing depends on laser power; thus it becomes important for breakdown with small focusing angles and short pulse durations
- For 100-fs pulses near breakdown threshold, self-focusing was observed if NA $\leq$ 0.9

(Schaffer et al., Opt. Lett. 26:93-95, 2001)

$\Rightarrow$ At small focusing angles, localized energy deposition is difficult to achieve !

$\Rightarrow$ Use large focusing angle !

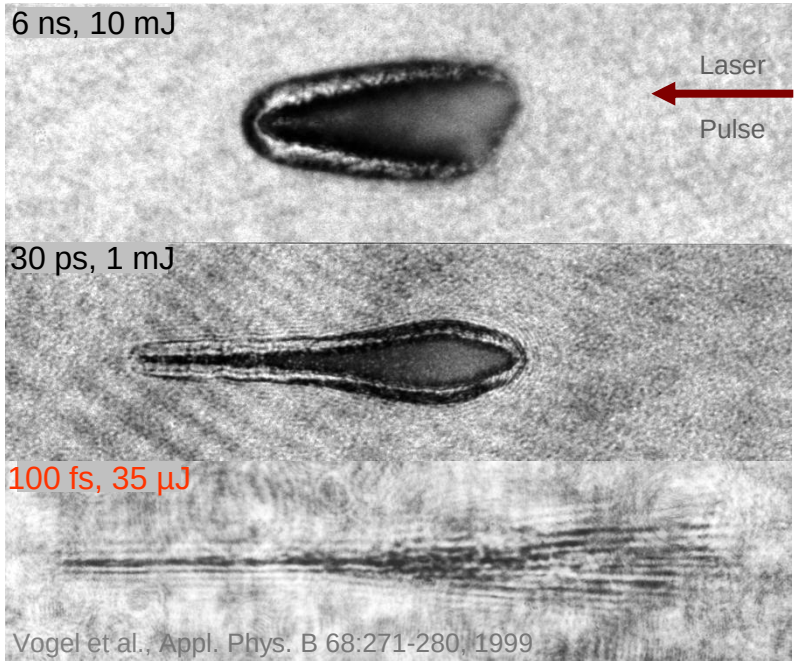

Filament formation in cornea, NA = 0.1

(Heisterkamp et al., Appl. Phys. B 74:419-425, 2004)

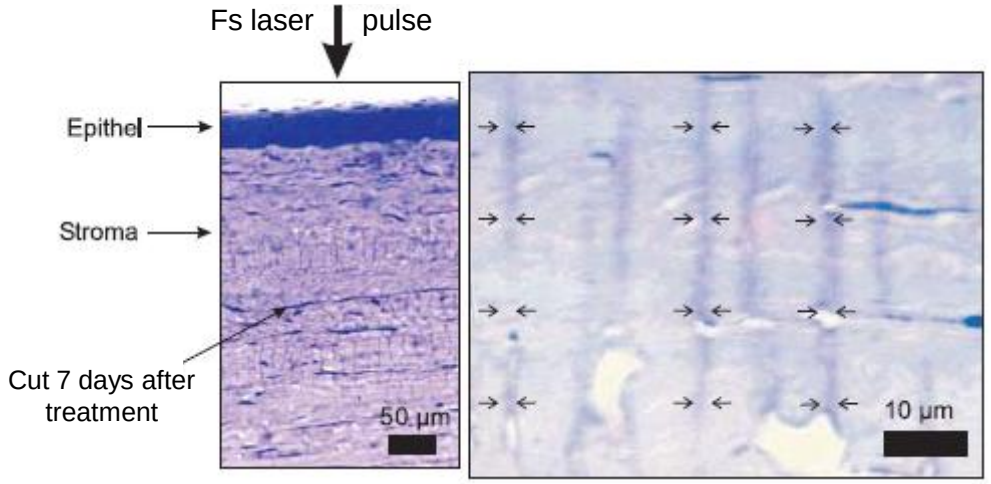

Self-focusing and plasma defocusing ⇒ filamentation

Intense electromagnetic radiation of intensity I produces a variation of the refractive index n as described by the formula $n = n_0 + n_2 I$,
where n_0 and n_2 are the linear and non-linear components of the refractive index

Self-focusing occurs if the radiation power is greater than the critical power

$$P_{cr} = \alpha \frac{\lambda^2}{4\pi n_0 n_2}$$

where λ is the radiation wavelength in vacuum and α is a constant
which depends on the initial spatial distribution of the beam.

"Catastrophic self-focusing": increase of I by self-focusing enhances the effect and leads to beam collapse that is limited only by plasma formation and subsequent defocusing

The refractive index in plasma is lower than in the undisturbed medium ⇒ plasma defocusing

The interplay of self-focusing and plasma defocusing results in a self-sustained plasma filament